ELECTROMAGNETIC FIELD ANALYSIS OF THE CONDUCTING SPHERICAL CAVITY AND SEGMENT

CHUWONG PHONGCHAROENPANICH

A THESIS SUBMITTED IN PARTIAL FULFILLMENT
OF THE REQUIREMENT FOR THE DEGREE
MASTER OF ENGINEERING IN ELECTRICAL ENGINEERING
SCHOOL OF GRADUATE STUDIES
KING MONGKUT'S INSTITUTE OF TECHNOLOGY LADKRABANG
1998

ISBN 974-622-102-7

หัวข้อวิทยานิพนธ์	การวิเคราะห์สนามแม่เหล็กไฟฟ้าของคาวิตี้และเซกเมนต์ตัวนำทรงกลม
นักศึกษา	นายชูวงค์ พงศ์เจริญพาณิชย์
อาจารย์ผู้ควบคุมวิทยานิพนธ์	รศ.ดร.โมไนย ไกรฤกษ์
ระดับการศึกษา	วิศวกรรมศาสตรมหาบัณฑิต สาขาวิชาวิศวกรรมไฟฟ้า สถาบันเทคโนโลยีพระจอมเกล้าเจ้าคุณทหารลาดกระบัง
พ.ศ.	2541

บทคัดย่อ

วิทยานิพนธ์นี้เป็นการพิสูจน์และวิเคราะห์สนามแม่เหล็กไฟฟ้าภายในคาวิตี้และเซกเมนต์ตัวนำทรงกลม โดยรูปทรงของปัญหาที่พิจารณาประกอบด้วย คาวิตี้ตัวนำทรงกลม คาวิตี้ตัวนำทรงกลมซ้อนกันที่ปิดด้วยส่วนของกรวยตัวนำ และเซกเมนต์ตัวนำทรงกลม โดยนิพจน์ของสนามจะแสดงทั้งกรณีที่มีและไม่มีแหล่งกำเนิด การพิสูจน์เริ่มจากการแก้สมการคลื่นในกรณีที่ไม่มีแหล่งกำเนิดโดยใช้เทคนิคการแยกตัวแปร จากนั้นหาคำตอบเฉพาะของแต่ละรูปทรงโดยการประยุกต์ค่าเงื่อนไขขอบเขต สนามแม่เหล็กไฟฟ้ากรณีที่มีแหล่งกำเนิดสามารถพิสูจน์ได้โดยใช้ฟังก์ชันกรีนไดแอดิก ซึ่งวิธีของฟังก์ชันกรีนไดแอดิกชนิดแม่เหล็ก จะใช้ฟังก์ชันคลื่นเวกเตอร์โซลีนอยด์จากการกระจายฟังก์ชันเจาะจงสเกลาร์กรณีไม่มีแหล่งกำเนิด และโดยใช้ความสัมพันธ์เชิงตั้งฉาก จะสามารถพิสูจน์หาฟังก์ชันกรีนไดแอดิกทั้งชนิดไฟฟ้าและแม่เหล็กได้ สนามแม่เหล็กไฟฟ้าจะหาค่าได้จากการอินทิเกรตผลคูณระหว่างฟังก์ชันกรีนไดแอดิกกับนิพจน์แหล่งกำเนิดตลอดโดเมนแหล่งกำเนิดนั้น ผลเฉลยเชิงเลขจะแสดงค่าเจาะจงในแต่ละโหมด และการกระจายสนามแม่เหล็กไฟฟ้าในกรณีไม่มีแหล่งกำเนิด ผลที่ได้นำไปประยุกต์ใช้ในการออกแบบสายอากาศร่องแถวลำดับที่ป้อนคลื่นด้วยคาวิตี้ตัวนำทรงกลม อันได้แก่สายอากาศร่องแถวลำดับบนผิวทรงกลมแบบลำคลื่นรูปกรวยที่มีการโพลาไรซ์เชิงวงกลม

Thesis Title	Electromagnetic Field Analysis of the Conducting Spherical Cavity and Segment
Student	Mr.Chuwong Phongcharoenpanich
Thesis Advisor	Assoc.Prof.Dr.Monai Krairiksh
Level of Study	Master of Engineering in Electrical Engineering
	King Mongkut's Institute of Technology Ladkrabang
Year	1998

Abstract

Electromagnetic fields inside the conducting spherical cavity and segment are derived and analyzed in this thesis. The geometry of the problem is composed of the conducting spherical cavity, the concentric conducting spherical cavity enclosed by the conducting conical surface and the conducting spherical segment. The field expression in case of the source and the source-free region are formulated. The wave equation in the source-free region is solved using variable separation technique and the particular solutions in each configuration are obtained by applying the boundary condition. The electromagnetic field in the source region is derived via the dyadic Green's function. In the method of magnetic dyadic Green's function, the solenoidal vector wave function is used and can be written in the form of scalar eigenfunction expansion which is derived from the event of the source-free region. By using the orthogonal relationship, the electric and magnetic dyadic Green's function can be determined. Integrating the product of that dyadic Green's function and the source expression throughout the source-configuration domain, the electromagnetic fields are obtained. Numerical results of the eigenmodes and electromagnetic field distribution in case of the source-free region are also demonstrated. Further application can be applied to the concentric conducting spherical cavity-backed slot array antennas such as the so-called circularly polarized conical beam spherical slot array antenna.

Acknowledgements

There are numerous individuals contributed whose assistance was crucial to the successful completion of this thesis.

First of all, I would like to express my profoundly invaluable gratitude to my advisor Associate Professor Monai Krairiksh for his continuously valuable guidance, helpful suggestion and constant encouragement since the first day I was his advisee. I would also like to express my gratitude to Associate Professor Jun-ichi Takada of Tokyo Institute of Technology for his generous suggestion and for keeping me on the right track in calculation.

I am particularly grateful to Associate Professor Wiwat Kiranon for his recommendation to apply for the local graduate scholarship, without his recommendation the research might not have progressed smoothly. I am also grateful to Associate Professor Charray Surawatpunya for his valuable comment and perspective suggestion.

I would like to extend my sincere appreciation to Professor Toshio Wakabayashi of Tokai University for his concentrated seminar in our lab. I would also like to sincerely thank to Assistant Professor Sompol Kosulvit to gain experience in doing experiments. Special thank to Dr. Kraisin Songwatana who gave me useful discussion and for proof-reading this thesis.

Again, the encouragement of the fellow members of Monai's Laboratory, Mr.Komsak Meksamoot who gave me kindly discussion, Mr. Montri Thanapakawat for his friendly entertainment especially when I was tensed from hard working, Mr.Duang-arthit Srimoon to help me

preparing the manuscript of this thesis and Mr.Wongsakorn Watcharananunt for his generousity.

I also would like to acknowledge to the National Science and Technology Development Agency (NSTDA) under the career development award for partially funding this research grant and local graduate scholarship program for providing the graduate scholarship during my graduate study.

I wish to thank the Japan International Cooperation Agency (JICA) for their funding to present this project in APMC'97 and to the School of Graduate Studies for supporting the preparation of this thesis.

Finally, I am greatly indebted to my parents for their unlimited patience, constantly supporting and helping me.

Chuwong Phongcharoenpanich

Content

Content (to)

Content (to)

List of Tables

Table page

List of Figures

List of Figures (to)

page

List of Figures (to)

page

Chapter 1

Introduction

Enclosed within this chapter is composed of the background of the spherical slot antennas which is the literature cited of the slot radiator imposed on the spherical surface, the purpose and the scope of the thesis and the outline of the remaining chapters which summarize the information of the succeeding chapters.

1.1 Background of the Spherical Slot Antennas

Since most of substantial amount of works have been done in the analysis of the slot on plane [1-1]-[1-4], cylindrical [1-5]-[1-6] and conical [1-7] surfaces but study of slot on sphere is few. Noticeably, the use of the spherical slot antennas is of particular importance in stationary structures and mobile vehicles, particularly those have portions of their bodies with the spherical shape. In addition, for radar applications which requires the constant radiation pattern in any direction, the spherical array antenna has long been employed [1-8]. At present, mobile satellite communication is maturing. The antenna on the mobile unit must have the capability of tracking satellite in a similar fashion as that of the radar system. Some spherical array antennas have been developed to serve such a system [1-9]-[1-10]. However, the development of the element of the spherical array that is cost effective is significant. To do so, we propose to cut the slot as the array elements on the spherical conductor

instead of mounting the array elements on the spherical surface. These slots are supported by a cavity or a segment that is excited by the feed network. The field inside this cavity or segment plays a key role in the investigation of this cavity-backed slot antenna. This fact has motivated the presentation of this thesis.

1.2 Purpose and Scope of the Thesis

The purpose of this thesis is to derive and analyze the electromagnetic field of the conducting spherical cavity and segment. The electromagnetic field expression is derived for both cases; source and source-free. The scope of this presentation is comprised of three categories by means of the configuration of the problem, they are

1. the conducting spherical cavity which the geometry under consideration is the a whole sphere made of conductor,

2. the concentric conducting spherical cavity which is a concentric conducting sphere enclosed by the conducting conical surface, and

3. the conducting spherical segment which is the axially partitioned in the azimuthal plane of the concentric conducting spherical cavity .

Furthermore, the practical applications in each case are also discussed.

1.3 Outline of the Remaining Chapters

As mentioned in the previous section that the objective of the presentation of this thesis is concerning about the derivation and analysis of the electromagnetic field of the conducting spherical cavity and

segment. The details of the derivation procedure which are in the remaining chapters will be summarized as follows:

Chapter 2 describes the starting point of the derivation procedure by begining with the Maxwell's equations and the continuity equation. To solve for the analytical solutions, the Maxwell's equations are raised its order to keep away from the coupled property. By this fashion the wave equation is derived. The separation of the variables technique is utilized to determine the analytical solution by separating the eigenfunction into three uncoupled variables in spherical coordinate. The general expression of the scalar eigenfunction and the vector potential after some lengthy manipulations are included in this chapter.

Chapter 3 presents the electromagnetic field expression of the spherical geometry in case of the source-free region. The problems under consideration consists of the conducting spherical cavity, the concentric conducting spherical cavity enclosed by the conducting conical surface and the conducting spherical segment, respectively. The electromagnetic field in the particular cases are obtained by imposing the boundary conditions correspond to the configuration in each cases and solving for the unknown scalar coefficients.

Chapter 4 discusses the theory of dyadic analysis, by that theorem we can write the Maxwell's equations and the wave equation in dyadic form. Electric and magnetic types dyadic Green's function of the first, second and third kinds and their properties are also discussed. The free space dyadic Green's function will be derived to demonstrate the derivation procedure. The results of the free space dyadic Green's functions consist of the electric and magnetic types. Additionally, the

concentric conducting spherical cavity and the conducting spherical segment are proposed in this chapter. The dyadic Green's functions of this geometries are derived.The electromagnetic field inside the cavity and segment due to the electric and magnetic sources region are obtain, subsequently.

Chapter 5 demonstrates the numerical results of eigenmodes and electromagnetic fields inside the conducting spherical cavity and the concentric conducting spherical cavity in various modes to verify the derivation.

Chapter 6 proposes the concentric conducting spherical cavity-backed slot array antenna namely the circularly polarized conical beam spherical slot array antenna, to demonstrate the practical application of the electromagnetic field which is derived in the preceding chapters.

Chapter 7 summarizes the consequence of the preceding chapters together with the discussion of the future studies.

Subsequently, vector analysis in the spherical coordinate system, spherical Bessel function and associated Legendre function are reported in the appendices.

References

[1-1] A.F.Stevenson, "Theory of Slots in Rectangular Waveguides," *J.Appl.Phys.*, vol.19, pp.24-38, Jan.1948.

[1-2] J.Galejs, "Admittance of a Rectangular Slot which is Backed by a Rectangular Cavity," *IEEE Trans.Antennas Propagat.*, vol.11, no.3, pp.119-126, 1963.

[1-3] H.Grunberg, "Theory of Waveguide-Fed Slots Radiating into

Parallel-Plate Regions," *J.Appl.Phys.*, vol.23, pp.733-737, Jul.1952.

[1-4] P.Kale, S.B.Sharma, R.K.Malavia and K.Vellimalai, "Slotted Waveguide Planar Array at C-Band," *The 3rd Asia-Pacific Microwave Conference Proceedings*, pp.87-90, 1990.

[1-5] S.Papatheodorou, J.R.Mautz and R.F.Harrington, "The Aperture Admittance of a Circumferential Slot in a Circular Cylinder," *IEEE Trans. Antennas Propagat.*, vol. 40, no.2, pp.240-244, Feb.1992.

[1-6] A.F.Peterson and R.Mittra, "Mutual Admittance between Slot in Cylinders of Arbitrary Shape," *IEEE Trans. Antennas Propagat.*, vol. 37, no.7, pp.858-864, Jul.1989.

[1-7] R.F.Goodrich, R.F.Kleinman, A.L.Maffett, C.E.Schensted, K.M. Siegel, M.G.Chernin, H.E.Shanks and R.E.Plummers, "Radiation from Slot Arrays on Cones," *IRE Trans.Antennas Propagat.*, vol.7, no.7, pp.213-222, Jul.1959.

[1-8] D.L.Sengupta, T.M.Smith and R.W.Larson, "Radiation Characteristics of a Spherical Array of Circularly Polarized Elements," *IEEE Trans. Antennas Propagat.*, vol 16, no.1, pp.2-7, Jan. 1968.

[1-9] T.Hori, N.Terada and K.Kagoshima, "Electronically Steerable Spherical Array Antenna for Mobile Earth Station," *Proc.IEE Conf.Antennas Propagat.*, IEE, London, pp.55-58, Mar.1987.

[1-10] M.E.Bialkowski, "Design of an Antenna and Associated Components for the Australian Mobilesat," *1995 Asia-Pacific Microwave Conference Proceedings*, pp. 740-745, Dec. 1995.

Chapter 2

Wave Equation and Its Analytical Solutions

Maxwell's equations are set of basic equations which were formulated according to experiments by many scientists such as Faraday, Ampere, Gauss, Lens, Coulomb, Volta and others and were summarized in the compact form by James Clerk Maxwell, a scottish physicist and mathematician [2-1]-[2-4]. Maxwell's equations can be classified into two forms by means of their operations, they are differential or point form and integral form. The differential form is most widely used for solving the boundary value problem. In case of the source, lossy regions and time harmonic $e^{-j\omega t}$ form, Maxwell's equations in the differential form can be written as

$$\nabla \times \overline{E} = -\overline{M}_i + j\omega \overline{B} \tag{2.1a}$$

$$\nabla \times \overline{H} = \overline{J}_i + \overline{J}_c - j\omega \overline{D} \tag{2.1b}$$

$$\nabla \cdot \overline{D} = q_{ev} \tag{2.1c}$$

$$\nabla \cdot \overline{B} = q_{mv}. \tag{2.1d}$$

Another equation which is frequently used together with the Maxwell's equations is the continuity equation:

$$\nabla \cdot \overline{J}_{ic} = j\omega q_{ev} \,, \tag{2.1e}$$

where

$\overline{E}$: electric field intensity (volts/meter),

$\overline{H}$: magnetic field intensity (amperes/meter),

$\overline{D}$: electric flux density (coulombs/square meter),

$\overline{B}$: magnetic flux density (webers/square meter),

$\overline{J}_i$: impressed (source) electric current density (amperes/square meter),

$\overline{J}_c$: conduction electric current density (amperes/square meter),

$\overline{M}_i$: impressed (source) magnetic current density (volts/square meter),

q_{ev} : electric charge density (coulombs/cubic meter),

q_{mv} : magnetic charge density (webers/cubic meter),

j : imaginary unit and

ω : operating angular frequency which equals to 2π times the frequency. The three medium relations which the expressions are referred to as the constitutive relations are

$$\overline{D} = \varepsilon \overline{E} \tag{2.2a}$$

$$\overline{B} = \mu \overline{H} \tag{2.2b}$$

$$\overline{J}_c = \sigma \overline{E}, \tag{2.2c}$$

where ε, μ, σ denote, respectively, the permittivity, the permeability and the conductivity of the medium.

$$\varepsilon = \varepsilon_o \varepsilon_r \tag{2.3a}$$

$$\mu = \mu_o \mu_r. \tag{2.3b}$$

ε_r, μ_r are the relative permittivity and permeability which depend on the electrical properties of the materials. ε_o is the free space permittivity and equals to 8.854×10^{-12} or about $10^{-9}/36\pi$ farads per meter. In the same manner, μ_o is the free space permeability which equals to $4\pi\times10^{-7}$ henries per meter. For free space the conductivity vanishes.

2.1 Wave Equation Construction

Generally, because of their first order coupled partial differential equation property of the Maxwell's equations, it is not convenient to solve analytically except by numerical techniques such as finite difference or finite volume time domain methods [2-5]-[2-9]. To solve the equation by an analytical method, that problem can be formulated by raising their order which leads to the second order uncoupled partial differential equation. It is referred to as the wave equation. The derivation is started by taking the curl of both sides of (2.1a) and (2.1b) with the homogeneous medium. By using the vector identity that

$$\nabla \times \nabla \times \overline{F} = \nabla(\nabla \cdot \overline{F}) - \nabla^2 \overline{F}, \tag{2.4}$$

substituting (2.1c) and after rearranging, (2.1a) can be written as

$$\nabla^2 \overline{E} = \nabla \times \overline{M}_i - j\omega\mu \overline{J}_i + \frac{1}{\varepsilon}\nabla q_{ev} - j\omega\mu\sigma\overline{E} - \omega^2 \mu\varepsilon \overline{E}. \tag{2.5}$$

In the same fashion, substituting (2.1d) into (2.1b), the magnetic wave equation can be represented as

$$\nabla^2 \overline{H} = -\nabla \times \overline{J}_i + \sigma\overline{M} - j\omega\varepsilon \overline{M}_i + \frac{1}{\mu}\nabla q_{mv} - j\omega\mu\sigma\overline{H} - \omega^2 \mu\varepsilon \overline{H}. \tag{2.6}$$

Equation 2.5 and 2.6 are referred to as the vector wave equations for the electric and magnetic fields, respectively.

2.2 Solutions of Wave Equation in the Spherical Coordinate

In case of the source-free region ($\overline{J}_i = \overline{M}_i = q_{ev} = q_{mv} = 0$) and lossless ($\sigma = 0$) media, the vector wave equation can be written in the simplest form as

$$\nabla^2 \overline{E} = -\omega^2 \mu\varepsilon \overline{E} \tag{2.7}$$

$$\nabla^2 \overline{H} = -\omega^2 \mu\varepsilon \overline{H}. \tag{2.8}$$

This simplification leads to an easiest way to solve. For the source region and lossy media, this solution can also be applied to the

eigenvalue problem. The details will be discussed in the succeeding chapters.

For the problems that involve spherical geometries such as electromagnetic fields inside the spherical cavity and segment the vector wave equation can not be separated into three uncoupled scalar wave equations in each orthogonal coordinates which is different from the rectangular coordinate. To solve this problem, it is advisable to use the scalar function (φ). This scalar function satisfies the scalar wave equation that

$$\nabla^2\varphi(R,\theta,\phi)+k^2\varphi(R,\theta,\phi) = 0, \tag{2.9}$$

where $k = \omega\sqrt{\mu\varepsilon}$ is the phase constant of the medium. The scalar function can be represented as the scalar field or the vector potential component which is used as the eigenvalue.

To solve the second order partial differential equation analytically, the separation of variables method [2-10]-[2-11] is used. In this way, the scalar function is separated into three uncoupled variable in the spherical coordinate as

$$\varphi(R,\theta,\phi) = \Re(R)\Theta(\theta)\Phi(\phi). \tag{2.10}$$

After expanding (2.9) in the spherical coordinate system, by substituting (2.10), dividing both sides of the equation by $\Re\Theta\Phi$, multiplying by $R^2 sin\theta$ and replacing the partials by the ordinary derivatives, thus the scalar wave equation (2.9) can be written as

$$\frac{\sin^2\theta}{\Re}\frac{d}{dR}\{R^2\frac{d\Re}{dR}\}+\frac{\sin\theta}{\Theta}\frac{d}{d\theta}\{\sin\theta\frac{d\Theta}{d\theta}\}+\frac{1}{\Phi^2}\frac{d^2\Phi}{d\phi^2} = -(kR\sin\theta)^2. \tag{2.11}$$

The ϕ - function is uncoupled so it can be isolated and set to

$$\frac{1}{\Phi^2}\frac{d^2\Phi}{d\phi^2} = -m^2, \tag{2.12}$$

or

$$\frac{d^2\Phi}{d\phi^2} = -m^2\Phi, \tag{2.13}$$

where m is the constant. This equation is well-known as the second order homogeneous equation with the constant coefficients [2-11].

By substituting (2.12) into (2.11), dividing the both sides by $\sin^2\theta$ and adding by $(kR)^2$, the scalar equation can be reduced to

$$\frac{1}{\Re}\frac{d}{dR}\{R^2\frac{d\Re}{dR}\}+(kR)^2+\frac{1}{\Theta\sin\theta}\frac{d}{d\theta}\{\sin\theta\frac{d\Theta}{d\theta}\}-\{\frac{m}{\sin\theta}\}^2 = 0. \tag{2.14}$$

In the same manner, θ - function can be set equal to $-n(n+1)$

$$\frac{1}{\Theta\sin\theta}\frac{d}{d\theta}\{\sin\theta\frac{d\Theta}{d\theta}\}-\{\frac{m}{\sin\theta}\}^2 = -n(n+1), \tag{2.15}$$

where n is the constant. The (2.15) is the associated Legendre differential equation [2-2]-[2-4], [2-12]-[2-14] of the cosine function. The R-function after substituting (2.15) into (2.14) can be reduced to

$$\frac{1}{\Re}\frac{d}{dR}\{R^2\frac{d\Re}{dR}\}+(kR)^2-n(n+1)\ =\ 0. \tag{2.16}$$

This equation is referred to as the ordinary spherical Bessel differential equation [2-2]-[2-4].

The analytical solutions of (2.13), (2.15) and (2.16), can be written, respectively as follows:

$$\Re(R)\ =\ \begin{cases} A_1 j_n(kR)+B_1 y_n(kR) & (2.17a) \\ A_2 h_n^{(1)}(kR)+B_2 h_n^{(2)}(kR) & (2.17b) \end{cases}$$

$$\Theta(\theta)\ =\ \begin{cases} C_1 P_n^m(cos\theta)+D_1 Q_n^m(cos\theta) & n=Integer \quad (2.17c) \\ C_2 P_n^m(cos\theta)+D_2 P_n^m(-cos\theta) & n\neq Integer \quad (2.17d) \end{cases}$$

$$\Phi(\phi)\ =\ \begin{cases} E_1 e^{-jm\phi}+F_1 e^{jm\phi} & (2.17e) \\ E_2 cos(m\phi)+F_2 sin(m\phi) & (2.17f) \end{cases}$$

where A_1, B_1, C_1, D_1, E_1, F_1, A_2, B_2, C_2, D_2, E_2 and F_2 are the arbitrary constants. In (2.17a), $j_n(kR)$ and $y_n(kR)$ stand for, respectively, the ordinary spherical Bessel function of the first and second kinds which correspond to the standing wave in the radial direction of the spherical coordinate. In (2.17b), $h_n^{(1)}(kR)$ and $h_n^{(2)}(kR)$ stand for, respectively, the ordinary spherical Hankel function of the first and second kinds. They

represent the traveling wave in the radial direction of the spherical coordinate. In (2.17c) and (2.17d) $P_n^m(cos\theta)$ and $Q_n^m(cos\theta)$ stand for, respectively, the associated Legendre function of the first and second kinds of the cosine function. The following solutions can be chosen according to the appropriate spherical configuration of the problem. Another spherical Bessel function which is usually used in the boundary value problems, this function was initially introduced by Schelkunoff [2-3],[2-15], denoted by $\hat{B}_n(kR)$ and satisfies the Schelkunoff spherical Bessel differential equation

$$\frac{1}{\hat{B}_n(kR)}\{R^2\frac{d^2\hat{B}_n(kR)}{dR^2}\}+(kR)^2-n(n+1)=0, \qquad (2.18)$$

$\hat{B}_n(kR)$ is either the Schelkunoff spherical Bessel ($\hat{J}_n(kR)$) Hankel functions
($\hat{H}_n(kR)$) or their linear combinations.

The electromagnetic fields inside the spherical cavity and segment can be determined via the vector potential by using the scalar eigenfunction which has been derived in the previous paragraph. The vector potential is classified into two types by means of the mode configurations, they are magnetic vector potential ($\overline{A}$) for the transverse magnetic mode and the electric vector potential ($\overline{F}$) for the transverse electric mode. In the analysis of the spherical geometry, the transverse mode field is subjected to the configuration is the transverse to the radial direction of the spherical coordinate (*TE to R* or TE^R and *TM to R* or

TM^R). The electric and magnetic fields after some lengthy derivations can be written in terms of the vector potential as follows:

Transverse electric to R mode (TE^R)

$$\overline{E}_F = -\frac{1}{\varepsilon}\nabla\times\overline{F} \tag{2.19}$$

or

$$E_R = 0 \tag{2.19a}$$

$$E_\theta = -\frac{1}{\varepsilon}\frac{1}{R\sin\theta}\frac{\partial F_R}{\partial\phi} \tag{2.19b}$$

$$E_\phi = \frac{1}{\varepsilon}\frac{1}{R}\frac{\partial F_R}{\partial\theta} \tag{2.19c}$$

and

$$\overline{H}_F = \frac{1}{j\omega\mu\varepsilon}\nabla\times\nabla\times\overline{F} \tag{2.20}$$

or

$$H_R = \frac{1}{j\omega\mu\varepsilon}\left(\frac{\partial^2}{\partial R^2}+k^2\right)F_R \tag{2.20a}$$

$$H_\theta = \frac{1}{j\omega\mu\varepsilon}\frac{1}{R}\frac{\partial^2 F_R}{\partial R\partial\theta} \tag{2.20b}$$

$$H_\phi = \frac{1}{j\omega\mu\varepsilon}\frac{1}{R\sin\theta}\frac{\partial^2 F_R}{\partial R\partial\phi} \tag{2.20c}$$

where $F_R = R\varphi_e.$ (2.21)

Transverse magnetic to R mode (TM^R)

$$\overline{E}_A = \frac{1}{j\omega\mu\varepsilon}\nabla\times\nabla\times\overline{A} \tag{2.22}$$

or

$$E_R = \frac{1}{j\omega\mu\varepsilon}\left(\frac{\partial^2}{\partial R^2}+k^2\right)A_R \tag{2.22a}$$

$$E_\theta = \frac{1}{j\omega\mu\varepsilon}\frac{1}{R}\frac{\partial^2 A_R}{\partial R\partial\theta} \tag{2.22b}$$

$$E_\phi = \frac{1}{j\omega\mu\varepsilon}\frac{1}{R\sin\theta}\frac{\partial^2 A_R}{\partial R\partial\phi} \tag{2.22c}$$

or

$$\overline{H}_A = -\frac{1}{\varepsilon}\nabla\times\overline{A} \tag{2.23}$$

$$H_R = 0 \tag{2.23a}$$

$$H_\theta = \frac{1}{\mu}\frac{1}{R\sin\theta}\frac{\partial A_R}{\partial\phi} \tag{2.23b}$$

$$H_\phi = -\frac{1}{\mu}\frac{1}{R}\frac{\partial A_R}{\partial\theta} \tag{2.23c}$$

where $$A_R = R\varphi_m. \tag{2.24}$$

φ_e and φ_m designated for the electric and magnetic scalar function which correspond to the transverse electric and transverse magnetic modes, respectively.

The vector potential can be obtained by substituting the scalar eigenfunction (2.10) in (2.21) for TE mode and (2.24) for TM mode. The solutions for the two kinds vector potential can be summarized as

$$\left.\begin{matrix}A_R\\F_R\end{matrix}\right\}(R,\theta,\phi) = \mathrm{R}(R)\Theta(\theta)\Phi(\phi) \tag{2.25}$$

$$\mathrm{R}(R) = \begin{cases} A_1\hat{J}_n(kR)+B_1\hat{Y}_n(kR) \\ A_2\hat{H}_n^{(1)}(kR)+B_2\hat{H}_n^{(2)}(kR) \end{cases} \tag{2.26}$$

For the $\Theta(\theta)$ and $\Phi(\phi)$ functions, they are still identical to (2.17c), (2.17 d) and (2.17e), (2.17f), respectively.

2.3 Conclusions

To determine the electromagnetic fields of the geometry under consideration such as the conducting spherical cavity and segment, we would start by solving the wave equations instead of the Maxwell's equations. Since the wave equations are the second order uncoupled partial differential equations whereas the Maxwell's equations are the first order coupled partial differential equation which are not convenient to solve analytically. The separation of variables method is utilized to solve the scalar wave equation of the scalar function instead of the electromagnetic field function because of its coupled property of their components in the spherical coordinate.

The derived scalar functions consist of

1. The spherical Bessel function of the first and second kinds ($j_n(kR)$ and $y_n(kR)$) for the standing wave and spherical Hankel function of the first and second kinds($h_n^{(1)}(kR)$ and $h_n^{(2)}(kR)$) for the traveling wave in the radial direction of the spherical coordinate.

2. The associated Legendre function of the first and second kinds of order (n,m) of the cosine function ($P_n^m(cos\theta)$ and $Q_n^m(cos\theta)$) for the wave in the θ - direction.

3. The complex exponential functions ($e^{-jm\phi}$ and $e^{jm\phi}$) and the cosinusoidal functions ($cos(m\phi)$ and $sin(m\phi)$) for the wave in the ϕ - direction.

The vector potentials are obtained by using that scalar eigenfunctions. The expression of the vector potential are identical to the scalar eigenfunctions in θ and ϕ components. Alternatively, for the R

omponent the ordinary spherical Bessel and Hankel functions become the Schelkunoff spherical Bessel and Hankel functions. The electromagnetic fields can be determined via these vector potentials.

References

[2-1] J.C.Maxwell, *A Treatise on Electricity and Magnetism*, vol.I-II, Dover Publications, New York, 1954.

[2-2] J.A.Stratton, *Electromagnetic Theory*, McGraw-Hill, New York, 1941.

[2-3] R.F.Harrington, *Time-Harmonic Electromagnetic Fields*, McGraw-Hill, New York, 1961.

[2-4] C.A.Balanis, *Advanced Engineering Electromagnetics*, Wiley, New York, 1989.

[2-5] K.S.Yee, "Numerical Solution of Initial Boundary Value Problems Involving Maxwell's Equations in Isotropic Media," *IEEE Trans.Antennas Propagat.*, vol.AP-14, no.3, pp.302-307, May 1966.

[2-6] M.N.O.Sadiku, *Numerical Techniques in Electromagnetic Theory*, CRC Press, Boca Raton, FL, 1992.

[2-7] K.S.Kunz and R.J.Luebbers, *The Finite Difference Time Domain Method for Electromagnetics*, CRC Press, Boca Raton, FL, 1993.

[2-8] A.Taflove, *Computational Electrodynamics: The Finite-Difference Time-Domain Method*, Artech House, Norwood, MA, 1995.

[2-9] K.S.Yee and J.S.Chen, "The Finite-Difference Time-Domain (FDTD) and the Finite-Volume Time-Domain (FVTD) Methods in Solving Maxwell's Equations," *IEEE Trans.Antennas Propagat.*, vol.AP-45, no.3, pp.302-307, Mar 1997.

[2-10] F.B.Hilderbrand, *Advanced Calculus for Applications*, Prentice-Hall, Englewood Cliffs, NJ, 1962.

[2-11] E.Kreyzig, *Advanced Engineering Mathematics*, 6th Ed.,Wiley, New York, 1988.

[2-12] P.M.Morse and H.Fesbach, *Methods of Theoretical Physics*, part I - II, McGraw-Hill, New York, 1953.

[2-13] M.Abramowitz and I.A.Stegun (eds.), *Handbook of Mathematical Functions with Formulas, Graphs and Mathematical Tables*, Dover Publications, New York, 1970.

[2-14] M.R.Spiegel, *Mathematical Handbook of Formulas and Tables*, Schaum's Outline Series, Singapore, 1990.

[2-15] S.A.Schelkunoff, *Electromagnetic Waves*, Van Nostrand, Princeton, NJ, 1943.

Chapter 3

Electromagnetic Field Expression of the Spherical Geometry in Source-Free Region

As the materials of the preceding chapters, the solutions of the wave equation in the spherical coordinate system are obtained and used as the scalar eigenfunction. The vector potentials are derived from that eigenfunction and the electromagnetic fields can be determined, subsequently. The general expressions of the electric and magnetic field in the spherical coordinate are also presented in the previous chapters. For the particular geometry, the solution is chosen and by applying the boundary condition which is satisfied the configuration problem, the unknown coefficients can be determined and the complete solution of that particular geometry is obtained. In this chapter the problem under consideration is comprised of the conducting spherical cavity, the concentric conducting spherical cavity enclosed by the conducting conical surface and the conducting spherical segment.

3.1 A Conducting Spherical Cavity

Let us consider the conducting whole sphere of the radius R_a located at the origin of the spherical coordinate system (R, θ, ϕ) which is depicted in fig.1.

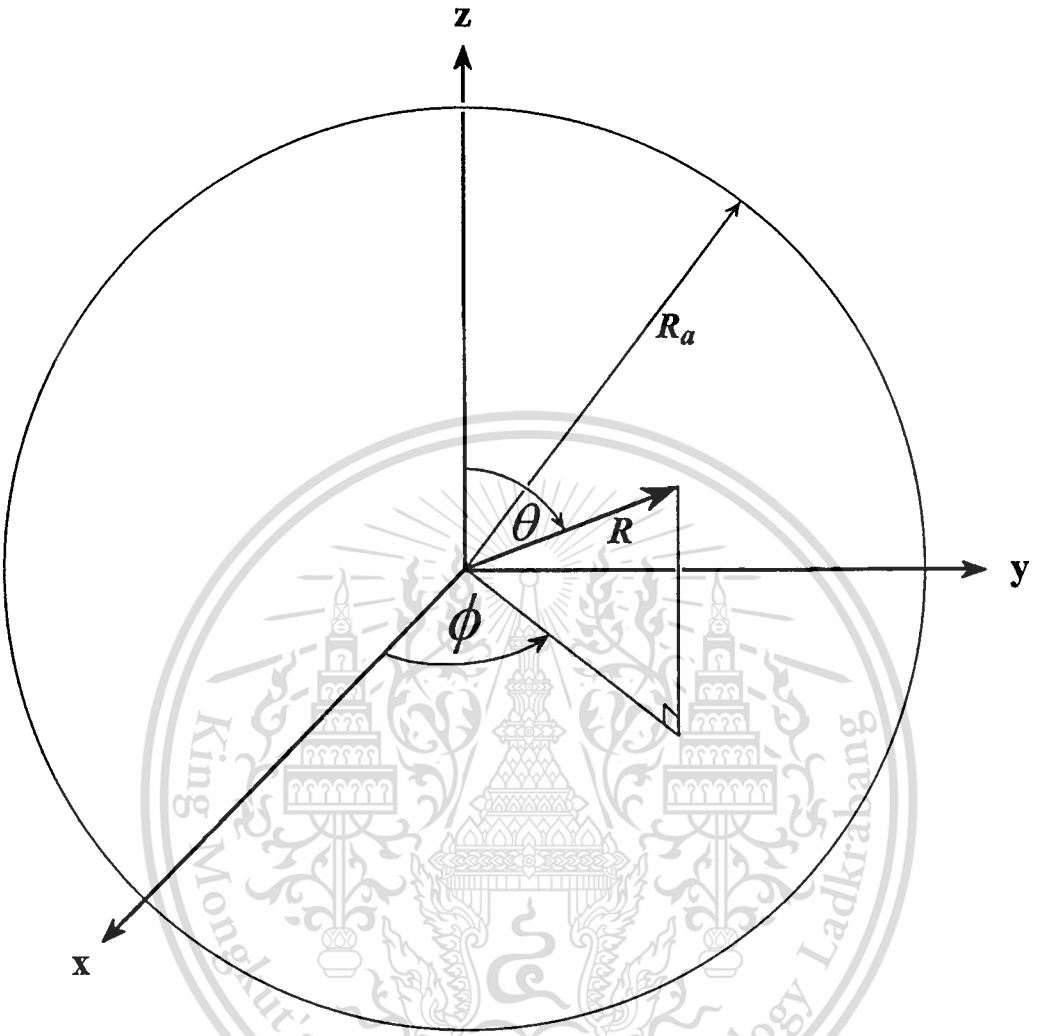

Fig.1 A Conducting Spherical Cavity

The linear, homogeneous, lossless and isotropic medium are assumed. The boundary of the problem is at $R=R_a$, $0\leq\theta\leq\pi$, $0\leq\phi\leq2\pi$. The general expression of the solution of the vector potential in the spherical coordinate system is

$$\left.\begin{matrix} A_R \\ F_R \end{matrix}\right\}(R,\theta,\phi) = [A_1\hat{J}_n(kR)+B_1\hat{Y}_n(kR)][C_1P_n^m(cos\theta)+D_1Q_n^m(cos\theta)] \times [E_1 cos\, m\phi + F_1 sin\, m\phi\,]. \tag{3.1}$$

By using the restriction that the field must be finite at anywhere i.e., at $R=0$ thus $B_1=0$ due to the singularity property of the second kind spherical Bessel function. In the similar way, in θ - direction, the second kind associated Legendre function possesses the singularity at $\theta=0$ and $\theta=\pi$ radians, therefore $D_1=0$. The solution after considerating the restriction of the field in case of the transverse electric and transverse magnetic mode, respectively can be reduced to

$$Z_R(R,\theta,\phi) = A_{mn}^{(\prime)}\hat{J}_n(kR)P_n^m(cos\theta)\left\{\begin{matrix} cos \\ sin \end{matrix}\right. m\phi\,, \tag{3.2}$$

where Z_R is either A_R or F_R depend on the transverse mode of the field, A_{mn} and A'_{mn} are the normalized TE and TM mode coefficients, respectively and $\left\{\begin{matrix} cos \\ sin \end{matrix}\right. m\phi$ denotes the linear combination of the cosine and the sine functions. By substituting the vector potentials in (2.19) and (2.22) for TE and TM mode, respectively, the three components of the electric and magnetic fields in the spherical coordinate system for the case of the transverse electric mode can be written as [3-1]-[3-3]

$$E_R = 0 \tag{3.3a}$$

$$E_\theta = \pm\frac{m}{\varepsilon}\frac{1}{Rsin\theta}A_{mn}\hat{J}_n(kR)P_n^m(cos\theta)\left\{\begin{matrix} sin \\ cos \end{matrix}\right. m\phi \tag{3.3b}$$

$$E_\phi = \frac{1}{\varepsilon}\frac{1}{R} A_{mn} \hat{J}_n(kR) \frac{dP_n^m(\cos\theta)}{d\theta} \begin{Bmatrix} \cos \\ \sin \end{Bmatrix} m\phi \quad (3.3c)$$

$$H_R = -\frac{n(n+1)}{j\omega\mu\varepsilon} A_{mn} \hat{J}_n(kR) P_n^m(\cos\theta) \begin{Bmatrix} \cos \\ \sin \end{Bmatrix} m\phi \quad (3.3d)$$

$$H_\theta = \frac{1}{j\omega\mu\varepsilon}\frac{1}{R} A_{mn} \frac{d\hat{J}_n(kR)}{dR} \frac{dP_n^m(\cos\theta)}{d\theta} \begin{Bmatrix} \cos \\ \sin \end{Bmatrix} m\phi \quad (3.3e)$$

$$H_\phi = \pm\frac{m}{j\omega\mu\varepsilon}\frac{1}{R\sin\theta} A_{mn} \frac{d\hat{J}_n(kR)}{dR} P_n^m(\cos\theta) \begin{Bmatrix} \sin \\ \cos \end{Bmatrix} m\phi \quad (3.3f)$$

and for the transverse magnetic mode

$$E_R = -\frac{n(n+1)}{j\omega\mu\varepsilon} A'_{mn} \hat{J}_n(kR) P_n^m(\cos\theta) \begin{Bmatrix} \cos \\ \sin \end{Bmatrix} m\phi \quad (3.4a)$$

$$E_\theta = \frac{1}{j\omega\mu\varepsilon}\frac{1}{R} A'_{mn} \frac{d\hat{J}_n(kR)}{dR} \frac{dP_n^m(\cos\theta)}{d\theta} \begin{Bmatrix} \cos \\ \sin \end{Bmatrix} m\phi \quad (3.4b)$$

$$E_\phi = \pm\frac{m}{j\omega\mu\varepsilon}\frac{1}{R\sin\theta} A'_{mn} \frac{d\hat{J}_n(kR)}{dR} P_n^m(\cos\theta) \begin{Bmatrix} \sin \\ \cos \end{Bmatrix} m\phi \quad (3.4c)$$

$$H_R = 0 \quad (3.4d)$$

$$H_\theta = \pm\frac{m}{\varepsilon}\frac{1}{R\sin\theta} A'_{mn} \hat{J}_n(kR) P_n^m(\cos\theta) \begin{Bmatrix} \sin \\ \cos \end{Bmatrix} m\phi \quad (3.4e)$$

$$H_\phi = \frac{1}{\varepsilon}\frac{1}{R}A'_{mn}\hat{J}_n(kR)\frac{dP_n^m(\cos\theta)}{d\theta}\begin{Bmatrix}\cos\\ \sin\end{Bmatrix} m\phi . \qquad (3.4f)$$

From the configuration of the problem, by using the boundary condition that the tangential electric field at the boundary must be vanished. For TE mode

at $R=R_a$, $E_\theta(R=R_a, 0\le\theta\le\pi, 0\le\phi\le 2\pi) = 0$

$$\pm\frac{m}{\varepsilon}\frac{1}{R_a\sin\theta}A_{mn}\hat{J}_n(kR_a)P_n^m(\cos\theta)\begin{Bmatrix}\sin\\ \cos\end{Bmatrix} m\phi = 0 \qquad (3.5)$$

and $E_\phi(R=R_a, 0\le\theta\le\pi, 0\le\phi\le 2\pi) = 0$

$$\frac{1}{\varepsilon}\frac{1}{R_a}A_{mn}\hat{J}_n(kR_a)\frac{dP_n^m(\cos\theta)}{d\theta}\begin{Bmatrix}\cos\\ \sin\end{Bmatrix} m\phi = 0, \qquad (3.6)$$

these equations lead to the characteristic equation

$$\hat{J}_n(kR_a) = 0. \qquad (3.7)$$

However, for the case of the TM mode

at $R=R_a$, $E_\theta(R=R_a, 0\le\theta\le\pi, 0\le\phi\le 2\pi) = 0$

$$\frac{1}{j\omega\mu\varepsilon}\frac{1}{R_a}A'_{mn}\frac{d\hat{J}_n(kR_a)}{dR}\frac{dP_n^m(\cos\theta)}{d\theta}\begin{Bmatrix}\cos\\ \sin\end{Bmatrix} m\phi = 0 \qquad (3.8)$$

and $E_\phi(R=R_a, 0\le\theta\le\pi, 0\le\phi\le 2\pi) = 0$

$$\pm\frac{m}{j\omega\mu\varepsilon}\frac{1}{R_a sin\theta}A'_{mn}\frac{d\hat{J}_n(kR_a)}{dR}P_n^m(cos\theta)\begin{Bmatrix}sin\\cos\end{Bmatrix}m\phi = 0. \quad (3.9)$$

In the same manner as the TE mode, the characteristic equation becomes

$$\frac{d\hat{J}_n(kR_a)}{dR} = 0. \quad (3.10)$$

The complete expression of electromagnetic fields inside the conducting spherical cavity is derived by using these characteristic equations. The numerical results of the field aspects are illustrated in the suceeding chapter, chapter 5.

3.2 A Concentric Conducting Spherical Cavity Enclosed by the Conducting Conical Surface

The geometry of the problem is the conducting sphere of the inner and outer spherical radii of R_a and R_b, respectively. This structure is enclosed by the conducting conical surface at an angle θ_c as illustrated in fig.2.

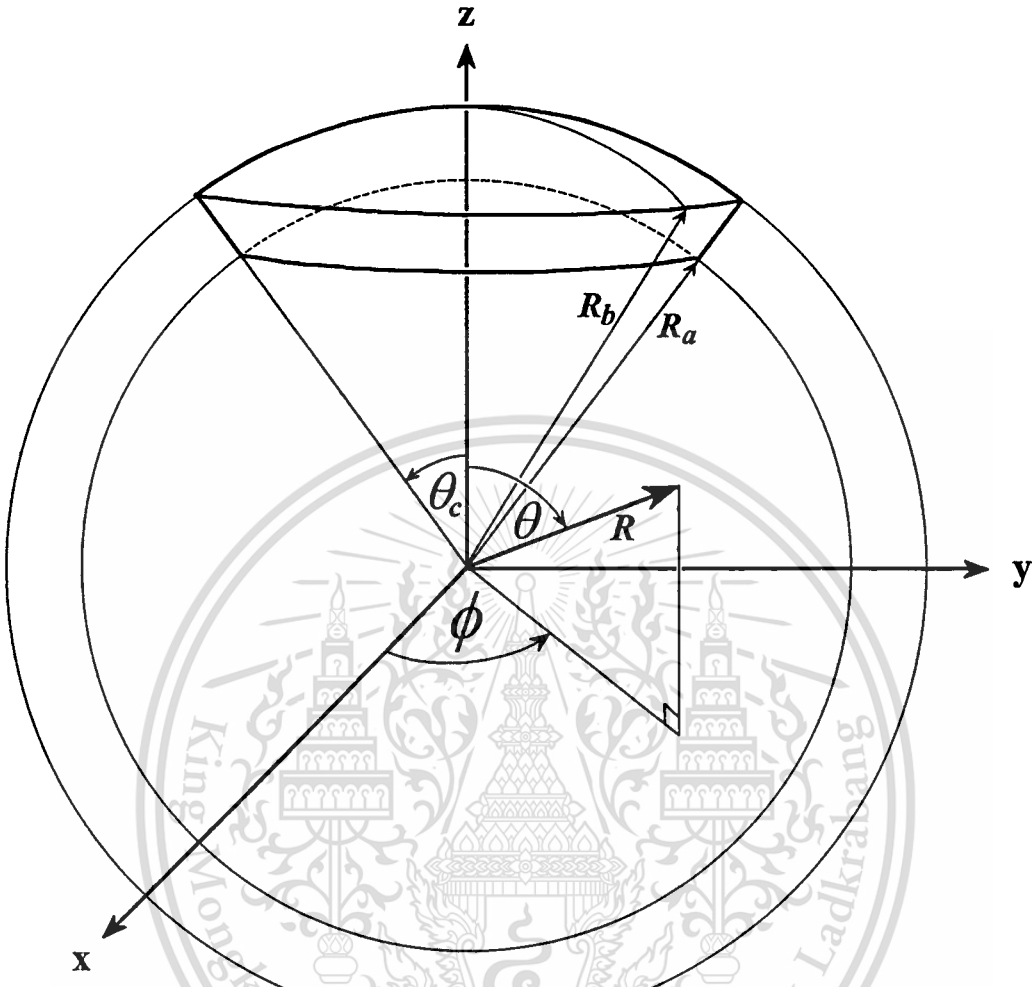

Fig.2 A Concentric Conducting Spherical Cavity

Again, the general expression of the vector is considered as

$$\begin{Bmatrix} A_R \\ F_R \end{Bmatrix}(R,\theta,\phi) = [A_1\hat{J}_n(kR)+B_1\hat{Y}_n(kR)][C_1P_n^m(\cos\theta)+D_1Q_n^m(\cos\theta)] \times [E_1\cos m\phi + F_1\sin m\phi]. \quad (3.11)$$

From the configuration under consideration, the solution of the vector potential in the radial direction includes the spherical Bessel function of the second kind which is different from the case of the conducting spherical cavity. However, the singularities occur in the θ - direction which is the same as the conducting spherical cavity because of the field must be finite at $\theta=0$ radian. The vector potential in this case can be written as

$$Z_R(R,\theta,\phi) = [B'_{mn}\hat{J}_n(kR)+C'_{mn}\hat{Y}_n(kR)]P_n^m(\cos\theta)\begin{Bmatrix}\cos\\ \sin\end{Bmatrix}m\phi, \quad (3.12)$$

where the unprimed and the primed coefficients stand for TE and TM mode, respectively.

The general expression of the electromagnetic field can be found by using the vector potential and in case of the transverse electric mode, that electromagnetic field can be written as [3-1]-[3-3]

$$E_R = 0 \quad (3.13a)$$

$$E_\theta = \pm\frac{m}{\varepsilon}\frac{1}{R\sin\theta}\hat{B}_n(kR)P_n^m(\cos\theta)\begin{Bmatrix}\sin\\ \cos\end{Bmatrix}m\phi \quad (3.13a)$$

$$E_\phi = \frac{1}{\varepsilon}\frac{1}{R}\hat{B}_n(kR)\frac{dP_n^m(\cos\theta)}{d\theta}\begin{Bmatrix}\cos\\ \sin\end{Bmatrix}m\phi \quad (3.13c)$$

$$H_R = -\frac{n(n+1)}{j\omega\mu\varepsilon}\hat{B}_n(kR)P_n^m(\cos\theta)\begin{Bmatrix}\cos\\ \sin\end{Bmatrix}m\phi \quad (3.13d)$$

$$H_\theta = \frac{1}{j\omega\mu\varepsilon}\frac{1}{R}\frac{d\hat{B}_n(kR)}{dR}\frac{dP_n^m(\cos\theta)}{d\theta}\begin{Bmatrix}\cos\\ \sin\end{Bmatrix} m\phi \qquad (3.13e)$$

$$H_\phi = \pm\frac{m}{j\omega\mu\varepsilon}\frac{1}{R\sin\theta}\frac{d\hat{B}_n(kR)}{dR}P_n^m(\cos\theta)\begin{Bmatrix}\sin\\ \cos\end{Bmatrix} m\phi \qquad (3.13f)$$

and for the transverse magnetic mode

$$E_R = -\frac{n(n+1)}{j\omega\mu\varepsilon}\hat{B}_n(kR)P_n^m(\cos\theta)\begin{Bmatrix}\cos\\ \sin\end{Bmatrix} m\phi \qquad (3.14a)$$

$$E_\theta = \frac{1}{j\omega\mu\varepsilon}\frac{1}{R}\frac{d\hat{B}_n(kR)}{dR}\frac{dP_n^m(\cos\theta)}{d\theta}\begin{Bmatrix}\cos\\ \sin\end{Bmatrix} m\phi \qquad (3.14b)$$

$$E_\phi = -\frac{m}{j\omega\mu\varepsilon}\frac{1}{R\sin\theta}\frac{d\hat{B}_n(kR)}{dR}P_n^m(\cos\theta)\begin{Bmatrix}\sin\\ \cos\end{Bmatrix} m\phi \qquad (3.14c)$$

$$H_R = 0 \qquad (3.14d)$$

$$H_\theta = \pm\frac{m}{\varepsilon}\frac{1}{R\sin\theta}\hat{B}_n(kR)P_n^m(\cos\theta)\begin{Bmatrix}\sin\\ \cos\end{Bmatrix} m\phi \qquad (3.14e)$$

$$H_\phi = \frac{1}{\varepsilon}\frac{1}{R}\hat{B}_n(kR)\frac{dP_n^m(\cos\theta)}{d\theta}\begin{Bmatrix}\cos\\ \sin\end{Bmatrix} m\phi, \qquad (3.14f)$$

where $\hat{B}_n(kR)$ denotes the linear combination of the Schelkunoff spherical Bessel function of the first and second kinds.

$$\hat{B}_n(kR) = B_{mn}^{(\prime)}\hat{J}_n(kR) + C_{mn}^{(\prime)}\hat{Y}_n(kR) \tag{3.15}$$

The particular solution in case of the concentric conducting spherical cavity enclosed by the conducting conical surface can be obtained by applying the boundary condition and solving for the unknown coefficients. From the boundary condition that the tangential electric field at the boundary is vanished.

for TE mode,

at $R=R_a$, $E_\theta(\ R=R_a,\ 0\le\theta\le\theta_c,\ 0\le\phi\le 2\pi) = 0$

$$\pm\frac{m}{\varepsilon}\frac{1}{R_a \sin\theta}\hat{B}_n(kR_a)P_n^m(\cos\theta)\begin{Bmatrix}\sin\\ \cos\end{Bmatrix} m\phi = 0 \tag{3.16}$$

and $E_\phi(\ R=R_a,\ 0\le\theta\le\theta_c,\ 0\le\phi\le 2\pi) = 0$

$$\frac{1}{\varepsilon}\frac{1}{R_a}\hat{B}_n(kR_a)\frac{dP_n^m(\cos\theta)}{d\theta}\begin{Bmatrix}\cos\\ \sin\end{Bmatrix} m\phi = 0 \tag{3.17}$$

one obtain

$$\hat{B}_n(kR_a) = 0 \tag{3.18}$$

and at $R=R_b$, $E_\theta(\ R=R_b,\ 0\le\theta\le\theta_c,\ 0\le\phi\le 2\pi) = 0$

$$\pm\frac{m}{\varepsilon}\frac{1}{R_b \sin\theta}\hat{B}_n(kR_b)P_n^m(\cos\theta)\begin{Bmatrix}\sin\\ \cos\end{Bmatrix} m\phi = 0 \tag{3.19}$$

and $E_\phi(\ R=R_b,\ 0\le\theta\le\theta_c,\ 0\le\phi\le 2\pi) = 0$

$$\frac{1}{\varepsilon}\frac{1}{R_b}\hat{B}_n(kR_b)\frac{dP_n^m(\cos\theta)}{d\theta}\begin{Bmatrix}\cos\\ \sin\end{Bmatrix} m\phi \;=\; 0, \qquad (3.20)$$

one obtains

$$\hat{B}_n(kR_b) \;=\; 0. \qquad (3.21)$$

From (3.18) and (3.21), the simultaneous equation which corresponds to the two characteristic equations:

$$B_{mn}\hat{J}_n(kR_a) + C_{mn}\hat{Y}_n(kR_a) \;=\; 0 \qquad (3.22a)$$

$$B_{mn}\hat{J}_n(kR_b) + C_{mn}\hat{Y}_n(kR_b) \;=\; 0, \qquad (3.22b)$$

which may be written in a matrix form

$$\begin{bmatrix}\hat{J}_n(kR_a) & \hat{Y}_n(kR_a)\\ \hat{J}_n(kR_b) & \hat{Y}_n(kR_b)\end{bmatrix}\begin{bmatrix}B_{mn}\\ C_{mn}\end{bmatrix} = \begin{bmatrix}0\\ 0\end{bmatrix}. \qquad (3.23)$$

The non-trivial solution of the linear equation system is

$$\hat{J}_n(kR_a)\hat{Y}_n(kR_b) - \hat{J}_n(kR_b)\hat{Y}_n(kR_a) \;=\; 0 \qquad (3.24)$$

or

$$\frac{\hat{J}_n(kR_a)}{\hat{Y}_n(kR_a)} = \frac{\hat{J}_n(kR_b)}{\hat{Y}_n(kR_b)}. \tag{3.25}$$

By substituting this (3.25) in (3.22a) or (3.22b), it is found that

$$-\frac{C_{mn}}{B_{mn}} = \frac{\hat{J}_n(kR_a)}{\hat{Y}_n(kR_a)} = \frac{\hat{J}_n(kR_b)}{\hat{Y}_n(kR_b)}. \tag{3.26}$$

This characteristic equation gives the solution

$$kR_a = x_{\zeta,\alpha} \tag{3.27}$$

and

$$kR_b = x_{\zeta,\beta} \tag{3.28}$$

such that

$$k(R_a - R_b) = x_{\zeta,\gamma}, \tag{3.29}$$

where x denotes the roots of zero of Bessel function ratio, α and β are the upper and the lower roots, respectively, γ is the interval between α and β which equals to α-β corresponds to the order of the root interval.

Additionally, for the case of the TM mode,

at $R=R_a$, $E_\theta(R=R_a, 0\le\theta\le\theta_c, 0\le\phi\le 2\pi) = 0$

$$\frac{1}{j\omega\mu\varepsilon}\frac{1}{R_a}\frac{d\hat{B}_n(kR_a)}{dR}\frac{dP_n^m(\cos\theta)}{d\theta}\begin{Bmatrix}\cos\\ \sin\end{Bmatrix} m\phi = 0 \qquad (3.30)$$

and $E_\phi(R=R_a,\ 0\le\theta\le\theta_c,\ 0\le\phi\le 2\pi) = 0$

$$\pm\frac{m}{j\omega\mu\varepsilon}\frac{1}{R_a\sin\theta}\frac{d\hat{B}_n(kR_a)}{dR}P_n^m(\cos\theta)\begin{Bmatrix}\sin\\ \cos\end{Bmatrix} m\phi = 0, \qquad (3.31)$$

one obtains

$$\frac{d\hat{B}_n(kR_a)}{dR} = 0 \qquad (3.32)$$

and at $R=R_b$, $E_\theta(R=R_b,\ 0\le\theta\le\theta_c,\ 0\le\phi\le 2\pi) = 0$

$$\frac{1}{j\omega\mu\varepsilon}\frac{1}{R_b}\frac{d\hat{B}_n(kR_b)}{dR}\frac{dP_n^m(\cos\theta)}{d\theta}\begin{Bmatrix}\cos\\ \sin\end{Bmatrix} m\phi = 0 \qquad (3.33)$$

and $E_\phi(R=R_b,\ 0\le\theta\le\theta_c,\ 0\le\phi\le 2\pi) = 0$

$$\pm\frac{m}{j\omega\mu\varepsilon}\frac{1}{R_b\sin\theta}\frac{d\hat{B}_n(kR_b)}{dR}P_n^m(\cos\theta)\begin{Bmatrix}\sin\\ \cos\end{Bmatrix} m\phi = 0, \qquad (3.34)$$

one obtains

$$\frac{d\hat{B}_n(kR_b)}{dR} = 0. \qquad (3.35)$$

From (3.32) and (3.35), the simultaneous equation which corresponds to the two characteristic equations are

$$B'_{mn}\frac{d\hat{J}_n(kR_a)}{dR} + C'_{mn}\frac{d\hat{Y}_n(kR_a)}{dR} = 0 \tag{3.36a}$$

$$B'_{mn}\frac{d\hat{J}_n(kR_b)}{dR} + C'_{mn}\frac{d\hat{Y}_n(kR_b)}{dR} = 0 \tag{3.36a}$$

or

$$\begin{bmatrix} \frac{d\hat{J}_n(kR_a)}{dR} & \frac{d\hat{Y}_n(kR_a)}{dR} \\ \frac{d\hat{J}_n(kR_b)}{dR} & \frac{d\hat{Y}_n(kR_b)}{dR} \end{bmatrix} \begin{bmatrix} B'_{mn} \\ C'_{mn} \end{bmatrix} = \begin{bmatrix} 0 \\ 0 \end{bmatrix} \tag{3.37}$$

The non-trivial solution of the linear equation system is

$$\frac{d\hat{J}_n(kR_a)}{dR}\frac{d\hat{Y}_n(kR_b)}{dR} - \frac{d\hat{J}_n(kR_b)}{dR}\frac{d\hat{Y}_n(kR_a)}{dR} = 0 \tag{3.38}$$

or

$$\frac{\frac{d\hat{J}_n(kR_a)}{dR}}{\frac{d\hat{Y}_n(kR_a)}{dR}} = \frac{\frac{d\hat{J}_n(kR_b)}{dR}}{\frac{d\hat{Y}_n(kR_b)}{dR}} \tag{3.39}$$

By substituting (3.39) in (3.36a) or (3.36b), it is found that

$$-\frac{C'_{mn}}{B'_{mn}} = \frac{\dfrac{d\hat{J}_n(kR_a)}{dR}}{\dfrac{d\hat{Y}_n(kR_a)}{dR}} = \frac{\dfrac{d\hat{J}_n(kR_b)}{dR}}{\dfrac{d\hat{Y}_n(kR_b)}{dR}}. \tag{3.40}$$

This characteristic equation gives the solution

$$kR_a = x'_{\zeta,\alpha} \tag{3.41}$$

and

$$kR_b = x'_{\zeta,\beta} \tag{3.42}$$

such that

$$k(R_a - R_b) = x'_{\zeta,\gamma}, \tag{3.43}$$

where x' denotes the roots of zero of derivative of Bessel function ratio and α, β, γ are the same as declared before.

Additionally, since the concentric conducting sphere is enclosed by the part of the conducting conical surface at θ_c so the boundary condition should be applied. For TE mode

at $\theta=\theta_c$, $E_\phi(R_a \le R \le R_b,\ \theta=\theta_c,\ 0 \le \phi \le 2\pi) = 0$

$$\frac{1}{\varepsilon}\frac{1}{R}\hat{B}_n(kR)\frac{dP_n^m(\cos\theta)}{d\theta}\bigg|_{\theta=\theta_c} \begin{Bmatrix}\cos\\ \sin\end{Bmatrix} m\phi = 0, \tag{3.44}$$

the characteristic equation which corresponds to the above equations

$$\left.\frac{dP_n^m(\cos\theta)}{d\theta}\right|_{\theta=\theta_c} = 0. \tag{3.45}$$

For TM mode

at $\theta=\theta_c$, $E_\phi(R_a \le R \le R_b, \theta=\theta_c, 0 \le \phi \le 2\pi) = 0$

$$\pm\frac{m}{j\omega\mu\varepsilon}\frac{1}{R\sin\theta_c}\frac{d\hat{B}_n(kR)}{dR}P_n^m(\cos\theta)\Big|_{\theta=\theta_c}\begin{Bmatrix}\sin\\ \cos\end{Bmatrix} m\phi = 0, \tag{3.46}$$

the characteristic equation is

$$P_n^m(\cos\theta)\Big|_{\theta=\theta_c} = 0. \tag{3.47}$$

It can be seen that after the boundary condition is applied, the unknown coefficient is determined and the complete expression of the electromagnetic field in such configuration of the problem is obtained, subsequently.

3.3 A Conducting Spherical Segment

A segmented in the azimuthal plane of the concentric conducting spherical cavity enclosed by the conducting conical surface will be considered in this section. The configuration of the problem is shown in fig.3.

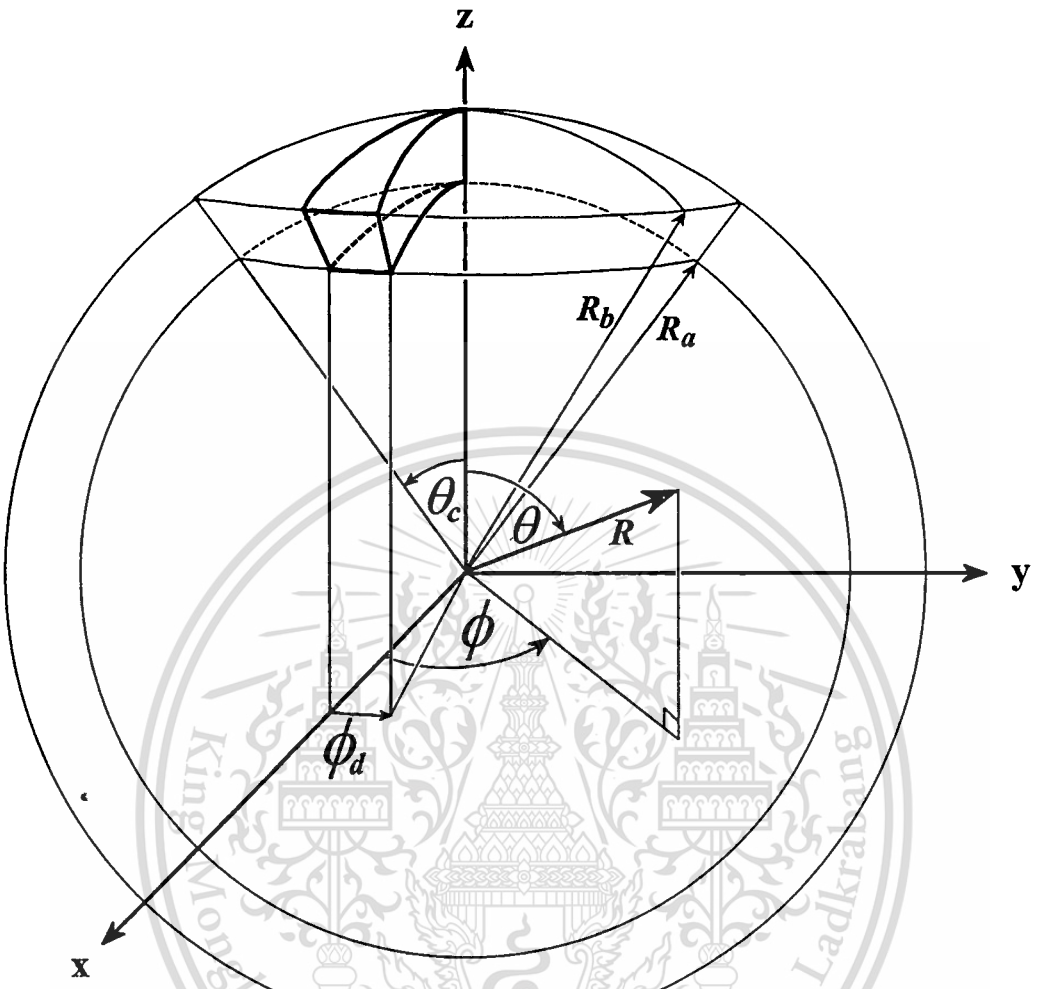

Fig.3 A Conducting Spherical Segment

Again, let us consider the concentric conducting spherical cavity of the inner and the outer spherical radii R_a and R_b, respectively. This structure is circumferential shorted between that radii at an angle θ_c and the azimuthal plane is bounded by two conducting axial half-planes at $\phi=0$ and $\phi=\phi_d$. The general expression of the vector potential under consideration is

$$\left.\begin{matrix} A_R \\ F_R \end{matrix}\right\}(R,\theta,\phi) = [A_1\hat{J}_n(kR)+B_1\hat{Y}_n(kR)][C_1P_n^m(\cos\theta)+D_1Q_n^m(\cos\theta)] \times [E_1\cos m\phi + F_1\sin m\phi\,]. \tag{3.48}$$

The general expression and the boundary condition in case of the spherical segment is identical to the concentric conducting spherical cavity but included the boundary condition in the azimuthal plane direction. The boundary condition for TE mode

at $\phi=0$, $E_\theta(R_a \le R \le R_b,\ 0\le\theta\le\theta_c,\ \phi=0) = 0$

$$-\frac{m}{\varepsilon}\frac{1}{R\sin\theta}\hat{B}_n(kR)P_n^m(\cos\theta)[-D_{mn}\sin m(0)+E_{mn}\cos m(0)] = 0 \tag{3.49}$$

$$\therefore E_{mn} = 0 \tag{3.50}$$

at $\phi=\phi_d$, $E_\theta(R_a \le R \le R_b,\ 0\le\theta\le\theta_c,\ \phi=\phi_d) = 0$

$$-\frac{m}{\varepsilon}\frac{1}{R\sin\theta}\hat{B}_n(kR)P_n^m(\cos\theta)[-D_{mn}\sin m\phi_d\,] = 0 \tag{3.51}$$

$$\sin m\phi_d = 0 \tag{3.52}$$

$$m = \frac{p\pi}{\phi_d}\ ;p = 0,1,2,... \tag{3.53}$$

For TM mode,

at $\phi=0$, $E_\theta(R_a \le R \le R_b,\ 0 \le \theta \le \theta_c,\ \phi=0) = 0$

$$\frac{1}{j\omega\mu\varepsilon}\frac{1}{R}\frac{d\hat{B}_n(kR)}{dR}\frac{dP_n^m(\cos\theta)}{d\theta}[D_{mn}\cos m(0) + E_{mn}\sin m(0)] = 0 \quad (3.54)$$

$$\therefore\ D_{mn} = 0 \quad (3.55)$$

at $\phi=\phi_d$, $E_\theta(R_a \le R \le R_b,\ 0 \le \theta \le \theta_c,\ \phi=\phi_d) = 0$

$$\frac{1}{j\omega\mu\varepsilon}\frac{1}{R}\frac{d\hat{B}_n(kR)}{dR}\frac{dP_n^m(\cos\theta)}{d\theta}[E_{mn}\sin m\phi_d] = 0 \quad (3.56)$$

$$\sin m\phi_d = 0 \quad (3.57)$$

$$m = \frac{q\pi}{\phi_d};\ q = 1,2,3\ldots \quad (3.58)$$

From these characteristic equations the electromagnetic field inside the conducting spherical segment for TE and TM modes can be obtained .

3.4 Conclusions

Electromagnetic fields in the source-free region of the spherical geometry such as the spherical cavity and segment are derived by using the vector potential as dictated in the previous chapter. The general

solutions of the vector potential after the restriction of the singularities are considered will be substituted to determine the electromagnetic field. The unknown coefficients can be found by enforcing the boundary condition that the tangential electric field at the boundary equal to zero. These particular solutions in each case can be applied to solve for the electromagnetic field of the source region which will be presented in the next chapter. The numerical results of the electromagnetic field inside the conducting spherical cavity is demonstrates to verify the derivation in the suceeding chapter, chapter5.

References

[3-1] J.A.Stratton, *Electromagnetic Theory*, McGraw-Hill, New York, 1941.

[3-2] R.F.Harrington, *Time-Harmonic Electromagnetic Fields*, McGraw-Hill, New York, 1961.

[3-3] C.A.Balanis, *Advanced Engineering Electromagnetics*, Wiley, New York, 1989.

Chapter 4

Dyadic Green's Functions of the Concentric Conducting Spherical Cavity and Segment

Green's function was first known in 1828 by George Green* [4-1] with his essay entitled "On the application of mathematical analysis to the theories of electricity and magnetism" in which he developed a method for obtaining solutions of Poisson's equation in potential theory. This method uses of a potential function that is the potential from a point or line source of unit strength.

The Green's function is the mathematical technique which is applied as a driving function of a unit source (unit impulse function or Dirac delta function) to determine the solution of the partial differential equation. The solution of the actual driving function can be obtained by superposition of the Green's function and the driving function. Following this reason, the Green's function is well-known as an impulse response or the transfer function in system or circuit theory [4-3].

---

*George Green '1793-1841, a self-educated English mathematician who started out as a baker and his dead was fellow of Caius College, Cambridge. His work concerned with potential theory in connection with electricity and magnetism, vibrations, waves and elasticity theory. It remained almost unknown, even in England, until after his death [4-2].

Dyadic Green's function is a very useful tool [4-4]-[4-9] for obtaining the electromagnetic field in the arbitrary source region such as free space and the bounded configurations [4-4]. This chapter summarizes the meaning and the concept of the various kinds of the dyadic Green's function and its application to the electromagnetic problems such as the dyadic Green's function of concentric conducting spherical cavity and segment.

4.1 Dyadic Analysis

Some essential formulas in dyadic analysis will be formulated in this section. In class, a vector function is represented as the expression $\overline{F}$ that [4-4]

$$\overline{F} = \sum_{i=1}^{3} F_i \hat{a}_i, \tag{4.1}$$

where $F_i(i=1,2,3)$ is defined as the three scalar components of $\overline{F}$ and $\hat{a}_i$ are the three unit vectors directed along the i direction.

For the dyadic function or a dyadic $\overline{\overline{F}}$, it is defined as

$$\overline{\overline{F}} = \sum_{j=1}^{3}\sum_{i=1}^{3} F_{ij} \hat{a}_i \hat{a}_j, \tag{4.2}$$

where F_{ij} $(i=1,2,3;j=1,2,3)$ denotes the nine scalar components of $\overline{\overline{F}}$ and $\hat{a}_i \hat{a}_j$ is the nine unit dyadics or dyads. It is noted that the anterior and the posterior position of the unit dyadics can not be commutatived.

The transpose of the dyadic function $(\overline{\overline{F}})^t$ is defined by

$$(\overline{\overline{F}})^t = \sum_{i=1}^{3}\sum_{j=1}^{3} F_{ij}\hat{a}_j\hat{a}_i. \tag{4.3}$$

It is obvious that the transpose operation in dyadic analysis is identical to the aspect of the matrix analysis, that is the members in rows and columns are interchanged. A symmetrical dyadic $\overline{\overline{F}}_s$ is the dyadic that the upper and lower triangular elements are identical. The characteristic of the symmetrical matrix is

$$\overline{\overline{F}}_s = (\overline{\overline{F}})^t. \tag{4.4}$$

An antisymmetical dyadic $\overline{\overline{F}}_a$ is the dyadic that the upper and the lower triangular elements are the same value but the opposite signs, therefore the diagonal elements vanished, and can be characterized by

$$(\overline{\overline{F}}_a)^t = -\overline{\overline{F}}_a. \tag{4.5}$$

Idem factor or the unit dyadic, denoted by $\overline{\overline{I}}$ is the identity dyadic which is the same as the identity matrix [4-5].

$$\overline{\overline{I}} = \sum_{i=1}^{3} \hat{a}_i\hat{a}_i\,. \tag{4.6}$$

In terms of the scalar components, the idem factor can be written as

$$F_{ij} = \delta_{ij}, \tag{4.7}$$

where δ_{ij} denotes the Kronecker delta function and equal unity if i equals j and vanishes at elsewhere.

The product of the vector and the dyadic can be classified into two forms by means of the position of the vector multiplier. They are the anterior and the posterior scalar products. The anterior scalar product $\overline{f} \cdot \overline{\overline{F}}$, is defined by

$$\overline{f} \cdot \overline{\overline{F}} = \sum_{i=1}^{3} \sum_{j=1}^{3} f_i F_{ij} \hat{a}_j . \tag{4.8}$$

and the posterior scalar products $\overline{\overline{F}} \cdot \overline{f}$, is defined by

$$\overline{\overline{F}} \cdot \overline{f} = \sum_{i=1}^{3} \sum_{j=1}^{3} f_j F_{ij} \hat{a}_i . \tag{4.9}$$

In case of the vector product of the vector and the dyadic, it is the same as the scalar product. The anterior vector product is defined by

$$\overline{f} \times \overline{\overline{F}} = \sum_{j=1}^{3} (\overline{f} \times \sum_{i=1}^{3} F_{ij} \hat{a}_i) \hat{a}_j \tag{4.10}$$

and the posterior vector product is defined by

$$\overline{\overline{F}} \times \overline{f} = \sum_{j=1}^{3} \left(\sum_{i=1}^{3} F_{ij} \hat{a}_i \right) (\hat{a}_j \times \overline{f}). \tag{4.11}$$

The result of the scalar product is vector whereas the vector product is dyadic.

4.2 Maxwell's equations and Wave Equation in Dyadic Form

As mentioned in Chapter 2, it is known that the Maxwell's equations are not appropriate to be solved analytically. The wave equation is derived to achieve the uncouple between the electric and magnetic fields. In that previous chapter, the electromagnetic field is obtained via the vector potential by using the boundary eigenvalue problem. However, by that way, the wave equation is simplified by assuming the medium is source-free and lossless. In case of the source region, the Maxwell's and the wave equations must be formulated in dyadic form, and then use the dyadic Green's function as the impulse response function. Integrating that dyadic Green's function and the source function throughout the source configuration domain, the electromagnetic field can be obtained.

We are now considering again, the Maxwell's equations in time harmonic $e^{-j\omega t}$ form after the constitutive relations are used, by juxtaposing the unit vector $\hat{a}_j$ at the posterior position and summing the three sets of equations with j, they can be written in dyadic form as [4-4]

$$\nabla \times \overline{\overline{E}} = j\omega\mu \overline{\overline{H}} \tag{4.12a}$$

$$\nabla \times \overline{\overline{H}} = \overline{\overline{J}}_{ic} - j\omega\varepsilon \overline{\overline{E}} \tag{4.12b}$$

$$\nabla \cdot (\varepsilon \overline{\overline{E}}) = \overline{q}_{ev} \tag{4.12c}$$

$$\nabla \cdot (\mu \overline{\overline{H}}) = 0. \tag{4.12d}$$

Next, the source term functions is considered. The Dirac delta function is used to represent the infinitesimal electric dipole. For the three dimensions, $\delta(\overline{R} - \overline{R'})$ is designated for that three infinitesimal dipoles located at the source point $\overline{R} = \overline{R'}$ as

$$\overline{J}_j = c_j \delta(\overline{R} - \overline{R'}) \hat{a}_j, \tag{4.13}$$

where c_j denotes the current moment of the dipoles.

Since the source function is the impulse function which the expression is the Dirac delta function, the electric and magnetic fields intensity become the dyadic Green's function of the electric and magnetic types, respectively. The relationships of these fields and the Green's functions are defined as follows:

$$\overline{\overline{E}} = \overline{\overline{G}}_e \tag{4.14a}$$

$$j\omega\mu \overline{\overline{H}} = \overline{\overline{G}}_m \tag{4.14b}$$

$$j\omega\mu \overline{\overline{J}} = \overline{\overline{I}} \delta(\overline{R} - \overline{R'}) \tag{4.14c}$$

$$\bar{q}_{ev} = -\frac{\varepsilon}{k^2}\nabla\delta(\bar{R}-\bar{R}') \tag{4.14d}$$

By substituting (4.14a) to (4.14d) in (4.12a) to (4.12d), the Maxwell's equations in dyadic form can be written as

$$\nabla\times\bar{\bar{G}}_e = \bar{\bar{G}}_m \tag{4.15a}$$

$$\nabla\times\bar{\bar{G}}_m = \bar{\bar{I}}\delta(\bar{R}-\bar{R}')+k^2\bar{\bar{G}}_e \tag{4.15b}$$

$$\nabla\cdot\bar{\bar{G}}_e = -\frac{1}{k^2}\nabla\delta(\bar{R}-\bar{R}') \tag{4.15c}$$

$$\nabla\cdot\bar{\bar{G}}_m = 0 \tag{4.15d}$$

We have discussed in chapter 2 that it is not convenient to solve the Maxwell's equations analytically. For this reason, the wave equations were derived. From Maxwell's equations, by the same procedure as described in chapter 2, the wave equations in dyadic form can be derived as

$$\nabla\times\nabla\times\bar{\bar{G}}_e - k^2\bar{\bar{G}}_e = \bar{\bar{I}}\delta(\bar{R}-\bar{R}') \tag{4.16a}$$

$$\nabla\times\nabla\times\bar{\bar{G}}_m - k^2\bar{\bar{G}}_m = \nabla\times[\bar{\bar{I}}\delta(\bar{R}-\bar{R}')] \tag{4.16b}$$

4.3 Various Kinds of Dyadic Green's Functions and Their Properties

Dyadic Green's functions can be classified into three categories by using the boundary condition which the problems are satisfied. Those boundary conditions are Dirichlet and Neumann boundary conditions [4-4]. The dyadic Green's function which is subjected to the Dirichlet boundary condition is called dyadic Green's function of the first kind. On the other hand, for the Neumann boundary condition, it is called dyadic Green's function of the second kind. For the region of more than one medium such as two media the dyadic Green's function involved are of the third kind. By means of the third kind dyadic Green's functions, the field functions are considered in each medium due to the source function. The electric and magnetic types dyadic Green's function of the first and second kinds are summarized in Table 1.

Table 1 Electric and magnetic types dyadic Green's function of the first and second kinds

Boundary condition→ *Source* ↓	*Dirichlet boundary condition*	*Neumann boundary condition*
Electric current source	$\nabla\times\overline{\overline{G}}_{e1} = 0$	$\nabla\times\nabla\times\overline{\overline{G}}_{m2} = 0$
Magnetic current source	$\nabla\times\overline{\overline{G}}_{m1} = 0$	$\nabla\times\nabla\times\overline{\overline{G}}_{e2} = 0$

4.4 Dyadic Green's Function of the Free Space

The dyadic Green's function of the free space is very important to obtain the electromagnetic field involving radiation in the free space. The method of the vector potential is one of the methods to determine the dyadic Green's function of the free space. From the vector potential in the previous chapter, the magnetic vector potential can be written as [4-4]

$$\overline{A}(\overline{R}) = \frac{1}{j\omega} G_o(\overline{R} - \overline{R'})\hat{a}_i \ . \tag{4.17}$$

By using (2.22) and electric field becomes electric type dyadic Green's function, one obtains

$$\overline{\overline{G}}_e(\overline{R}-\overline{R'}) = (\overline{\overline{I}} + \frac{1}{k^2}\nabla\nabla)G_o(\overline{R}-\overline{R'}) \tag{4.18}$$

where

$$G_o(\overline{R}-\overline{R'}) = \frac{e^{jk|\overline{R}-\overline{R'}|}}{4\pi|\overline{R}-\overline{R'}|} \tag{4.19}$$

represents the scalar Green's function of the free space. Magnetic type dyadic Green's function of the free space can be determined by substituting (4.18) into (4.15a) and can be written as

$$\overline{\overline{G}}_m(\overline{R}-\overline{R'}) = \nabla G_o(\overline{R}-\overline{R'})\times\overline{\overline{I}} \tag{4.20}$$

4.5 Eigenfunction Expansion and Solenoidal Vector Wave Function

From the structure of the concentric conducting spherical cavity in the spherical coordinate system (R,θ,ϕ) which is illustrated in fig.2. The cavity consists of two parts of concentric conducting spheres where the inner and outer spherical radii are R_a and R_b, respectively. This structure is enclosed by a part of a conducting cone which the conical angle is θ_c. For the conducting spherical segment, it is the concentric conducting spherical cavity as described aboved, in addition the azimuth plane is bounded by the two conducting axial half-planes at $\phi=0$ and $\phi = \phi_d$.

The eigenfunction expansion method is used for determining the electromagnetic field in the source region. A lossless homogeneous medium is considered and the time convention $e^{-j\omega t}$ is omitted. The scalar eigenfunction ($\varphi_{\substack{e\\o}m\xi}(\kappa_\zeta)$), as derived in chapter 3, which is a solution of the homogeneous Helmholtz equation [4-4]

$$\nabla^2\varphi + \kappa_\zeta{}^2\varphi = 0 \tag{4.21}$$

in the spherical coordinate system is considered in the form

$$\varphi_{\substack{e\\o}m\xi}(\kappa_\zeta) = b_\xi(\kappa_\zeta R)L_\xi^m(cos\theta)\begin{Bmatrix}cos\\sin\end{Bmatrix}m\phi\,, \tag{4.22}$$

where $b_\xi(\kappa_\zeta R)$ denotes the linear combination of the spherical Bessel function of the first kind ($j_\xi(\kappa_\zeta R)$) and second kind ($y_\xi(\kappa_\zeta R)$) of order ξ which satisfies the spherical Bessel differential equation [4-4]

$$\frac{d^2}{dx^2}[xb_\xi(x)]+[1-\frac{\xi(\xi+1)}{x^2}]xb_\xi(x) = 0, \qquad (4.23)$$

where x is $\kappa_\zeta R$, with the unknown normalized coefficient $A_\xi(\kappa_\zeta)$:

$$b_\xi(\kappa_\zeta R) = j_\xi(\kappa_\zeta R) + A_\xi(\kappa_\zeta) y_\xi(\kappa_\zeta R). \qquad (4.24)$$

κ_ζ is either κ_p or κ_q corresponds to TE and TM mode, respectively.
By applying the boundary condition that the tangential electric field in the radial direction vanishes, the unknown coefficient $A_\xi(\kappa_\zeta)$ can be determined from the characteristic equation as derived in chapter 3. For TM mode

$$A_\xi(\kappa_\zeta) = -\frac{j'_\xi(\kappa_\zeta R_a)}{y'_\xi(\kappa_\zeta R_a)} = -\frac{j'_\xi(\kappa_\zeta R_b)}{y'_\xi(\kappa_\zeta R_b)}, \qquad (4.25)$$

where the prime denotes the differentiation with respect to the argument. This characteristic equation gives the solution

$$\kappa_\zeta R_a = x'_{\zeta,\alpha} \qquad (4.26)$$

and

$$\kappa_\zeta R_b = x'_{\zeta,\beta} \tag{4.27}$$

such that

$$\kappa_\zeta (R_a - R_b) = x'_{\zeta,\gamma}, \tag{4.28}$$

where x' denotes the roots of zero of derivative of the ordinary spherical Bessel function ratio and γ is the interval between the roots α and β. The γ equals to α-β corresponds to the order of the root interval. For TE mode counterpart, the characteristic equation becomes

$$A_\xi(\kappa_\zeta) = -\frac{j_\xi(\kappa_\zeta R_a)}{y_\xi(\kappa_\zeta R_a)} = -\frac{j_\xi(\kappa_\zeta R_b)}{y_\xi(\kappa_\zeta R_b)}. \tag{4.29}$$

The solution of the above equation are

$$\kappa_\zeta R_a = x_{\zeta,\alpha} \tag{4.30}$$

and

$$\kappa_\zeta R_b = x_{\zeta,\beta} \tag{4.31}$$

such that

$$\kappa_\zeta (R_a - R_b) = x_{\zeta,\gamma}, \tag{4.32}$$

where x denotes the roots of zero of the ordinary spherical Bessel function ratio and α, β, γ is the same as declared before.

The function $L_\xi^m(cos\theta)$ denotes the linear combination of the associated Legendre function of the first kind ($P_\xi^m(cos\theta)$) and second kind ($Q_\xi^m(cos\theta)$) of order (ξ,m) which satisfies the associated Legendre differential equation [4-4]

$$\frac{1}{sin\theta}\frac{d}{d\theta}[sin\theta\frac{d}{d\theta}L_\xi^m(cos\theta)] + [\xi(\xi+1) - \frac{m^2}{sin^2\theta}]L_\xi^m(cos\theta) = 0 \tag{4.33}$$

with the unknown normalized coefficient B_ξ^m :

$$L_\xi^m(cos\theta) = P_\xi^m(cos\theta) + B_\xi^m Q_\xi^m(cos\theta). \tag{4.34}$$

The unknown coefficient B_ξ^m can be obtained by enforcing the finite condition of the dyadic at θ equal $180°$ as[4-10]

$$B_\xi^m = -\frac{2}{\pi}tan[\pi(\xi+m)] . \tag{4.35}$$

In the event of the concentric conducting spherical cavity enclosed by the conducting conical surface at $\theta = 0$ and θ_c, because of $\theta = 0$ is contained, hence $B_{\xi}^{m}=0$ due to the integer of ξ.

The eigenvalues m is determined from the dimension in the azimuthal direction of the cavity. ξ is either μ or λ and can be determined from the auxiliary equation [4-4]

$$\frac{dL_{\lambda}^{m}(cos\theta)}{d\theta}\Big|_{\theta=\theta_c} = 0 \tag{4.36}$$

and

$$L_{\mu}^{m}(cos\theta)\Big|_{\theta=\theta_c} = 0. \tag{4.37}$$

They satisfy the field in the TE and TM modes, respectively.

The eigenvalues κ_{ζ} is κ_p or κ_q that after being multiplied by the certain radii of concentric conducting spheres of the spherical coordinate system are the roots of the indical equation [4-4]

$$b_{\xi}(\kappa_p R)\Big|_{R=R_a} = b_{\xi}(\kappa_p R)\Big|_{R=R_b} = 0, \tag{4.38}$$

for TE mode, and

$$\frac{d[\kappa_q R b_{\xi}(\kappa_q R)]}{d(\kappa_q R)}\Big|_{R=R_a} = \frac{d[\kappa_q R b_{\xi}(\kappa_q R)]}{d(\kappa_q R)}\Big|_{R=R_b} = 0 \tag{4.39}$$

for TM mode.

In the method of magnetic dyadic Green's function ($\overline{\overline{G}}_m$), for the configuration of the conducting spherical cavity, the eight sets of solenoidal spherical vector wave functions with discrete eigenvalues are required. They are

$$\overline{M}^{e}_{o}{}_{m\xi}(\kappa_\zeta) = \nabla\times[\varphi_{e_{o}m\xi}(\kappa_\zeta)\overline{R}], \tag{4.40}$$

$$\overline{N}^{e}_{o}{}_{m\xi}(\kappa_\zeta) = \frac{1}{\kappa_\zeta}\nabla\times\nabla\times[\varphi_{e_{o}m\xi}(\kappa_\zeta)\overline{R}]. \tag{4.41}$$

Where ξ and ζ can be either μ or λ and p or q, respectively. Both of these functions are the solutions of the vector wave equation

$$\nabla\times\nabla\times\overline{F} - \kappa_\zeta^2\overline{F} = 0, \tag{4.42}$$

where $\overline{F}$ is $\overline{M}$ or $\overline{N}$ and satisfies the symmetrical relationships

$$\overline{N}^{e}_{o}{}_{m\xi}(\kappa_\zeta) = \frac{1}{\kappa_\zeta}\nabla\times\overline{M}^{e}_{o}{}_{m\xi}(\kappa_\zeta) \tag{4.43}$$

and

$$\overline{M}^{e}_{o}{}_{m\xi}(\kappa_\zeta) = \frac{1}{\kappa_\zeta}\nabla\times\overline{N}^{e}_{o}{}_{m\xi}(\kappa_\zeta) \ . \tag{4.44}$$

By substituting the eigenfunction into (4.40) and (4.41), the complete expressions of the vector wave function can be written in the form

$$\overline{M}^{e}_{omn\xi}(\kappa\zeta) = \mp\frac{m}{\sin\theta} b_\xi(\kappa\zeta R) L^m_\xi(\cos\theta)\begin{Bmatrix}\sin\\ \cos\end{Bmatrix} m\phi\hat{\theta} - b_\xi(\kappa\zeta R)\frac{\partial L^m_\xi(\cos\theta)}{\partial\theta}\begin{Bmatrix}\cos\\ \sin\end{Bmatrix} m\phi\hat{\phi}, \tag{4.45}$$

$$\overline{N}^{e}_{omn\xi}(\kappa\zeta) = \frac{\xi(\xi+1)}{\kappa\zeta} b_\xi(\kappa\zeta R) L^m_\xi(\cos\theta)\begin{Bmatrix}\cos\\ \sin\end{Bmatrix} m\phi\hat{R} + \frac{1}{\kappa\zeta R}\frac{\partial[Rb_\xi(\kappa\zeta R)]}{\partial R}\times\left[\frac{\partial L^m_\xi(\cos\theta)}{\partial\theta}\begin{Bmatrix}\cos\\ \sin\end{Bmatrix} m\phi\hat{\theta}\right. \mp\left.\frac{m}{\sin\theta} L^m_\xi(\cos\theta)\begin{Bmatrix}\sin\\ \cos\end{Bmatrix} m\phi\hat{\phi}\right]. \tag{4.46}$$

4.6 Dyadic Green's Functions of the Concentric Conducting Spherical Cavity and Segment

To derive the dyadic Green's function of the structure under consideration, the method of $\overline{\overline{G}}_m$ approach will be applied. The magnetic type of dyadic Green's function was first derived by using [4-4]

$$\nabla\times\nabla\times\overline{\overline{G}}_{m2}(\overline{R},\overline{R'}) - k^2\overline{\overline{G}}_{m2}(\overline{R},\overline{R'}) = \nabla\times[\overline{\overline{I}}\delta(\overline{R}-\overline{R'})], \tag{4.47}$$

where $\overline{\overline{G}}_{m2}$ denotes the magnetic dyadic Green's function of the second kind that satisfies the boundary condition

$$\bar{n}\times\nabla\times\bar{\bar{G}}_{m2}(\bar{R},\bar{R}') = 0 \tag{4.48}$$

at R equals R_a and R_b, θ equals 0 and θ_c for the concentric conducting spherical cacity and for the conducting spherical segment, $\phi=0$ and $\phi = \phi_d$ is included. k is the propagation constant of the medium which equals $\omega\sqrt{\mu\varepsilon}$, ω is the operating angular frequency, μ, ε are the permeability and permittivity of the medium, respectively, $\bar{\bar{I}}$ is the Idem factor and $\delta(\bar{R}-\bar{R}')$ is the three dimensional delta function.

According to Ohm-Rayleigh method [4-4], the source function in case of the concentric conducting spherical cavity is expanded in the form of solenoidal vector wave functions

$$\nabla\times[\bar{\bar{I}}\delta(\bar{R}-\bar{R}')] = \sum_{l,m}[\sum_{\mu}\bar{C}^{e}_{omn\lambda}(\kappa_p)\bar{N}^{e}_{omn\lambda}(\kappa_p) + \sum_{\lambda}\bar{D}^{e}_{omn\mu}(\kappa_q)\bar{M}^{e}_{omn\mu}(\kappa_q)], \tag{4.49}$$

where the integer l represents the discrete eigenvalues κ_p and κ_q. $\bar{C}^{e}_{omn\lambda}(\kappa_p)$ and $\bar{D}^{e}_{omn\mu}(\kappa_q)$ are two unknown vector coefficients to be determined. By taking the anterior scalar product of (4.49) with $\bar{N}'^{e}_{omn\lambda'}(\kappa'_p)$and $\bar{M}'^{e}_{omn\mu'}(\kappa'_q)$, respectively, integrating the resultant equation throughout the cavity configuration domain and using the orthogonal relationship between the vector wave function, one obtains

$$\bar{C}^{e}_{omn\lambda}(\kappa_p) = \frac{(2-\delta_0)\kappa_p}{2\pi I_{\lambda p}}\bar{M}'^{e}_{omn\lambda}(\kappa_p) \tag{4.50}$$

and

$$\overline{D}^{e}_{o}{}_{m\mu}(\kappa_q) = \frac{(2-\delta_0)\kappa_q}{2\pi I_{\mu q}} \overline{N'}^{e}_{o}{}_{m\mu}(\kappa_q), \tag{4.51}$$

where

$$I_{\xi\zeta} = \frac{1}{\kappa_\zeta \kappa'_\zeta} \int_0^{\theta_c} \int_{R_a}^{R_b} \{\xi^2(\xi+1)^2 j_\xi(\kappa_\zeta R) j_\xi(\kappa'_\zeta R)[P_\xi^m(cos\theta)]^2 + \frac{\partial[Rj_\xi(\kappa_\zeta R)]}{\partial R} \frac{\partial[Rj_\xi(\kappa'_\zeta R)]}{\partial R} [(\frac{\partial P_\xi^m(\cos\theta)}{\partial\theta})^2 + (\frac{mP_\xi^m}{\sin\theta})^2]\} sin\theta dR d\theta. \tag{4.52}$$

When $\xi\zeta$ is λp and μq, respectively and δ_0 represents the Kronecker delta function. To find $\overline{\overline{G}}_{m2}$, we will expand $\overline{\overline{G}}_{m2}$ by using the same expression of the source function as shown in (4.49), but the two different scalar unknown coefficients $E(\kappa_p)$ and $F(\kappa_q)$ as

$$\overline{\overline{G}}_{m2}(\overline{R},\overline{R'}) = \sum_{l,m} \frac{2-\delta_0}{2\pi} [\sum_{\mu} \frac{\kappa_p}{I_{\lambda p}} E(\kappa_p) \overline{M'}^{e}_{o}{}_{m\lambda}(\kappa_p) \overline{N}^{e}_{o}{}_{m\lambda}(\kappa_p) + \sum_{\lambda} \frac{\kappa_q}{I_{\mu q}} F(\kappa_q) \overline{N'}^{e}_{o}{}_{m\mu}(\kappa_q) \overline{M}^{e}_{o}{}_{m\mu}(\kappa_q)] \tag{4.53}$$

By substituting (4.53) in (4.47), the unknown coefficients $E(\kappa_p)$ and $F(\kappa_q)$ can be determined

$$E(\kappa_p) = \frac{1}{(\kappa_p^2 - k^2)} \tag{4.54}$$

$$F(\kappa_q) = \frac{1}{(\kappa_q^2 - k^2)} \tag{4.55}$$

and $\overline{\overline{G}}_{m2}$ can be written in the form

$$\overline{\overline{G}}_{m2}(\overline{R},\overline{R'}) = \sum_{l,m} \frac{2-\delta_0}{2\pi} [\sum \frac{\kappa_p}{\mu(\kappa_p^2 - k^2) I_{\lambda p}} \times \overline{M'^{e}}_{o m\lambda}(\kappa_p) \overline{N}^{e}_{o m\lambda}(\kappa_p)$$
$$+ \sum \frac{\kappa_q}{\lambda(\kappa_q^2 - k^2) I_{\mu q}} \times \overline{N'^{e}}_{o m\mu}(\kappa_q) \overline{M}^{e}_{o m\mu}(\kappa_q)] \tag{4.56}$$

After $\overline{\overline{G}}_{m2}$ was derived, by considering the singularities of the source point and using the Maxwell's coupled differential equation in dyadic form,

$$\nabla \times \overline{\overline{G}}_{m2} = \overline{\overline{I}}\delta(\overline{R} - \overline{R'}) + k^2 \overline{\overline{G}}_{e1}, \tag{4.57}$$

where $\overline{\overline{G}}_{e1}$ denotes the electric dyadic Green's function of the first kind that satisfied the boundary condition

$$\overline{n} \times \overline{\overline{G}}_{e1}(\overline{R},\overline{R'}) = 0. \tag{4.58}$$

$\overline{\overline{G}}_{e1}(\overline{R},\overline{R'})$ could be derived as [4-11]

$$\overline{\overline{G}}_{e1}(\overline{R},\overline{R'}) = -\frac{1}{k^2}\overline{\overline{I}}\delta(\overline{R}-\overline{R'}) + \frac{1}{k^2}\sum_{l,m}\frac{2-\delta_0}{2\pi}$$
$$[\sum_{\mu}\frac{\kappa_p^{\,2}}{(\kappa_p^2-k^2)I_{\lambda p}}\overline{M'}^{e}_{omn\lambda}(\kappa_p)\overline{M}^{e}_{omn\lambda}(\kappa_p) \qquad (4.59)$$
$$+\sum_{\lambda}\frac{\kappa_q^{\,2}}{(\kappa_q^2-k^2)I_{\mu q}}\overline{N'}^{e}_{omn\mu}(\kappa_q)\overline{N}^{e}_{omn\mu}(\kappa_q)].$$

Based on the electric dyadic Green's function of the first kind, the primed functions ($\overline{M'}$and $\overline{N'}$) are the excitation functions and the unprimed functions ($\overline{M}$ and $\overline{N}$) are the field functions. The former and the latter term correspond to the transverse electric and transverse magnetic mode, respectively.

Alternatively, by using the symmetrical relationship between the electric and magnetic dyadic Green's functions, the electric dyadic Green 's function of the second kind and the magnetic dyadic Green;s function of the first kind can be expressed as

$$\overline{\overline{G}}_{e2}(\overline{R},\overline{R'}) = -\frac{1}{k^2}\overline{\overline{I}}\delta(\overline{R}-\overline{R'}) + \frac{1}{k^2}\sum_{l,m}\frac{2-\delta_0}{2\pi}$$
$$[\sum_{\mu}\frac{\kappa_p^{\,2}}{(\kappa_p^2-k^2)I_{\lambda p}}\overline{N'}^{e}_{omn\lambda}(\kappa_p)\overline{N}^{e}_{omn\lambda}(\kappa_p)$$
$$+\sum_{\lambda}\frac{\kappa_q^{\,2}}{(\kappa_q^2-k^2)I_{\mu q}}\overline{M'}^{e}_{omn\mu}(\kappa_q)\overline{M}^{e}_{omn\mu}(\kappa_q)].$$

(4.60)

and

$$\overline{\overline{G}}_{m1}(\overline{R},\overline{R'}) = \sum_{l,m}\frac{2-\delta_0}{2\pi}[\sum_{\mu}\frac{\kappa_p}{(\kappa_p^2-k^2)I_{\lambda p}}\times \overline{N'}^{e}_{omn\lambda}(\kappa_p)\overline{M}^{e}_{omn\lambda}(\kappa_p)$$

$$+ \sum_{\lambda}\frac{\kappa_q}{(\kappa_q^2-k^2)I_{\mu q}}\times \overline{M'}^{e}_{omn\mu}(\kappa_q)\overline{N}^{e}_{omn\mu}(\kappa_q)] \qquad (4.61)$$

Additionally, the expression of the dyadic Green's function of the conducting spherical segment can be derived by using the same method as the concentric conducting spherical cavity and adding the boundary in the azimuth plane. The complete expressions of the dyadic Green's function of the conducting spherical segment are summarized as follows: [4-12]

$$\overline{\overline{G}}_{m2}(\overline{R},\overline{R'}) = \sum_{l,\upsilon}[\sum_{\mu}\frac{\kappa_p}{(\kappa_p^2-k^2)I_{\upsilon\lambda p}}\overline{M'}^{e}_{o\upsilon\lambda}(\kappa_p)\overline{N}^{e}_{o\upsilon\lambda}(\kappa_p)$$

$$+ \sum_{\lambda}\frac{\kappa_q}{(\kappa_q^2-k^2)I_{\upsilon\mu q}}\overline{N'}^{e}_{o\upsilon\mu}(\kappa_q)\overline{M}^{e}_{o\upsilon\mu}(\kappa_q)] \qquad (4.62)$$

$$\overline{\overline{G}}_{e1}(\overline{R},\overline{R'}) = -\frac{1}{k^2}\overline{\overline{I}}\delta(\overline{R}-\overline{R'}) + \frac{1}{k^2}\sum_{l,\upsilon}$$
$$[\sum_{\mu}\frac{\kappa_p{}^2}{(\kappa_p^2-k^2)I_{\upsilon\lambda p}}\overline{M'}^{e}_{o\upsilon\lambda}(\kappa_p)\overline{M}^{e}_{o\upsilon\lambda}(\kappa_p) + \tag{4.63}$$
$$\sum_{\lambda}\frac{\kappa_q{}^2}{(\kappa_q^2-k^2)I_{\upsilon\mu q}}\overline{N'}^{e}_{o\upsilon\mu}(\kappa_q)\overline{N}^{e}_{o\upsilon\mu}(\kappa_q)]$$

$$\overline{\overline{G}}_{e2}(\overline{R},\overline{R'}) = -\frac{1}{k^2}\overline{\overline{I}}\delta(\overline{R}-\overline{R'}) + \frac{1}{k^2}\sum_{l,\upsilon}$$
$$[\sum_{\mu}\frac{\kappa_p{}^2}{(\kappa_p^2-k^2)I_{\upsilon\lambda p}}\overline{N'}^{e}_{o\upsilon\lambda}(\kappa_p)\overline{N}^{e}_{o\upsilon\lambda}(\kappa_p) + \tag{4.64}$$
$$\sum_{\lambda}\frac{\kappa_q{}^2}{(\kappa_q^2-k^2)I_{\upsilon\mu q}}\overline{M'}^{e}_{o\upsilon\mu}(\kappa_q)\overline{M}^{e}_{o\upsilon\mu}(\kappa_q)].$$

$$\overline{\overline{G}}_{m1}(\overline{R},\overline{R'}) = \sum_{l,\upsilon}[\sum_{\mu}\frac{\kappa_p}{(\kappa_p^2-k^2)I_{\upsilon\lambda p}}\overline{N'}^{e}_{o\upsilon\lambda}(\kappa_p)\overline{M}^{e}_{o\upsilon\lambda}(\kappa_p)$$
$$+\sum_{\lambda}\frac{\kappa_q}{(\kappa_q^2-k^2)I_{\upsilon\mu q}}\overline{M'}^{e}_{o\upsilon\mu}(\kappa_q)\overline{N}^{e}_{o\upsilon\mu}(\kappa_q)] \tag{4.65}$$

where

$$I_{\upsilon\xi\zeta} = \frac{1}{\kappa_\zeta\,\kappa'_\zeta}\int_0^{\phi_d}\int_0^{\theta_c}\int_{R_a}^{R_b}\{\xi^2(\xi+1)^2 j_\xi(\kappa_\zeta R)j_\xi(\kappa'_\zeta R)$$
$$[P_\xi^\upsilon(cos\theta)]^2 + \frac{\partial[Rj_\xi(\kappa_\zeta R)]}{\partial R}\frac{\partial[Rj_\xi(\kappa'_\zeta R)]}{\partial R} \tag{4.66}$$
$$[(\frac{\partial P_\xi^\upsilon(\cos\theta)}{\partial\theta})^2 + (\frac{\upsilon P_\xi^\upsilon}{\sin\theta})^2]\}R^2 sin\theta dRd\theta d\phi.$$

and υ is the same variable as m in the concentric conducting spherical cavity but in case of the conducting spherical segment the eigenvalue must be satisfied the boundary condition in the azimuth direction of TE and TM modes as

$$\upsilon = \frac{m\pi}{\phi_d} ; m = 1,2,... \text{ for TM mode} \tag{4.67}$$

$$\upsilon = \frac{n\pi}{\phi_d} ; n = 0,1,... \text{ for TE mode} \tag{4.68}$$

Knowing the dyadic Green's function, integrating the product of that dyadic Green's function and the source current density throughout the source configuration domain, the field inside the cavity and segment excited by the electric current source such as the linear electric probe can be analyzed as

$$\overline{E}(\overline{R}) = i\omega\mu\iiint \overline{\overline{G}}_{e1}(\overline{R},\overline{R'}) \cdot \overline{J}(\overline{R'})\, dV, \tag{4.69}$$

whereas the cavity and segment excited by the magnetic current source such as the aperture or slot in its wall can be analyzed as

$$\overline{E}(\overline{R}) = -\oiint_{S_A} [\nabla \times \overline{\overline{G}}_{e2}(\overline{R},\overline{R'})] \cdot [\hat{n}' \times \overline{E}'(\overline{R})] ds' \tag{4.70}$$

where $\overline{E}(\overline{R})$ denotes the electric field intensity inside the cavity as a function of the field point, $\overline{J}(\overline{R'})$ is the electric current density and $\overline{E}(\overline{R'})$

is the electirc field distribution along the aperture as the function of the source point.

4.7 Conclusions

This chapter describes the theory and concept of the dyadic analysis and dyadic Green's function in electromagnetic theory such as various kinds of dyadic Green's functions and their properties. The free space dyadic Green's function which is very useful in calculating of the radiation in free space is derived and extend to derive the dyadic Green's function of the concentric conducting spherical cavity and segment. The electromagnetic fields in the source region are derived by using the expression of the dyadic Green's function. Numerical results of the electromagnetic field in the source region of the concentric conducting spherical cavity and segment are left for the further study.

References

[4-1] R.E.Collin, *Field Theory of Guided Waves*, 2nd Ed.,IEEE Press, New York, 1991.

[4-2] E.Kreyzig, *Advanced Engineering Mathematics*, 6th Ed.,Wiley, New York, 1988.

[4-3] J.Takada, "Method of Moments Applied to the Slotted Waveguide Antenns, Record of a Seminar in KMITL on Jan.23, 1996," *Bulletin of INCOCSAT(Tokyo Institute of Technology)*, vol.2, 1996.

[4-4] C.T.Tai, *Dyadic Green Functions in Electromagnetic Theory.* IEEE Press, New York, 1993.

[4-5] C.T.Tai, *Generalized Vector and Dyadic Analysis*, IEEE Press,

Piscataway, N.J., 1992.

[4-6] C.T.Tai, "On the eigen-function expansion of dyadic Green's functions," *Proc.IEEE*, vol.61, pp. 480-481, 1973.

[4-7] H.T.Hui and E.K.N.Yung, "The eigenfunction expansion of dyadic Green's functions for chirowaveguides," *IEEE Trans. Microwave Theory Tech.*, vol.44, no.9, pp. 1575-1583, Sep. 1996.

[4-8] H.T.Hui and E.K.N.Yung, "Corrections to the eigenfunction expansion of dyadic Green's functions for chirowaveguides," *IEEE Trans. Microwave Theory Tech.*, vol.45, no.5, p. 561, May 1997.

[4-9] H.T.Hui and E.K.N.Yung, "Modal expansion of dyadic Green's functions of the cylindrical chirowaveguide," *IEEE Microwave and Guided Wave Letters*, vol.6, no.10, pp. 360-362, Oct. 1996.

[4-10] J.R.Descardeci, "A Note on Using Dyadic Green's Functions on Spheres and Cones," *IEEE Antenna and Propagation Magazine,* vol.38, no.1, p.59, Feb. 1996.

[4-11] C.Phongcharoenpanich, M.Krairiksh and J.Takada, "Dyadic Green 's functions of the concentric conducting spherical cavity," *Proceeding of the 1997 Asia-Pacific Microwave Conference*, vol.2, pp.757-760, 1997.

[4-12] C.Phongcharoenpanich, and M.Krairiksh, "Modal expansion of dyadic Green's functions of the conducting spherical segment," *Proceeding of the 20th Electrical Engineering Conference*, vol.1, pp. 243-248, 1997.

Chapter 5

Numerical Results of the Eigenmodes and Electromagnetic Field of the Conducting Spherical Cavity

Numerical results of the eigenmodes and the electromagnetic fields of the conducting spherical cavity and the concentric conducting spherical cavity are demonstrated to verify the derivation . The electric and magnetic fields of the source-free region, which the expressions are derived in chapter 3, in case of the transverse electric and transverse magnetic modes are illustrated.

5.1 A Conducting Spherical Cavity

According to the characteristic equation, as described in chapter 3, of both cases, TE and TM modes, the characteristic parameters consist of the operating mode number *(n)*, the phase constant expression *(k)* which also implied the meaning of the frequency *(f)* and the radius or the size of the conducting spherical cavity *(R_a)*, respectively. These parameters have to satisfy the characteristic equation, e.g., for the specified operating mode, *n*, the operating frequency and the constant radius of the cavity must be chosen according to that mode. On this viewpoint, the relationship between the Schelkunoff spherical Bessel function of the first kind and its derivative with respect to the argument versus their

abscissas for TE and TM modes, respectively where *n=1-3* are illustrated to help in finding the root of the characteristic equation in fig.4 and fig.5.

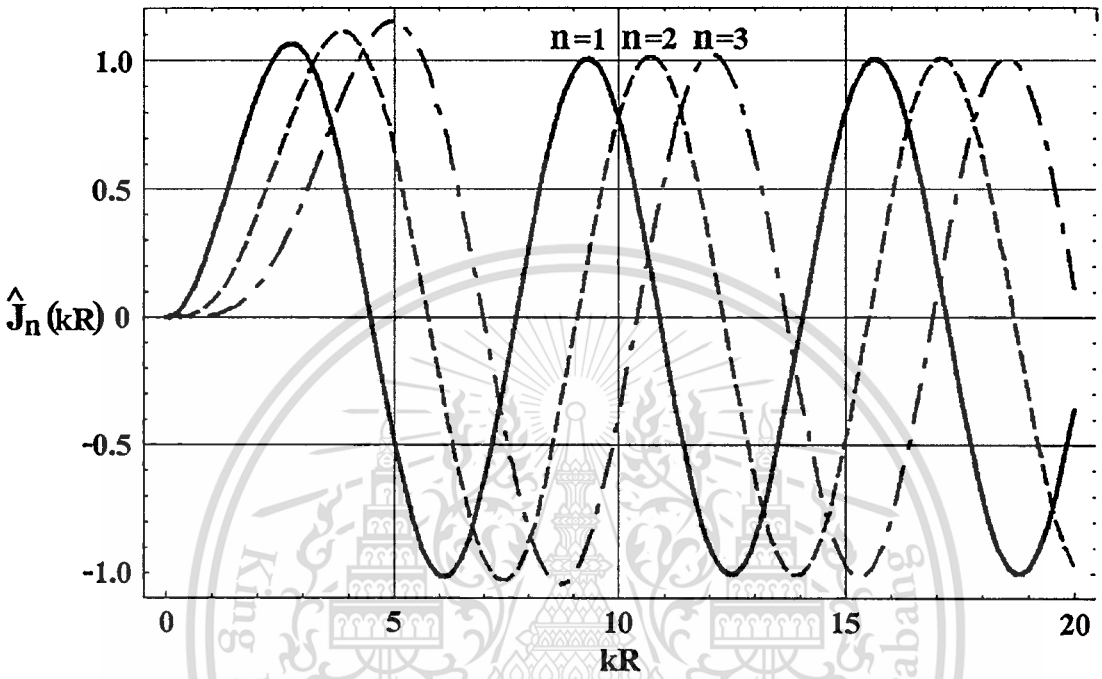

Fig.4 Graphical characteristic in the radial direction for TE mode

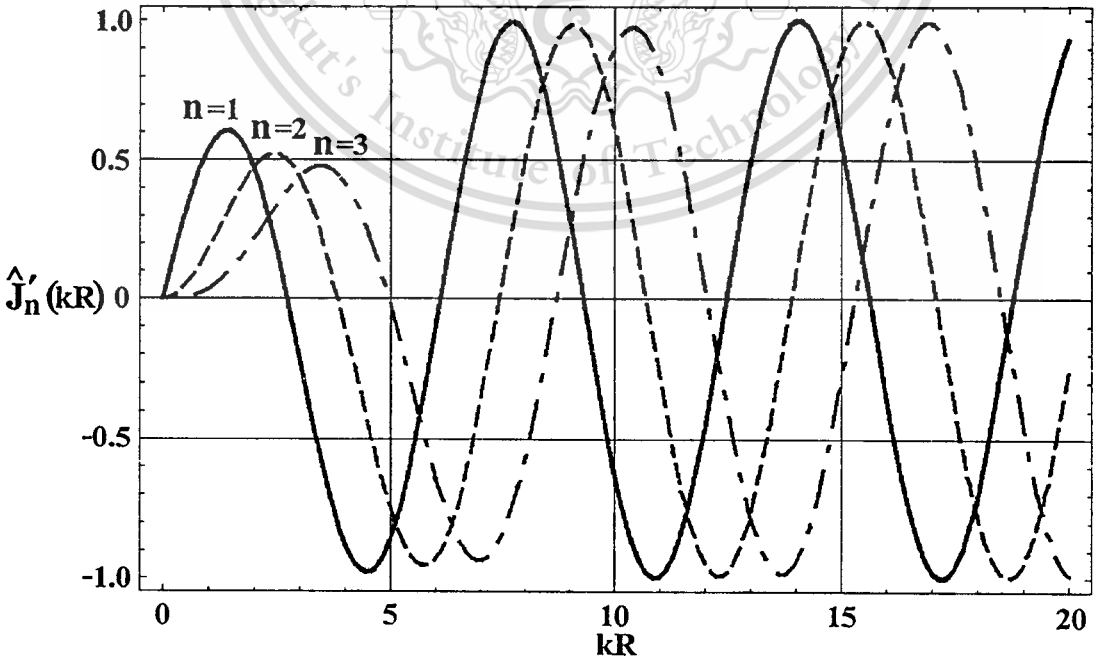

Fig.5 Graphical characteristic in the radial direction for TM mode

To solve for the root of the characteristic equation in both cases of TE and TM modes, the secant method [5-1] is used. The characteristic equation for TE mode is

$$\hat{J}_n(kR_a) = 0 \tag{5.1}$$

$$kR_a = \varsigma_{nl} \tag{5.2}$$

$$k = \frac{\varsigma_{nl}}{R_a} \tag{5.3}$$

$$\omega\sqrt{\mu\varepsilon} = \frac{\varsigma_{nl}}{R_a} \tag{5.4}$$

$$\therefore \quad f_{mnl}^{TE} = \frac{1}{2\pi\sqrt{\mu\varepsilon}}\frac{\varsigma_{nl}}{R_a}. \tag{5.5}$$

This frequency is referred to as the resonant frequency for the TE_{mnl} mode. By the same procedure, for TM_{mnl} mode the characteristic equation becomes

$$\hat{J}_n'(kR_a) = 0 \tag{5.6}$$

$$kR_a = \varsigma_{nl}' \tag{5.7}$$

$$k = \frac{\varsigma'_{nl}}{R_a} \tag{5.8}$$

$$\omega\sqrt{\mu\varepsilon} = \frac{\varsigma'_{nl}}{R_a} \tag{5.9}$$

$$\therefore \quad f_{mnl}^{TM} = \frac{1}{2\pi\sqrt{\mu\varepsilon}}\frac{\varsigma'_{nl}}{R_a} \tag{5.10}$$

where ς_{nl} and ς'_{nl} denote, respectively the root and its derivative of the Schelkunoff spherical Bessel function of the first kind which can be found by using the secant method as dictated before. The relation between the operating mode and the root of the characteristic equation for TE and TM modes for $n = 1\text{-}10$ and $l = 1\text{-}10$ are tabulated in Tables 2 and 3, respectively.

Table 2 The relation between the operating mode *(n)* and the root of the characteristic equation *(l)* for TE mode

↓n l→	1	2	3	4	5
1	4.493	7.725	10.904	14.066	17.221
2	5.763	9.095	12.323	15.515	18.689
3	6.988	10.417	13.698	16.924	20.122
4	8.183	11.705	15.040	18.301	21.525
5	9.356	12.967	16.355	19.653	22.905
6	10.513	14.207	17.648	20.984	24.263
7	11.657	15.431	18.923	22.295	25.603
8	12.791	16.641	20.183	23.591	26.927
9	13.916	17.839	21.429	24.873	28.237
10	15.034	19.026	22.663	26.143	29.535

↓n l→	6	7	8	9	10
1	20.371	23.520	26.666	29.812	32.956
2	21.854	25.013	28.168	31.320	34.471
3	23.304	26.477	29.643	32.804	35.961
4	24.728	27.916	31.094	34.256	37.432
5	26.128	29.333	32.525	35.708	38.884
6	27.508	30.730	33.937	37.123	40.319
7	28.870	32.111	35.333	38.541	41.739
8	30.217	33.477	36.715	39.636	43.145
9	31.550	34.829	38.083	41.318	44.539
10	32.871	36.168	39.438	42.688	45.921

Table 3 The relation between the operating mode *(n)* and the root of the characteristic equation *(l)* for TM mode

↓n l→	1	2	3	4	5
1	2.744	6.117	9.317	12.486	15.644
2	3.870	7.443	10.713	13.921	17.103
3	4.973	8.722	12.064	15.314	18.524
4	6.062	9.968	13.380	16.674	19.915
5	7.140	11.189	14.670	18.009	21.281
6	8.211	12.391	15.939	19.321	22.626
7	9.275	13.579	17.190	20.615	23.953
8	10.335	14.753	18.425	21.894	25.263
9	11.391	15.917	19.649	23.159	26.560
10	12.443	17.072	20.860	24.411	27.844

↓n l→	6	7	8	9	10
1	18.796	21.946	25.093	28.239	34.529
2	20.272	23.434	26.591	29.744	32.895
3	21.174	24.891	28.060	31.224	34.383
4	23.128	26.322	29.505	32.680	35.848
5	24.518	27.731	30.929	34.117	37.296
6	25.887	29.121	32.335	35.536	38.726
7	27.239	30.492	33.723	36.938	40.141
8	28.575	31.849	35.097	38.326	41.542
9	29.897	33.192	36.457	39.701	42.929
10	31.206	34.522	37.805	41.064	44.306

where n stands for the cardinal number of the operating mode and l stands for the ordinal number of the root.

From the characteristic equation, it is apparent that for the known operating mode and the frequency, the size (radius) of the cavity can be chosen to provide the field distribution. On the other hand, for the specified operating mode and the cavity size, the resonant frequency can be calculated.

To clarify, the field distribution inside the conducting spherical cavity at the fundamental (TM_{011}) and the first three higher order (TM_{012}, TM_{021} and TE_{011}) modes are revealed. In case of TM_{0nl}, $m=0$, $n=1,2$, $l=1,2$ and the characteristic equation which satifies these modes are

$$\hat{J}'_n(kR_a) = 0 \tag{5.11}$$

$$kR_a = \varsigma'_{nl} \tag{5.12}$$

$$k = \frac{\varsigma'_{nl}}{R_a} \tag{5.13}$$

$$\omega\sqrt{\mu\varepsilon} = \frac{\varsigma'_{nl}}{R_a} \tag{5.14}$$

$$f_{0nl}^{TM} = \frac{1}{2\pi\sqrt{\mu\varepsilon}}\frac{\varsigma'_{nl}}{R_a}. \tag{5.15}$$

The expressions of electric and magnetic fields in this case are

$$E_R = -\frac{n(n+1)}{j\omega\mu\varepsilon} A'_{0n} \hat{J}_n(kR) P_n^0(\cos\theta) \tag{5.16}$$

$$E_\theta = \frac{1}{j\omega\mu\varepsilon} \frac{1}{R} A'_{0n} \frac{d\hat{J}_n(kR)}{dR} \frac{dP_n^0(\cos\theta)}{d\theta} \tag{5.17}$$

$$E_\phi = 0 \tag{5.18}$$

$$H_R = 0 \tag{5.19}$$

$$H_\theta = 0 \tag{5.20}$$

$$H_\phi = \frac{1}{\varepsilon} \frac{1}{R} A'_{0n} \hat{J}_n(kR) \frac{dP_n^0(\cos\theta)}{d\theta}. \tag{5.21}$$

For TE_{011} mode, the expression of the electromagnetic fields are

$$E_R = 0 \tag{5.22}$$

$$E_\theta = 0 \tag{5.23}$$

$$E_\phi = \frac{1}{\varepsilon} \frac{1}{R} \hat{J}_1(kR) \frac{dP_1^0(\cos\theta)}{d\theta} \tag{5.24}$$

$$H_R = -\frac{2}{j\omega\mu\varepsilon}\hat{J}_1(kR)P_1^0(cos\theta) \tag{5.25}$$

$$H_\theta = \frac{1}{j\omega\mu\varepsilon}\frac{1}{R}\frac{d\hat{J}_1(kR)}{dR}\frac{dP_1^0(cos\theta)}{d\theta} \tag{5.26}$$

$$H_\phi = 0 \tag{5.27}$$

The aspect of these fields are realized by plotting the electric and magnetic fields in each component versus the orthogonal variables in the spherical coordinate.

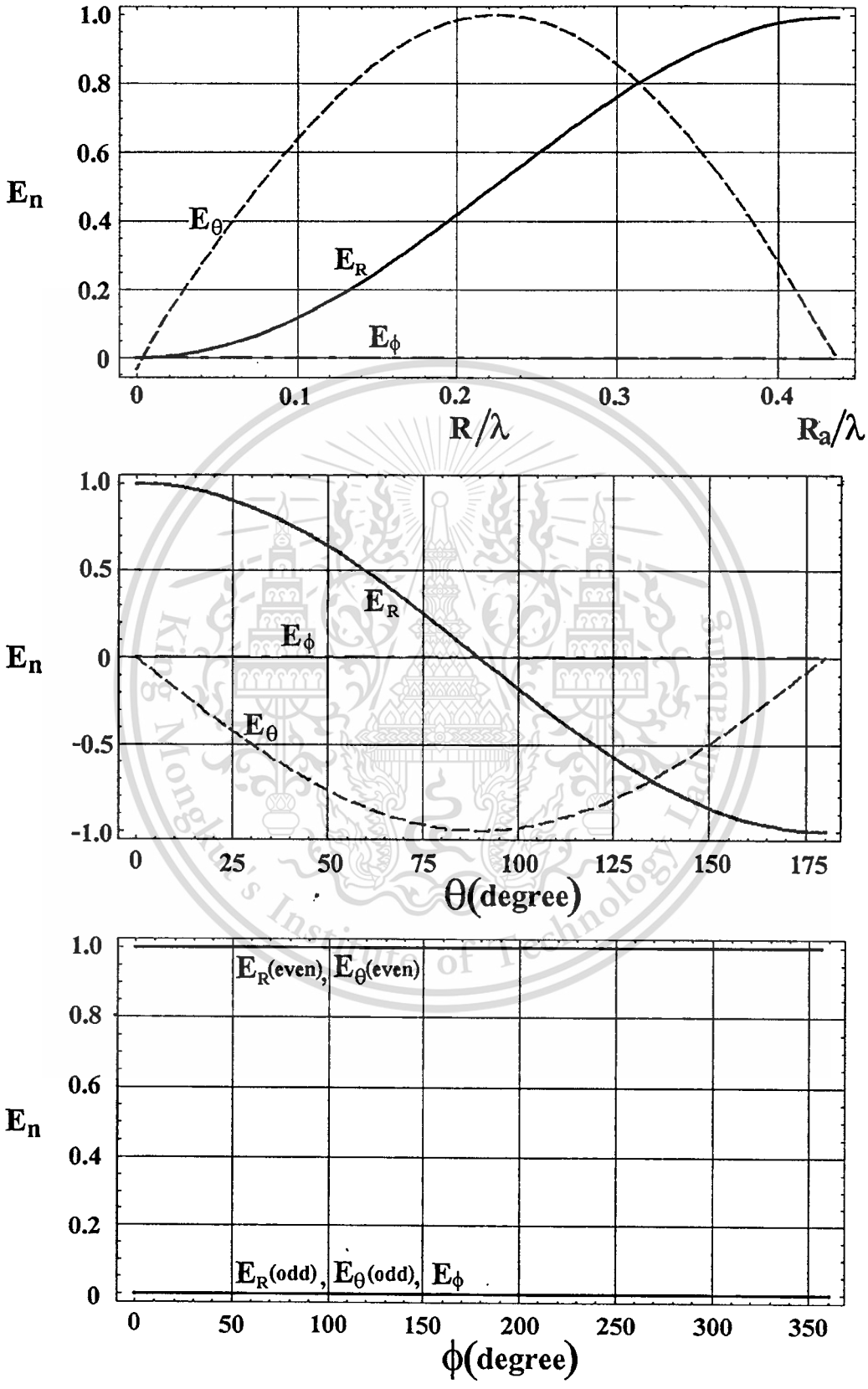

Fig.6 Electric field of the fundamental TM_{011} mode

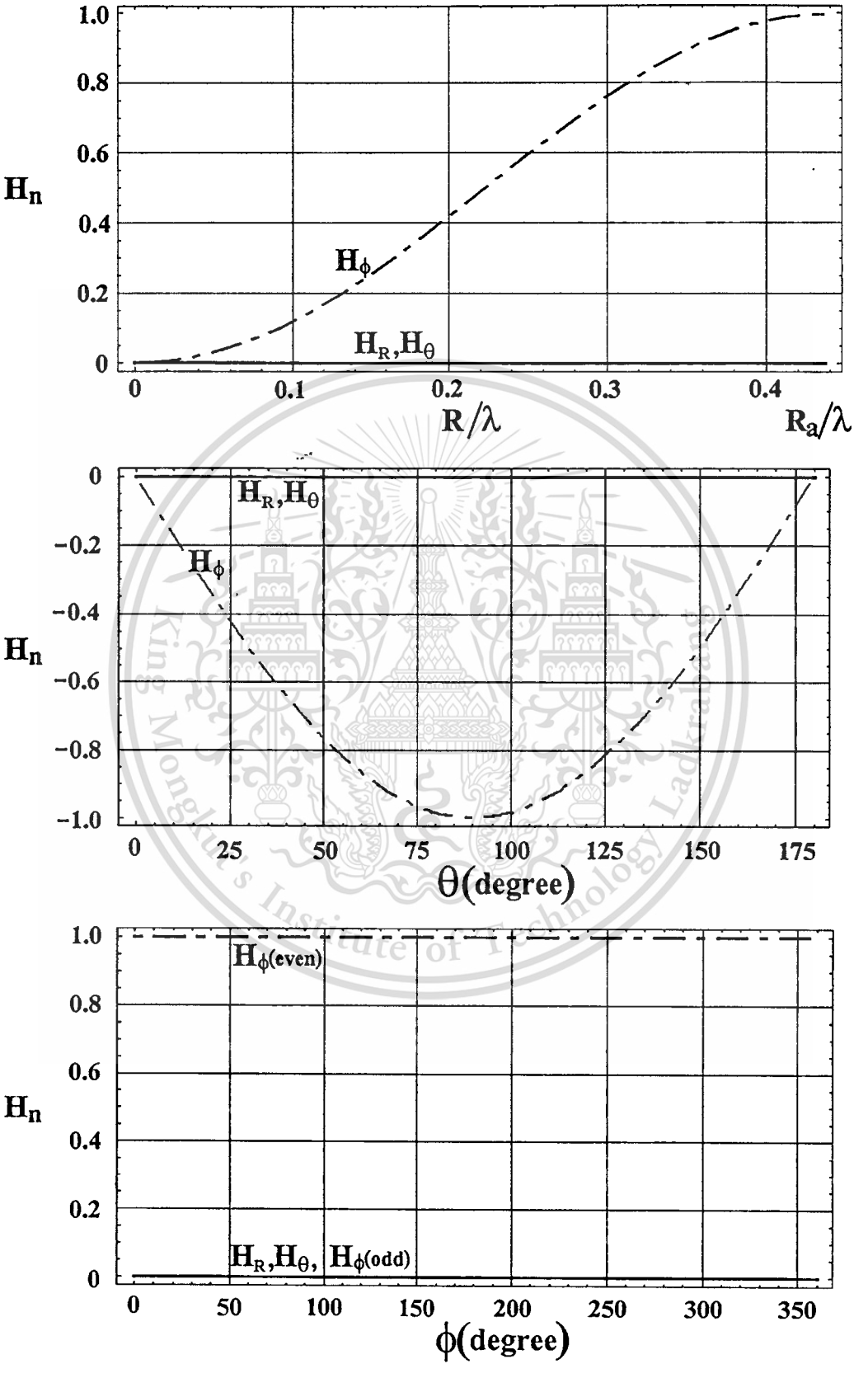

Fig.7 Magnetic field of the fundamental TM_{011} mode

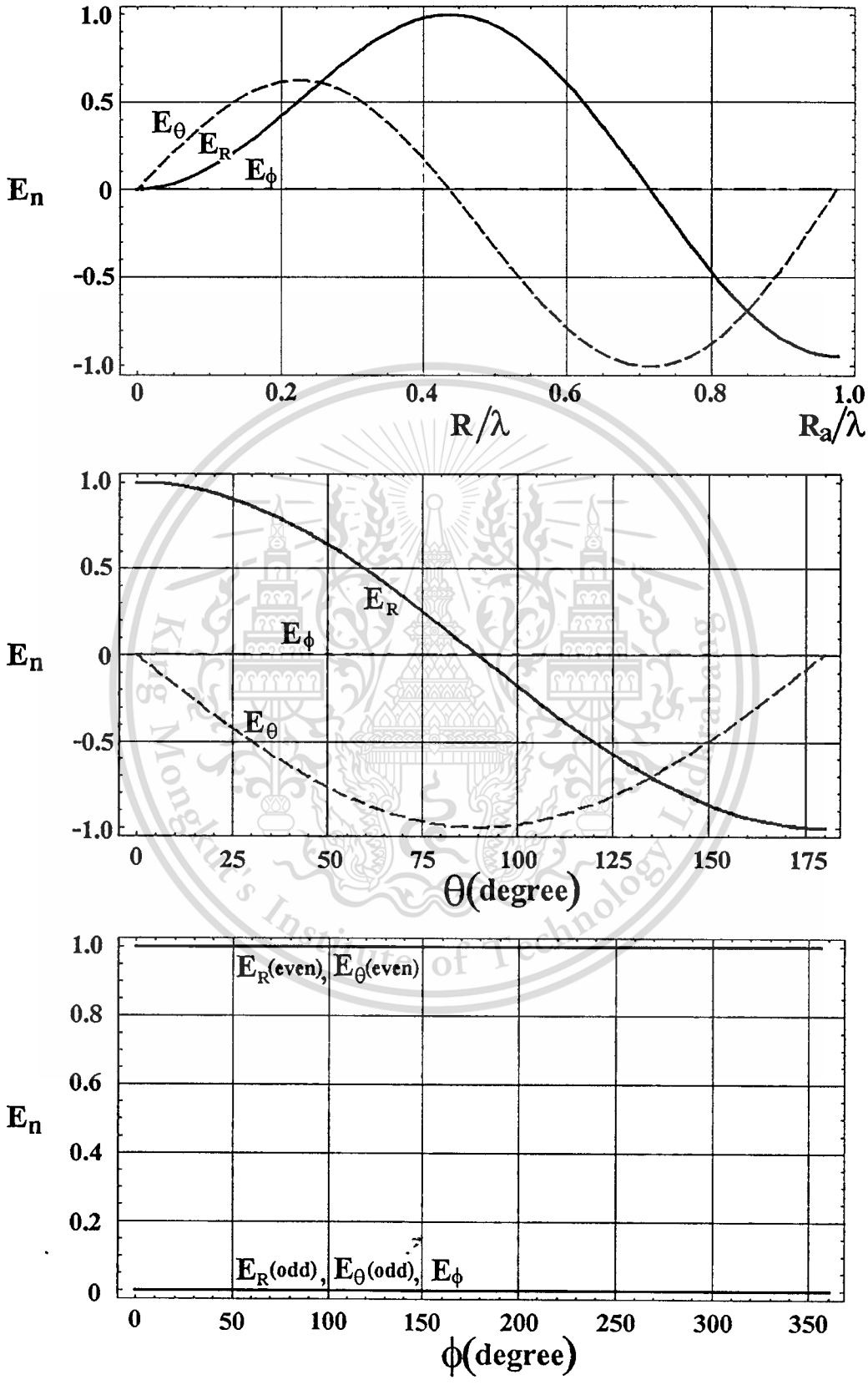

Fig.8 Electric field of the TM_{012} mode

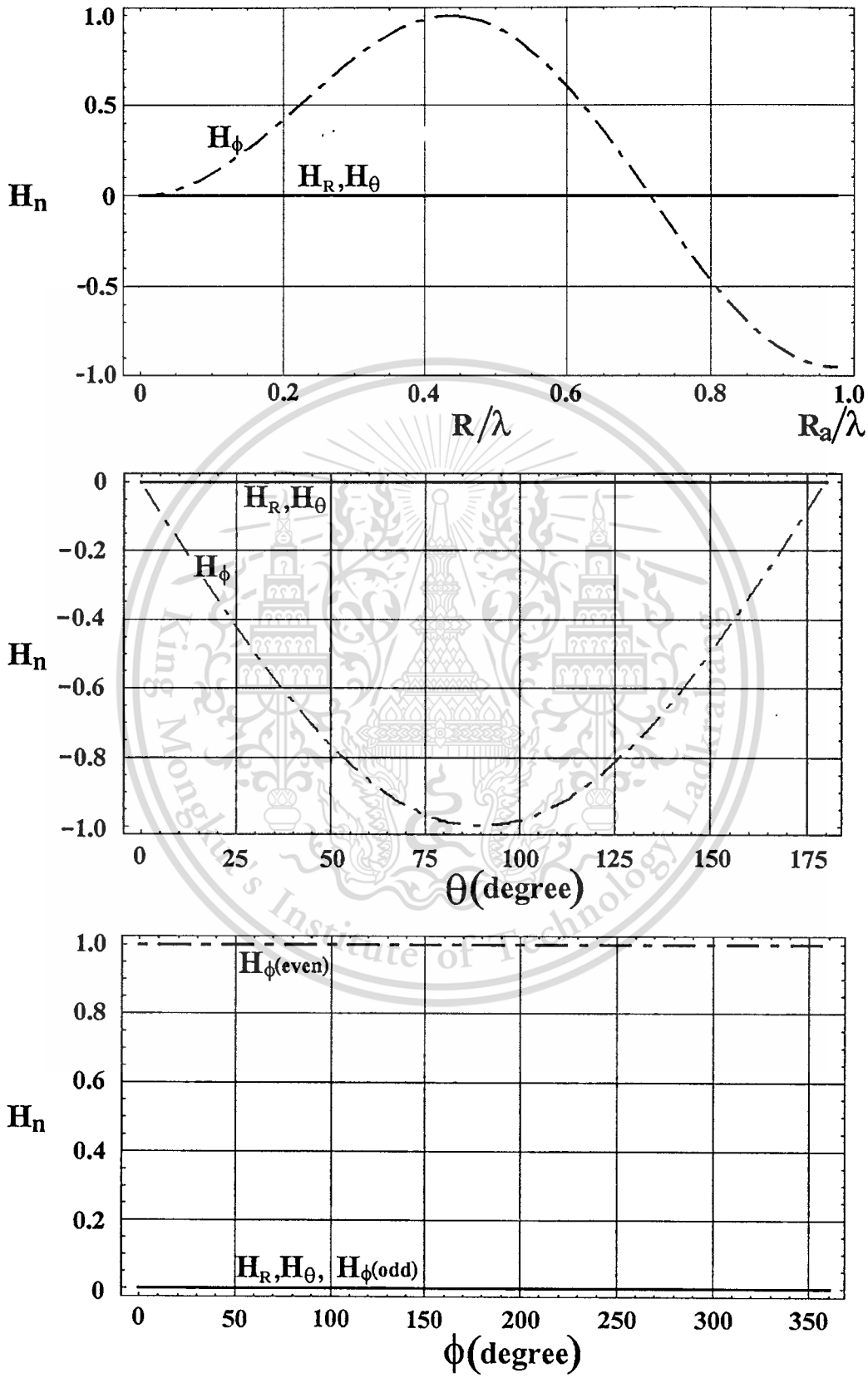

Fig.9 Magnetic field of the TM_{012} mode

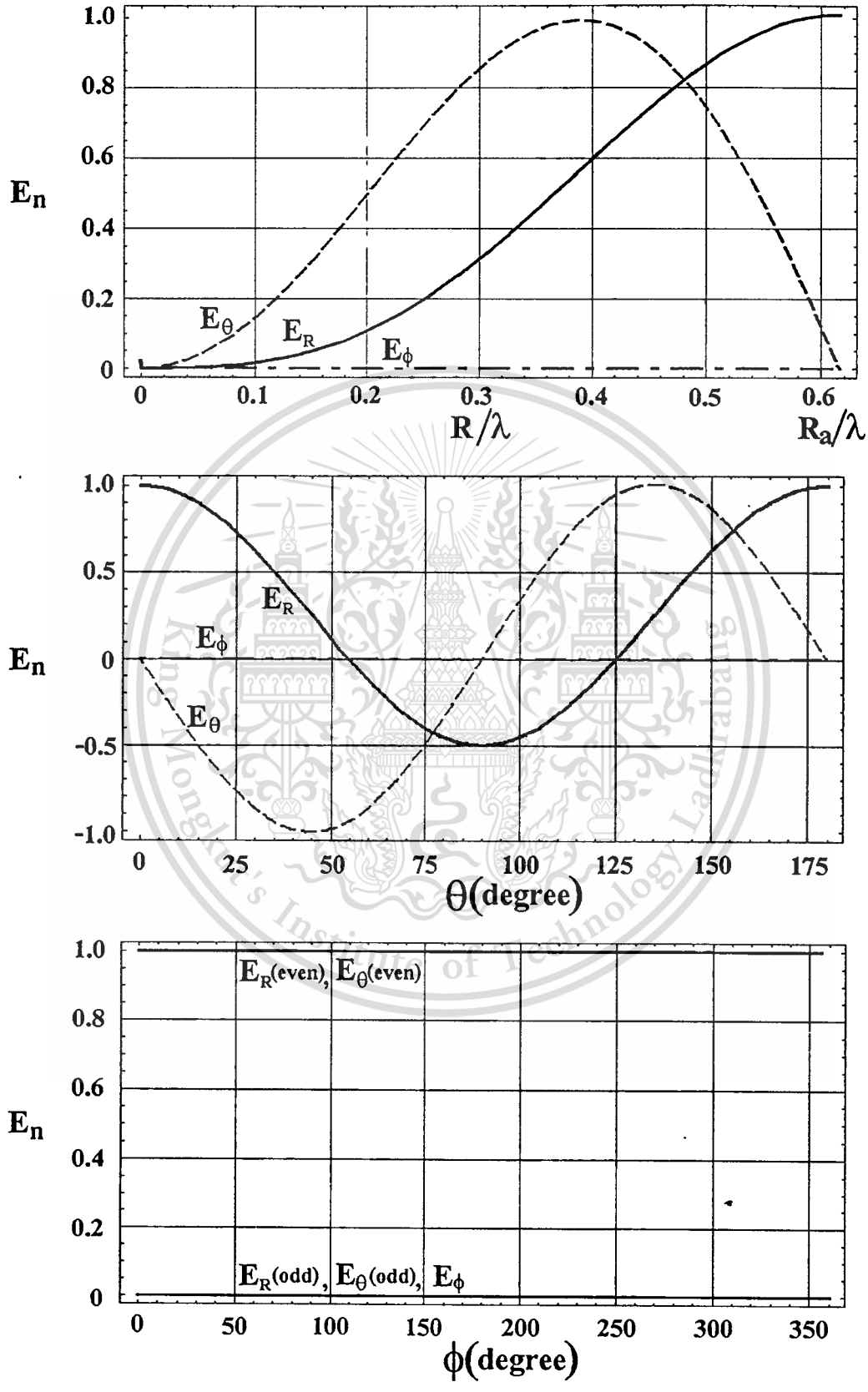

Fig.10 Electric field of the TM_{021} mode

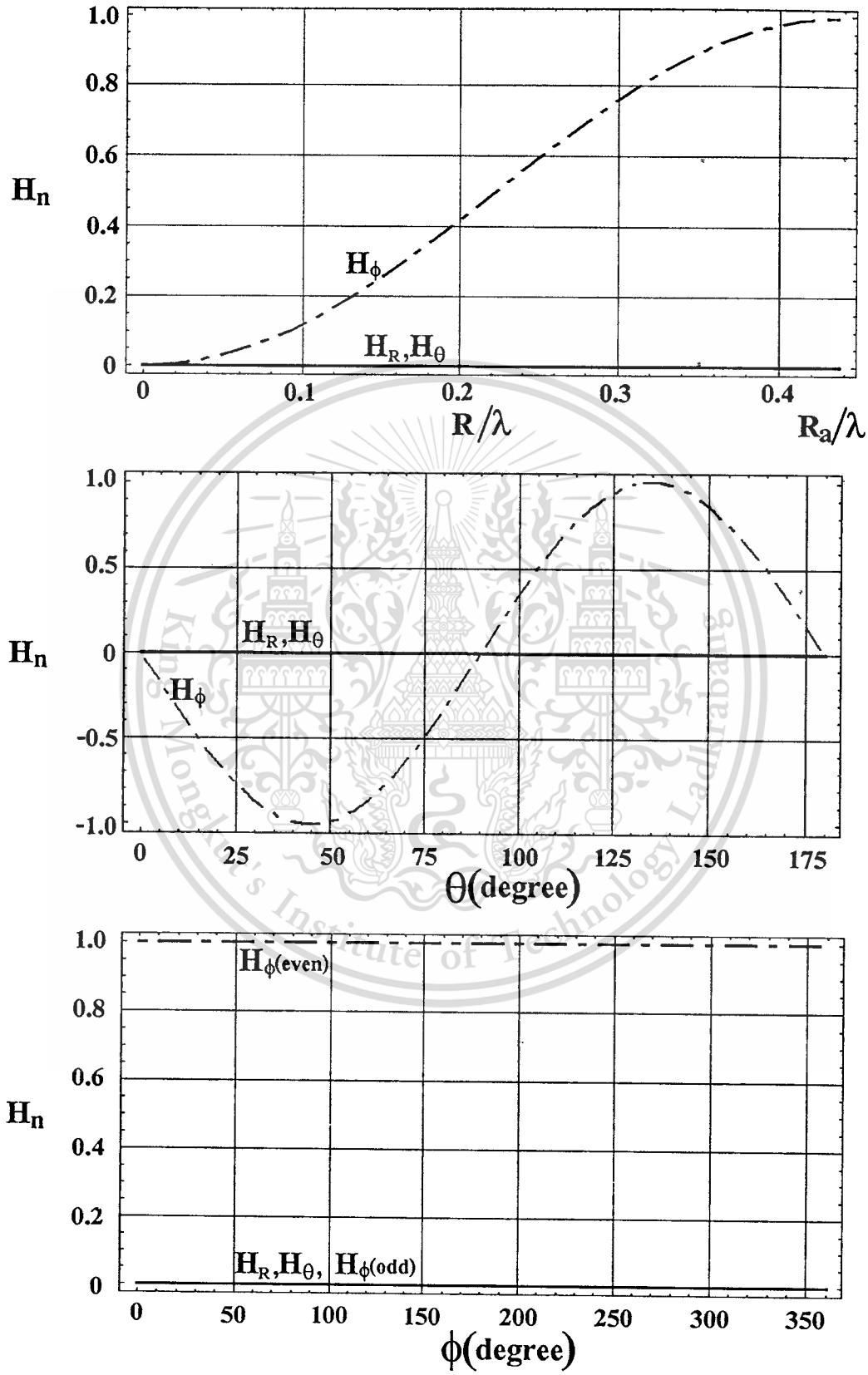

Fig.11 Magnetic field of the TM_{021} mode

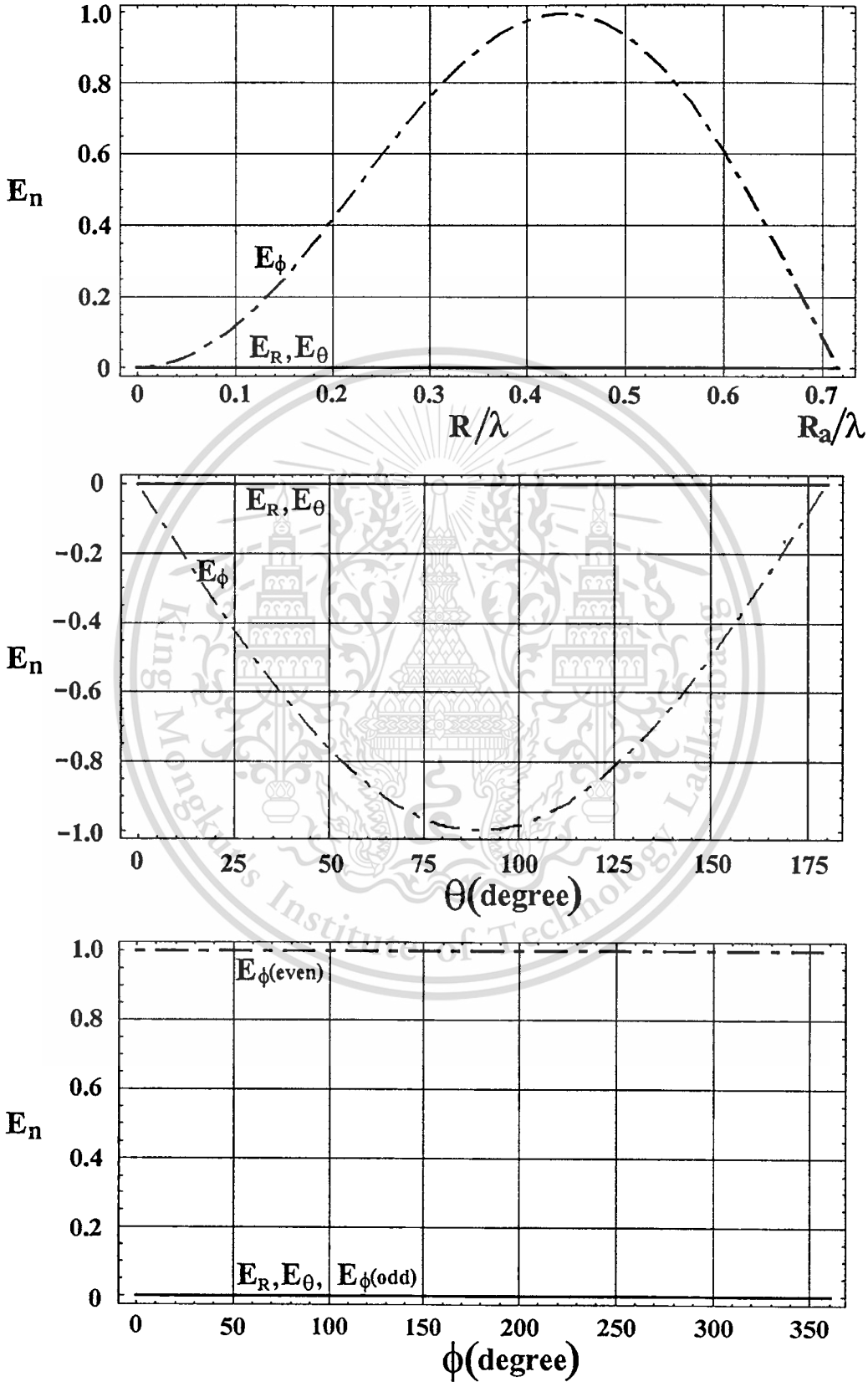

Fig.12 Electric field of the TE_{011} mode

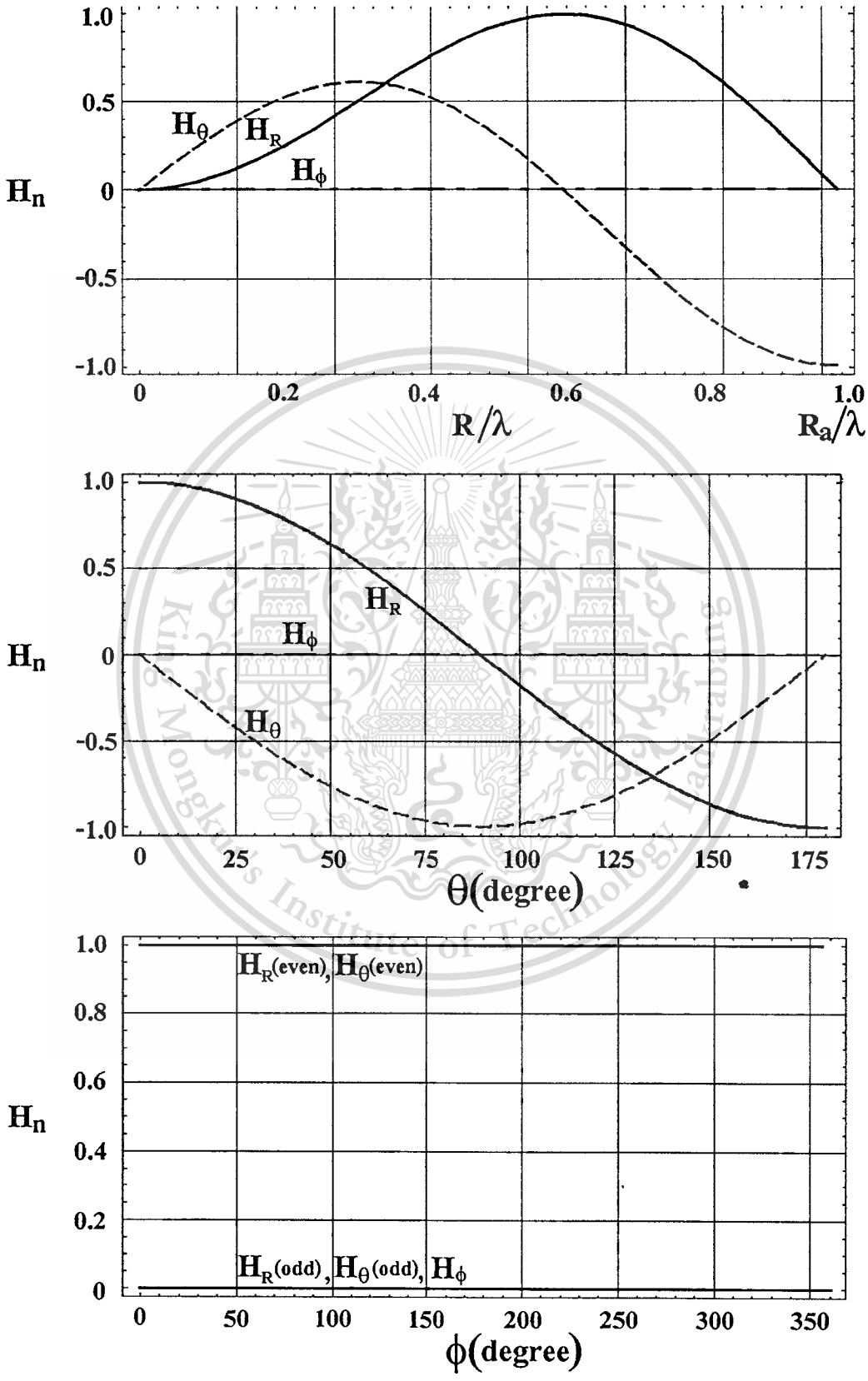

Fig.13 Magnetic field of the TE_{011} mode

From the field distribution, it can be found the position of the maximum and minimum field. By this viewpoint, the cavity can be designed correspond to the practical application.

5.2 A Concentric Conducting Spherical Cavity

From the structure of the concentric conducting spherical cavity enclosed by the conducting conical surface, it is obvious that the boundary condition in the radial and the elevation angle direction must be imposed and after that the characteristic equation is obtained.

To solve for the solution of the characteristic equation in the radial direction, one method is to solve by graphical method which could be done by plotting the ratio of the Schelkunoff spherical Bessel function of the first and second kinds versus their abscissas. The solution will be obtained from the point of intersection. The lower abscissa represents the solution of the inner spherical radius whereas the greater one for the outer spherical radius.

The parameters in this configuration are the inner and the outer spherical radii *(R_a and R_b)*, the angle of the conical surface *(θ_c)*, the phase constant *(k)* and the operating mode *(n)*, respectively. The relationship between the ratio of the Schelkunoff spherical Bessel function of the first kind and the second kind and its derivative ratio versus the abscissas for TE and TM modes are illustrated to find the root of the characteristic equation where *n=1-3* in fig.14 and fig.15.

For TE mode

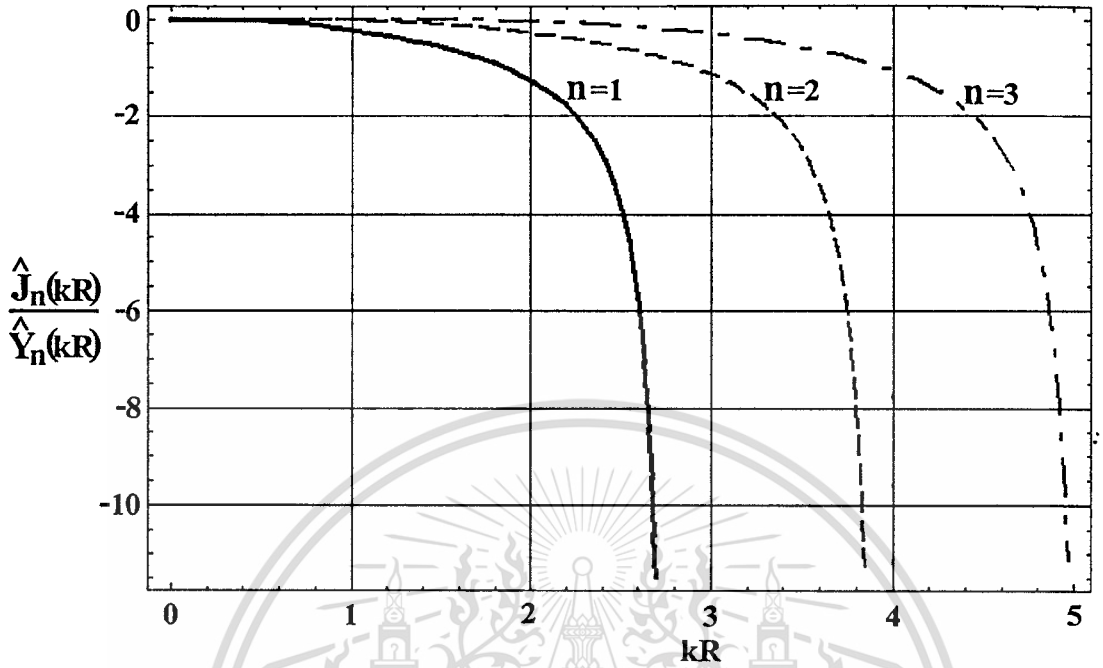

Fig.14 Ratio of the spherical Bessel function of the first to the second kinds *(n=1,2,3)*

For TM mode

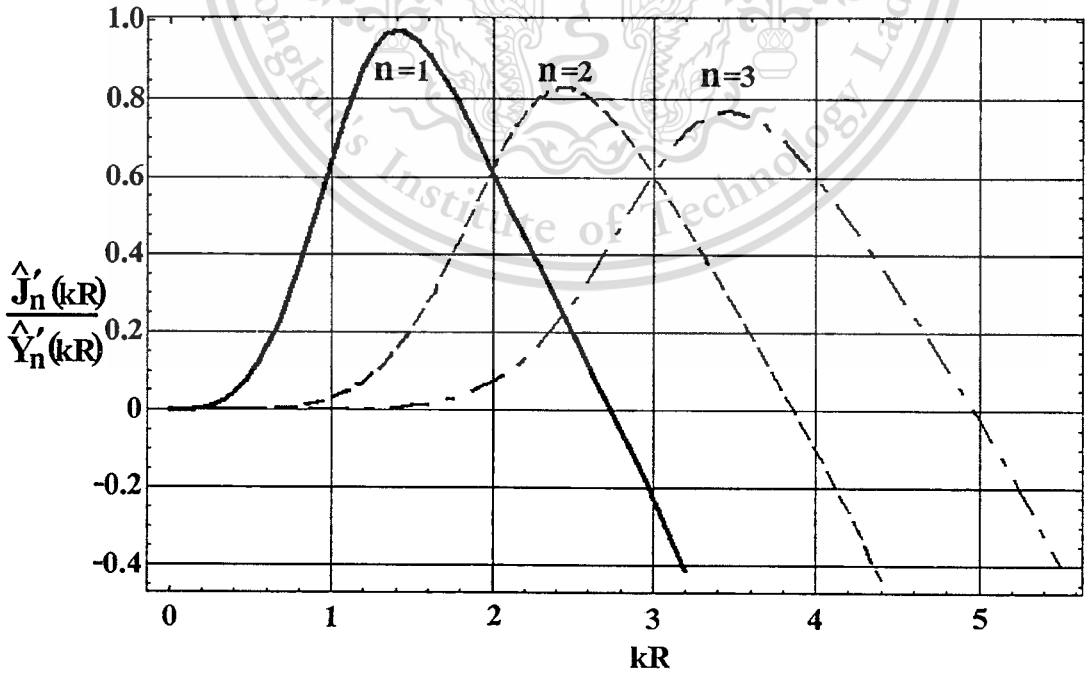

Fig.15 Ratio of the derivative of the spherical Bessel function of the first to the second kinds *(n=1,2,3)*

The resonant frequency for TE and TM mode can be derived by using the same method as the conducting spherical cavity, after some manipulations it can be written, for TE mode as

$$f_{mnl}^{TE} = \frac{1}{2\pi\sqrt{\mu\varepsilon}} \frac{x_{\zeta,\gamma}}{(R_b - R_a)} \tag{5.28}$$

and for TM mode as

$$f_{mnl}^{TM} = \frac{1}{2\pi\sqrt{\mu\varepsilon}} \frac{x'_{\zeta,\gamma}}{(R_b - R_a)} \tag{5.29}$$

Another method to solve for the solution of the characteristic equation could be achieved by using the secant method which is determining the point that the non-trivial solution become zero, for TE mode as

$$\hat{J}_n(kR_a)\hat{Y}_n(kR_b) - \hat{J}_n(kR_b)\hat{Y}_n(kR_a) = 0 \tag{5.30}$$

and for TM mode, counterpart as

$$\frac{d\hat{J}_n(kR_a)}{dR}\frac{d\hat{Y}_n(kR_b)}{dR} - \frac{d\hat{J}_n(kR_b)}{dR}\frac{d\hat{Y}_n(kR_a)}{dR} = 0. \tag{5.31}$$

Similarly, to determine the characteristic equation in the elevation angle direction, the boundary condition in that direction must be enforced as estimated in (3.45) and (3.46) for TE and TM modes, respectively. Accordingly, the parameters in this direction consists of the

order of the modes *n,m* and the conical angle (θ_c). These parameters must be satisfied the field distribution inside the cavity. The graphical characteristic for the TE and TM modes in the elevation angle direction. Fig.16 and fig.17 show the graphical characteristic in the elevation angle direction of TM mode for fixed *m=0*, varied *n=1,2,3* and varied *m=0,1,2,* fixed *n=2* ,respectively whereas fig.18 and fig.19 are for TE mode.

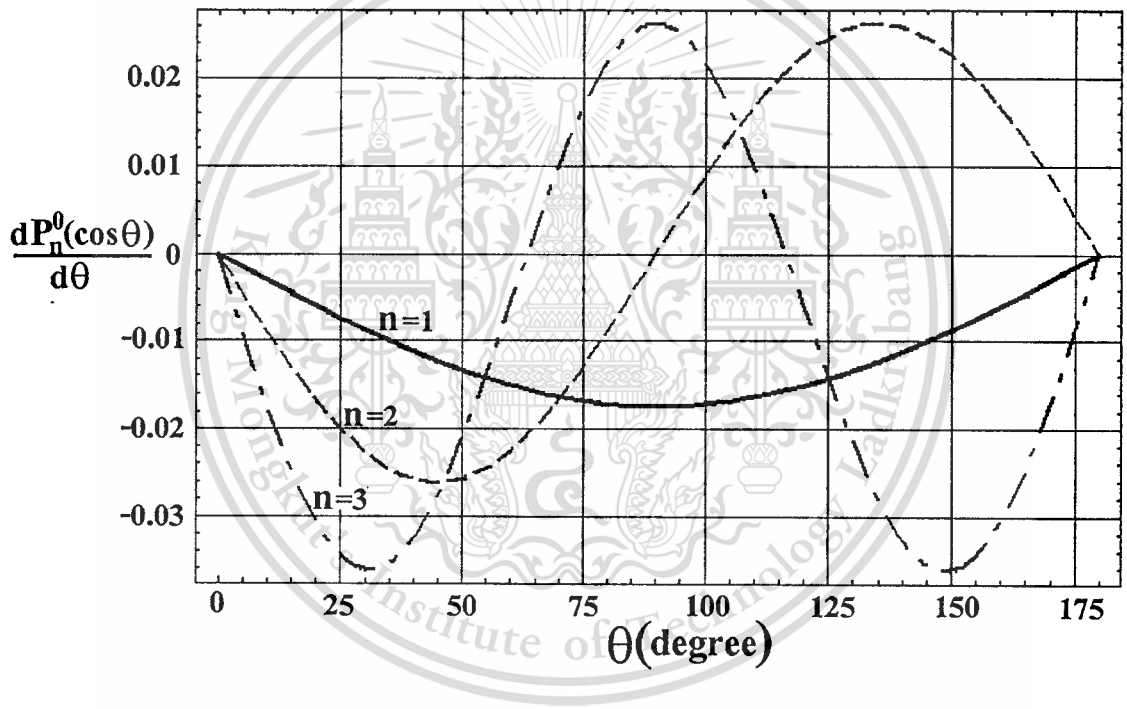

Fig.16 Graphical characteristic in the elevation angle direction for TE mode (fixed *m=0*, varied *n=1,2,3*)

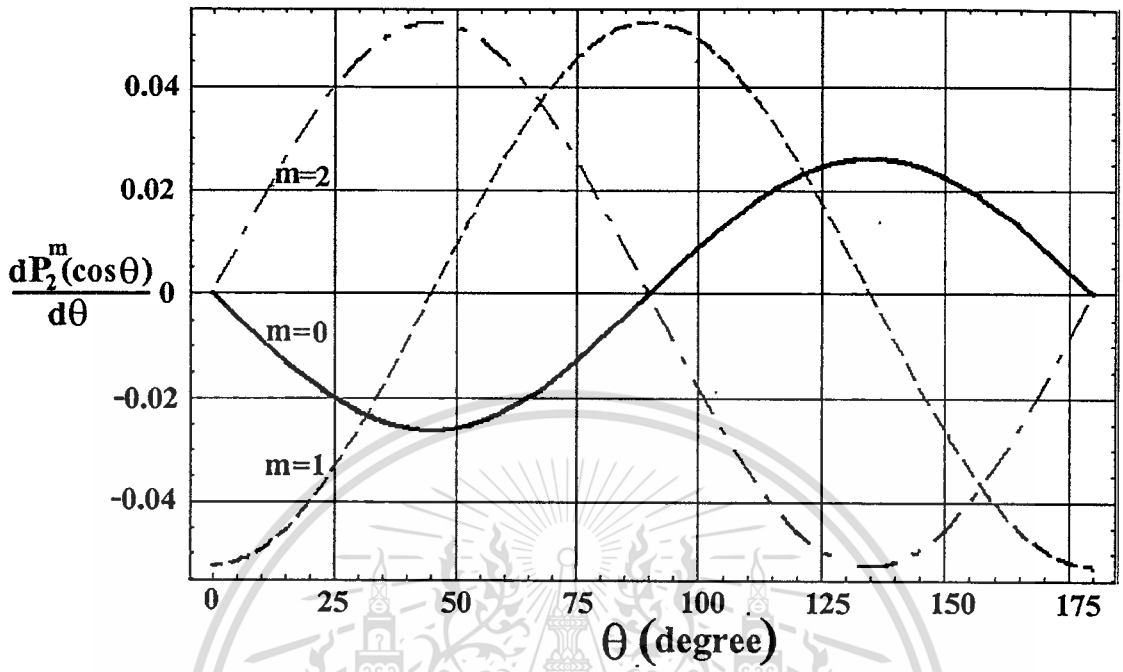

Fig.17 Graphical characteristic in the elevation angle direction for TE mode (varied *m=0,1,2,* fixed *n=2*)

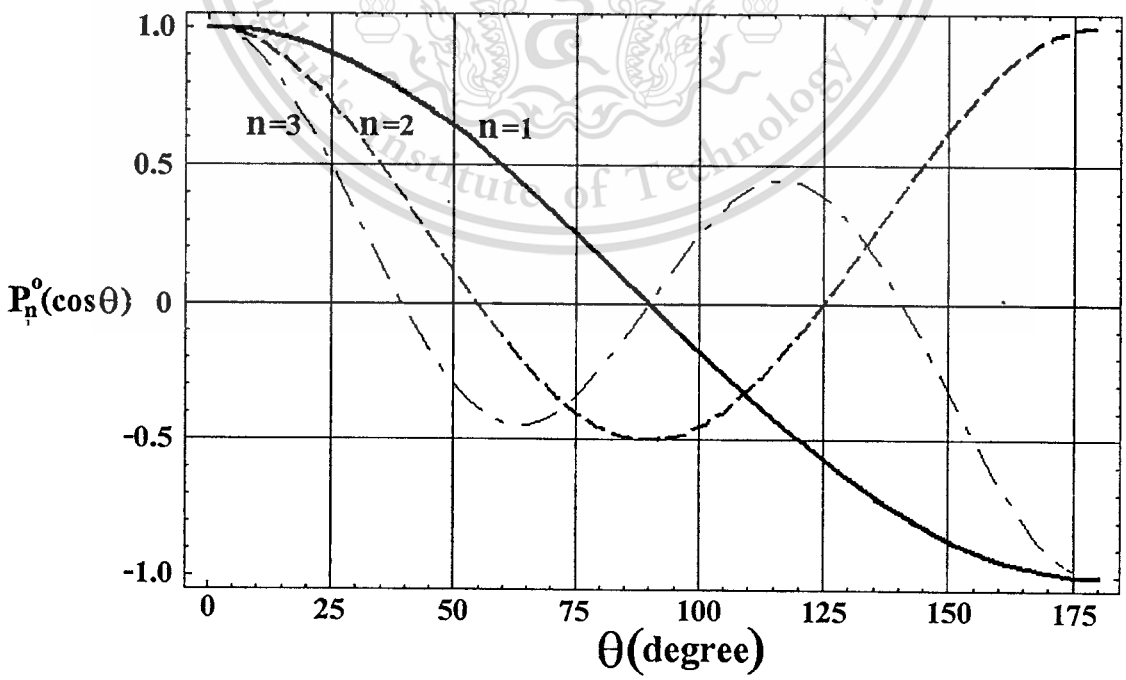

Fig.18 Graphical characteristic in the elevation angle direction for TM mode(fixed *m=0*, varied *n=1,2,3*)

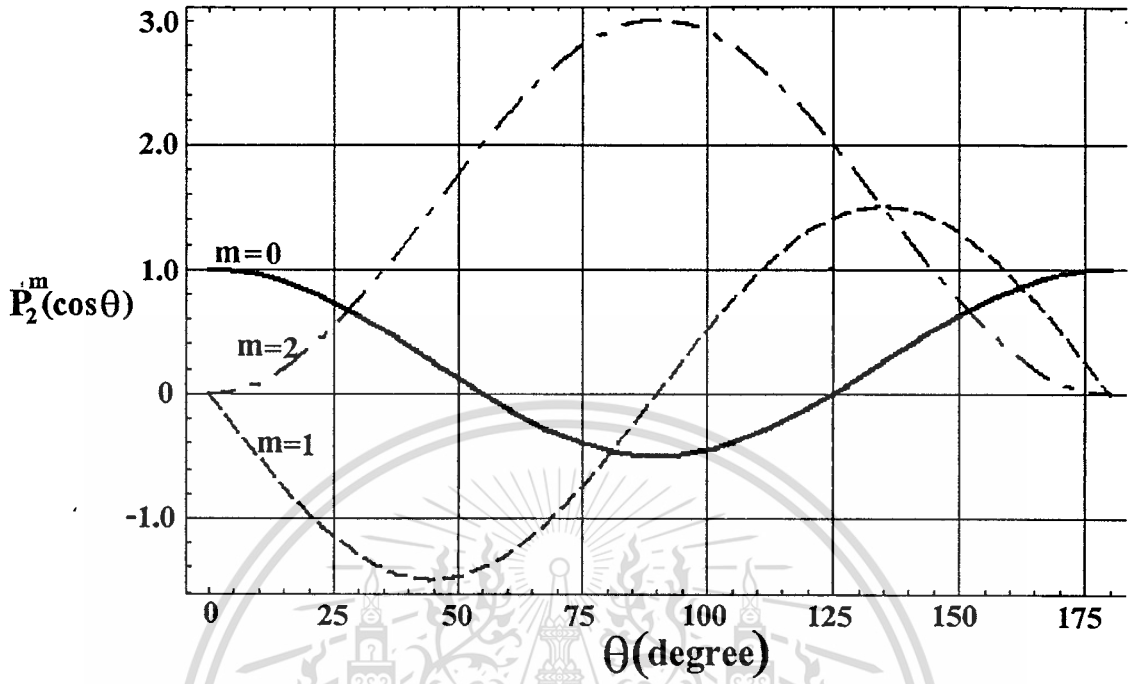

Fig.19 Graphical characteristic in the elevation angle direction for TM mode (varied *m=0,1,2,* fixed *n=2*)

The relation between that mode (*m,n*) and the conical angle (θ_c) could be accomplished by using the graphical method which is shown above or the sacant method which the results after some lengthy manipulations are summarized for *m=0,1,2* and *n=0,1,2* in table 4 for TM mode and table 5 for TE mode.

Table 4 Relationship between the mode number TM_{mnl} and the conical angle (θ_c)

m	*n*	$\theta_c(°)$
0	*1*	*90.00*
0	*2*	*54.74* *125.26*
0	*3*	*39.23* *90.00* *140.77*
1	*2*	*0.00* *90.00* *180.00*
2	*2*	*0.00*

Table 5 Relationship between the mode number TE_{mnl} and the conical angle (θ_c)

m	n	$\theta_c(°)$
0	1	0.00
0	2	0.00 90.00
0	3	0.00 63.43 116.57
1	2	45.00 135.00 180.00
2	2	0.00 90.00

Eventually, the electric and magnetic field of the fundamental TM_{011} mode and the higher order (TM_{021} and TM_{111}) are demonstrated. The electric and magnetic fields for the concentric conducting spherical cavity are summarized as follows:

$$E_R = -\frac{n(n+1)}{j\omega\mu\varepsilon}[B'_{mn}\hat{J}_n(kR)+C'_{mn}\hat{Y}_n(kR)]P_n^m(\cos\theta)\begin{Bmatrix}\cos\\ \sin\end{Bmatrix}m\phi \qquad (5.28)$$

$$E_\theta = \frac{1}{j\omega\mu\varepsilon}\frac{1}{R}\frac{d[B'_{mn}\hat{J}_n(kR)+C'_{mn}\hat{Y}_n(kR)]}{dR}\frac{dP_n^m(\cos\theta)}{d\theta}\begin{Bmatrix}\cos\\ \sin\end{Bmatrix}m\phi \qquad (5.29)$$

$$E_\phi = \pm \frac{m}{j\omega\mu\varepsilon} \frac{1}{R\sin\theta} \frac{d[B_{mn}^{(')} \hat{J}_n(kR) + C_{mn}^{(')} \hat{Y}_n(kR)]}{dR} P_n^m(\cos\theta) \begin{Bmatrix} \sin \\ \cos \end{Bmatrix} m\phi \quad (5.30)$$

$$H_R = 0 \quad (5.31)$$

$$H_\theta = \pm \frac{m}{\varepsilon} \frac{1}{R\sin\theta} [B_{mn}^{(')} \hat{J}_n(kR) + C_{mn}^{(')} \hat{Y}_n(kR)] P_n^m(\cos\theta) \begin{Bmatrix} \sin \\ \cos \end{Bmatrix} m\phi \quad (5.32)$$

$$H_\phi = \frac{1}{\varepsilon} \frac{1}{R} [B_{mn}^{(')} \hat{J}_n(kR) + C_{mn}^{(')} \hat{Y}_n(kR)] \frac{dP_n^m(\cos\theta)}{d\theta} \begin{Bmatrix} \cos \\ \sin \end{Bmatrix} m\phi . \quad (5.33)$$

The aspect of these fields are realized by plotting the electric and magnetic fields in each component versus the abscissas in the spherical coordinate.

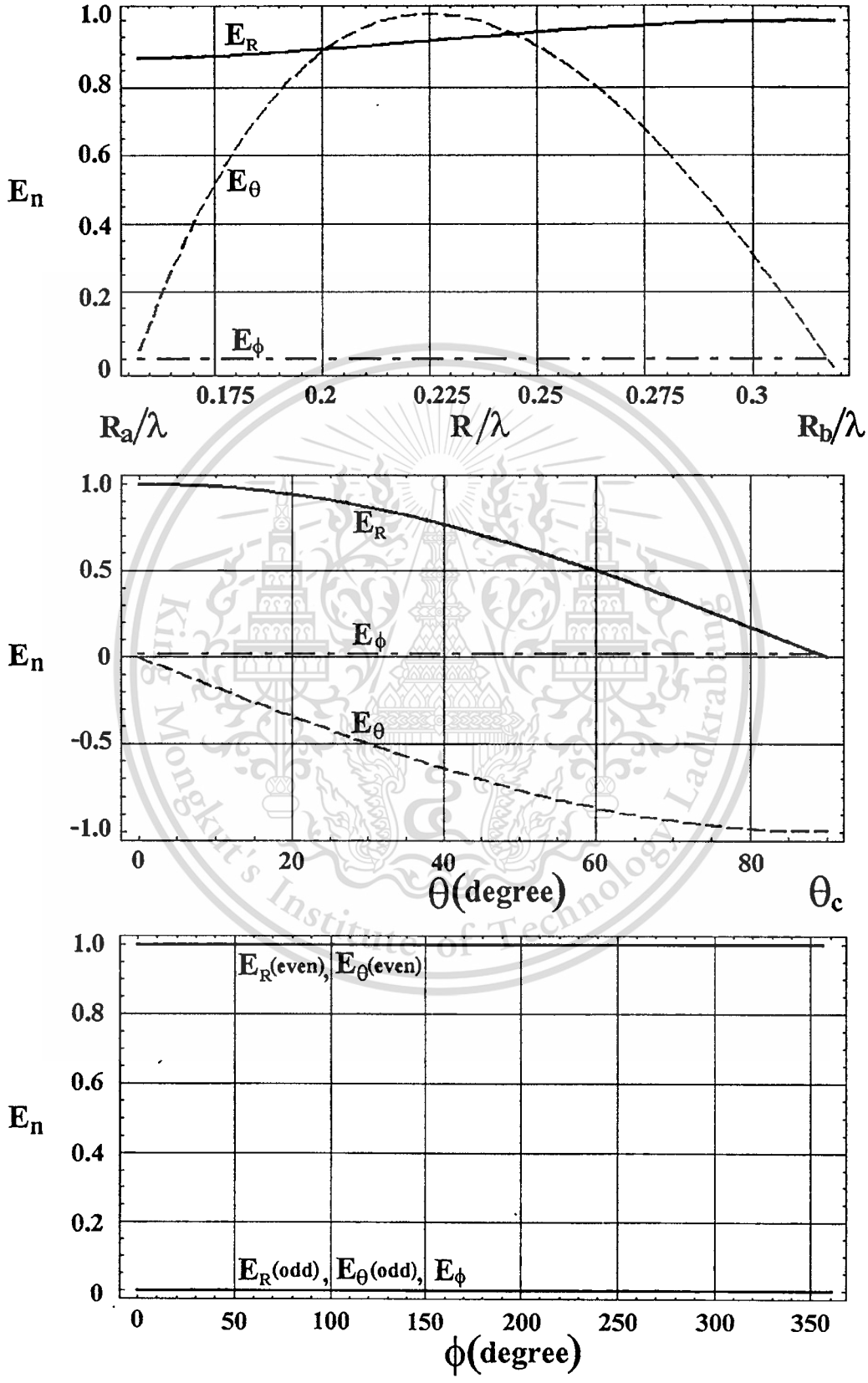

Fig.20 Electric field of the TM_{011} mode

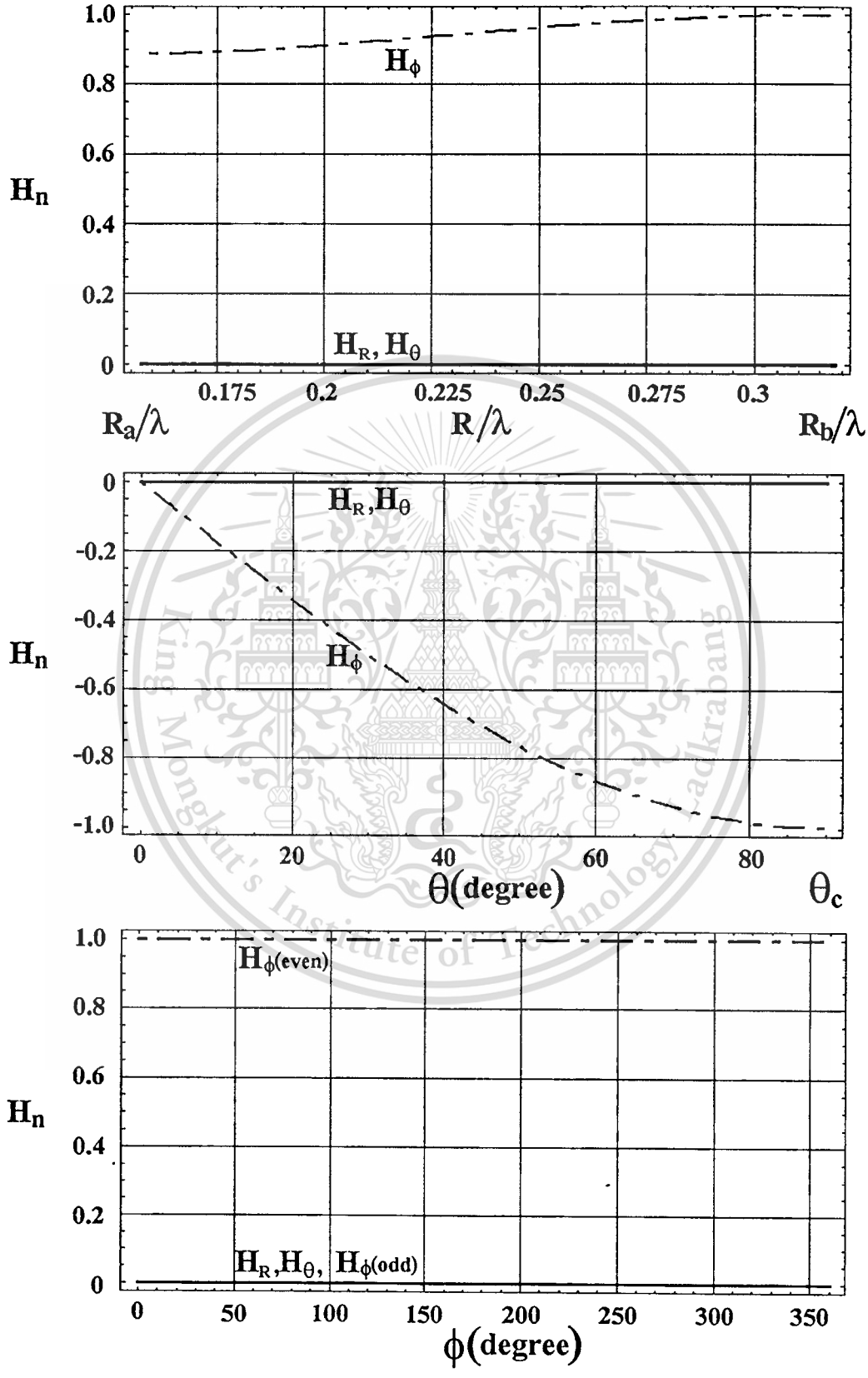

Fig.21 Magnetic field of the TM_{011} mode

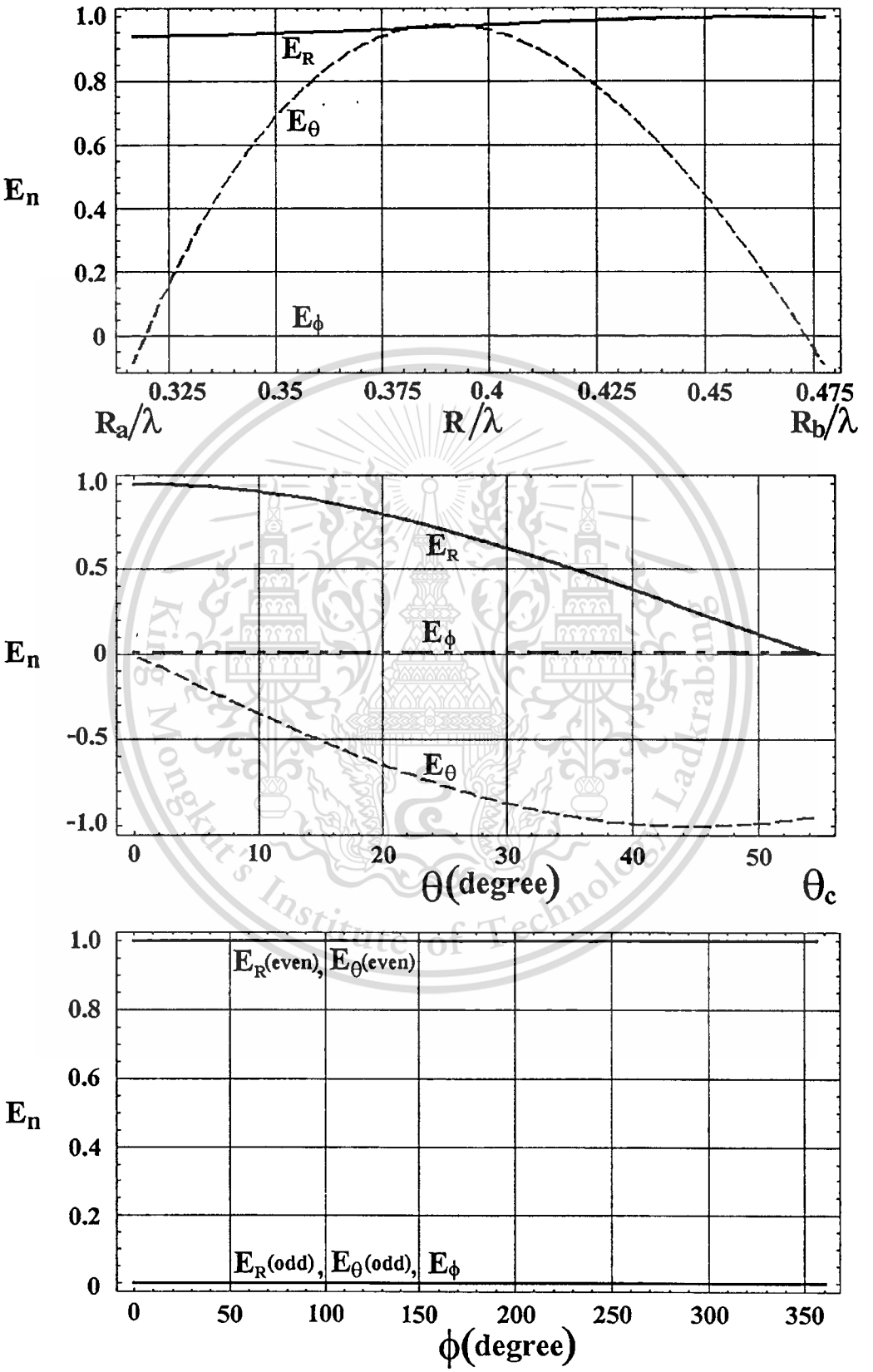

Fig.22 Electric field of the TM_{021} mode

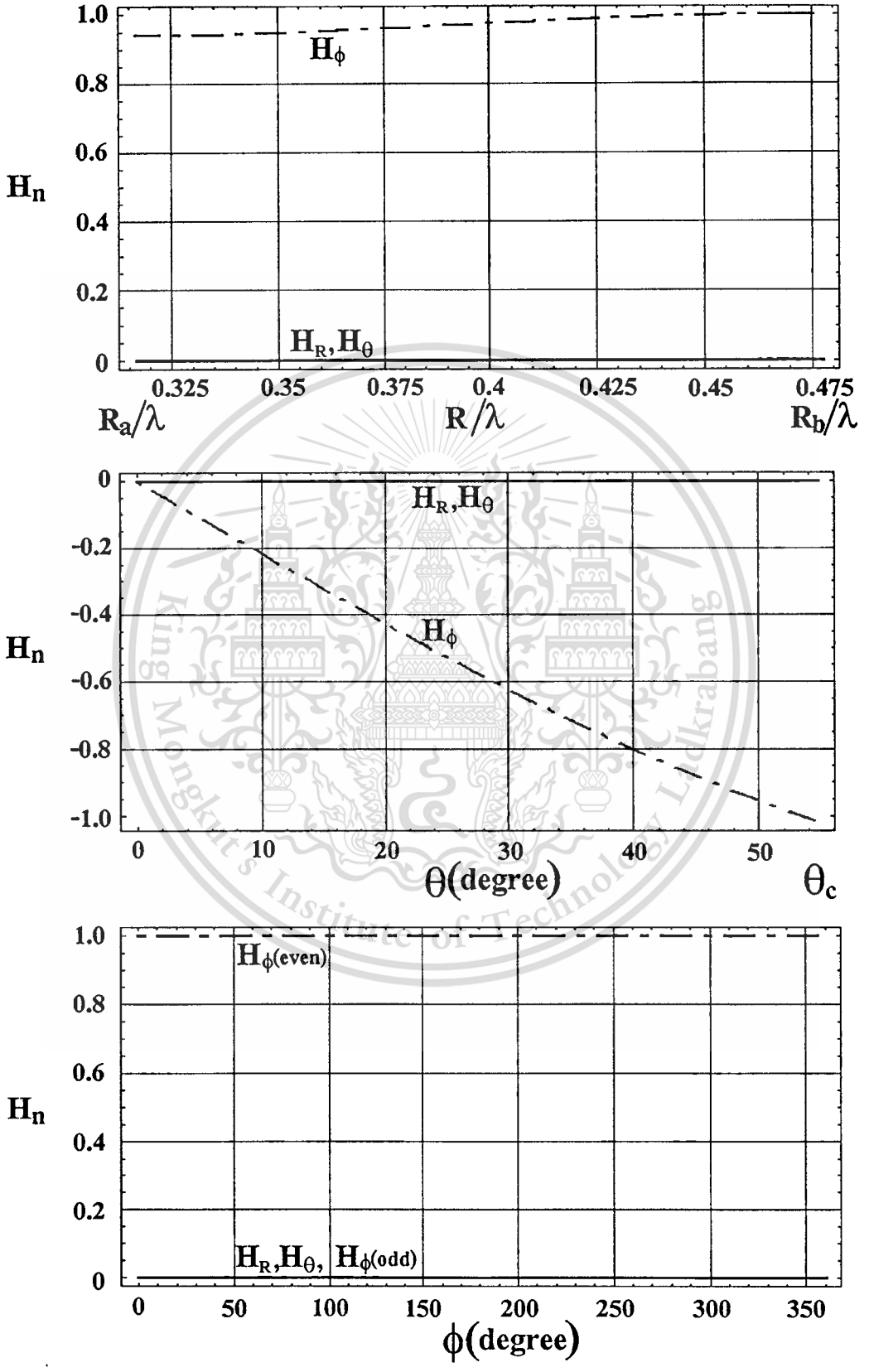

Fig.23 Magnetic field of the TM_{021} mode

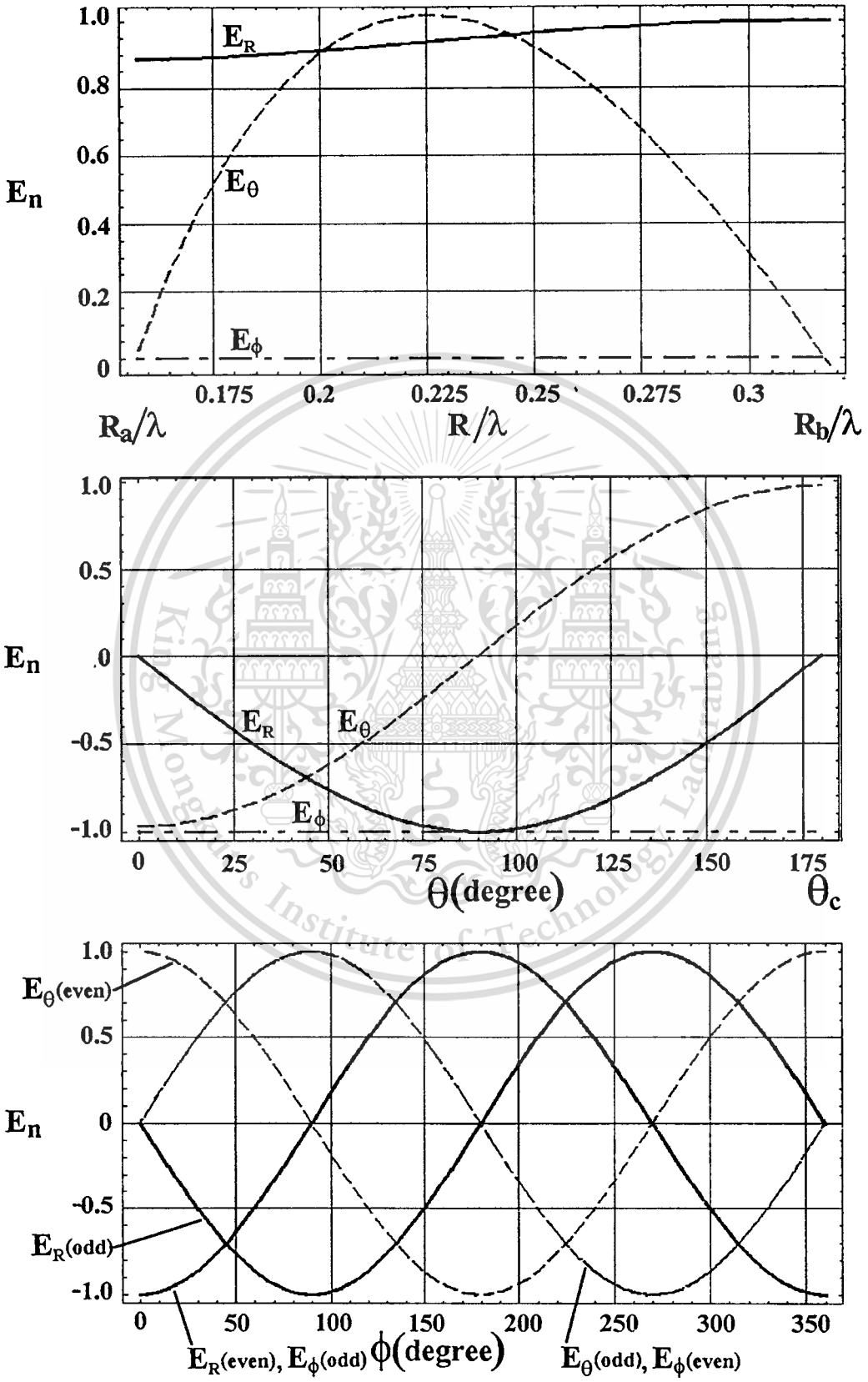

Fig.24 Electric field of the TM_{111} mode

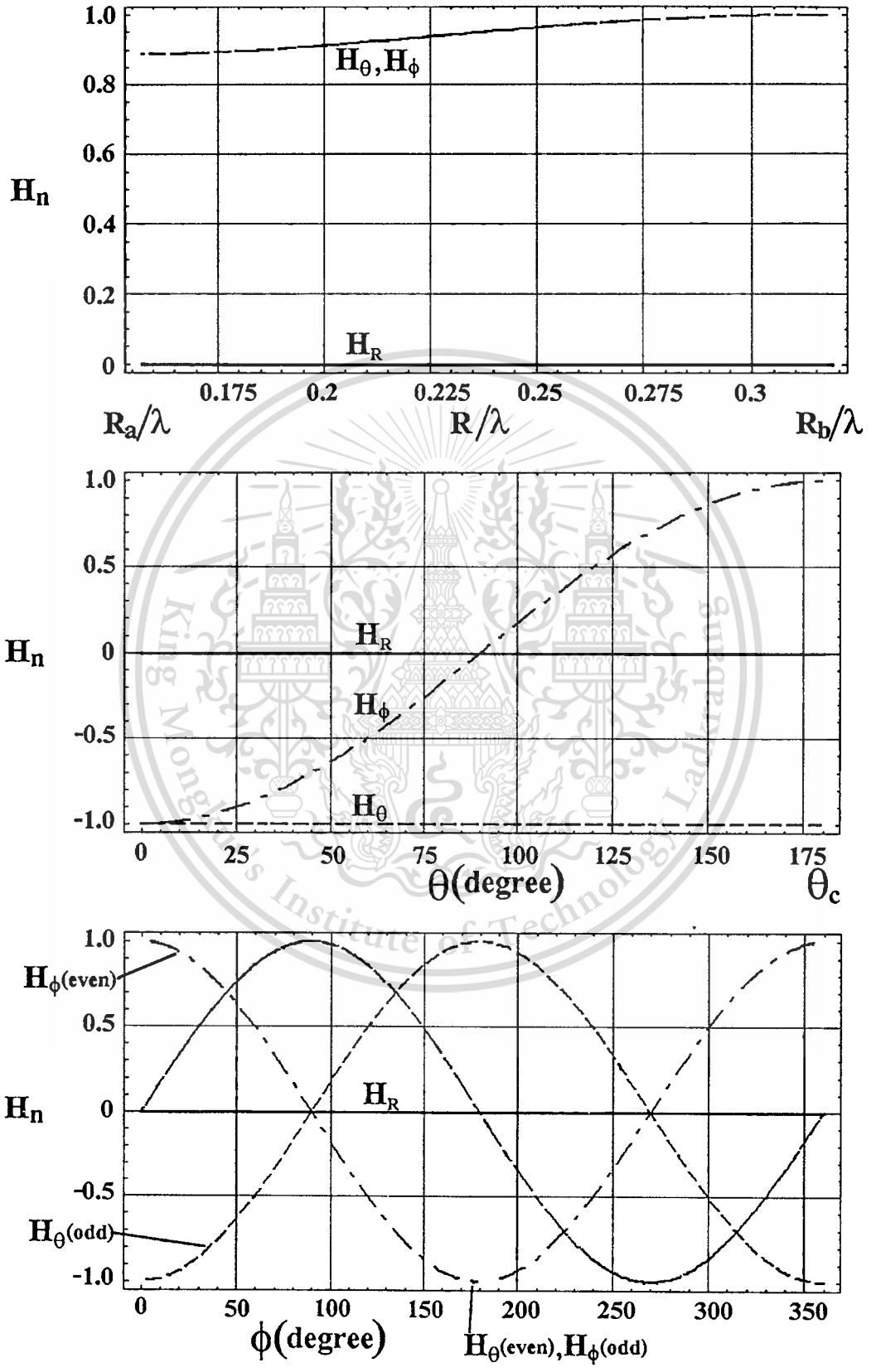

Fig.25 Magnetic field of the TM_{111} mode

5.3 Conclusions

Numerical results of the eigenmodes and electromagnetic fields of the conducting spherical cavity and the concentric conducting spherical cavity are realized by using the expression which is derived in chapter 3. By this powerpoint, the futher application of these fields can be applied to determine the position of the slot orientation on the spherical surface such as the concentric conducting spherical cavity-backed slot array antenna which will be presented in the next chapter.

References

[5-1] S.C.Chapra and R.P.Canal, *Numerical Methods for Engineers*, McGraw-Hill, New York, 1990.

Chapter 6

A Concentric Conducting Spherical Cavity-Backed Slot Array Antenna

Electromagnetic field inside a concentric conducting spherical cavity, which is formulated in the preceding chapters, is utilized in designing a concentric conducting spherical cavity-backed slot array antenna such as a circularly polarized conical beam spherical slot array antenna. The details of such typical antenna will be presented in this chapter.

A circularly polarized conical beam spherical slot array antenna is proposed for a low elevation angle land mobile satellite communication subscriber. The structure of this antenna type is very simple to fabricate i.e., the ring of the perpendicular slot pairs cut on an outer surface of a concentric conducting spherical cavity. From the assumption of the weak coupling of the slots from the cavity, the conical beam pattern can be obtained. However, the circular polarization characteristic must be improved by using traveling wave design of the exciting structure which is left for further study. Experimental results, that verify the conical beam radiation are in good agreement with the design.

6.1 A Circularly Polarized Conical Beam Spherical Slot Array Antenna

Conical beam antenna is widely used in a low bit rate or a low G/T land mobile satellite communication subscriber [6-1] in addition to the wireless LAN basestation [6-2]. Recently, Takada, *et.al.*, [6-3] developed the so-called circularly polarized conical beam radial line slot antenna which a circular array of slot pairs was excited by a radial line waveguide. This antenna radiated a circularly polarized conical beam pattern. However, it was found that the beam direction was about $30°$ from broadside. Therefore, the elevation angle of the beam is relatively high. To lower the elevation angle, to apply this antenna to the land mobile satellite subscriber located far from the equator, Takada, *et.al.*, [6-4]-[6-6] proposed the rotating mode generator to feed the slot array antenna. The requirement was accomplished at some expenses of gain degradation and more complicated feeding structure.

The objective of this presentation is to propose a simple structure circularly polarized conical beam antenna which provides a pattern in an elevation plane directs toward a low angle direction. The design of this antenna are discussed and experimental results which demonstrate the conical beam pattern with low elevation angle are included.

6.2 Antenna Structure

A circularly polarized conical beam spherical slot array antenna consists of a number of perpendicular slot pairs cut on an outer surface of a concentric conducting spherical cavity. They are arranged as a ring along an azimuthal circumference of the spherical surface at the positions

that the adjacent pairs are out of phase to form a conical beam. Fig.26a shows the local coordinate of the slot element. Each slot on a pair is separated, along an elevation plane, at a distance so that the phase quadrature is obtained to provide a circularly polarized radiation. Fig.26b shows the perspective view of a circularly polarized conical beam spherical slot array antenna. One of the slots in a pair is oriented at $45°$ counterclockwise with respect to the horizontal line of the spherical surface whereas the perpendicular counterpart is oriented at an angle of $135°$.

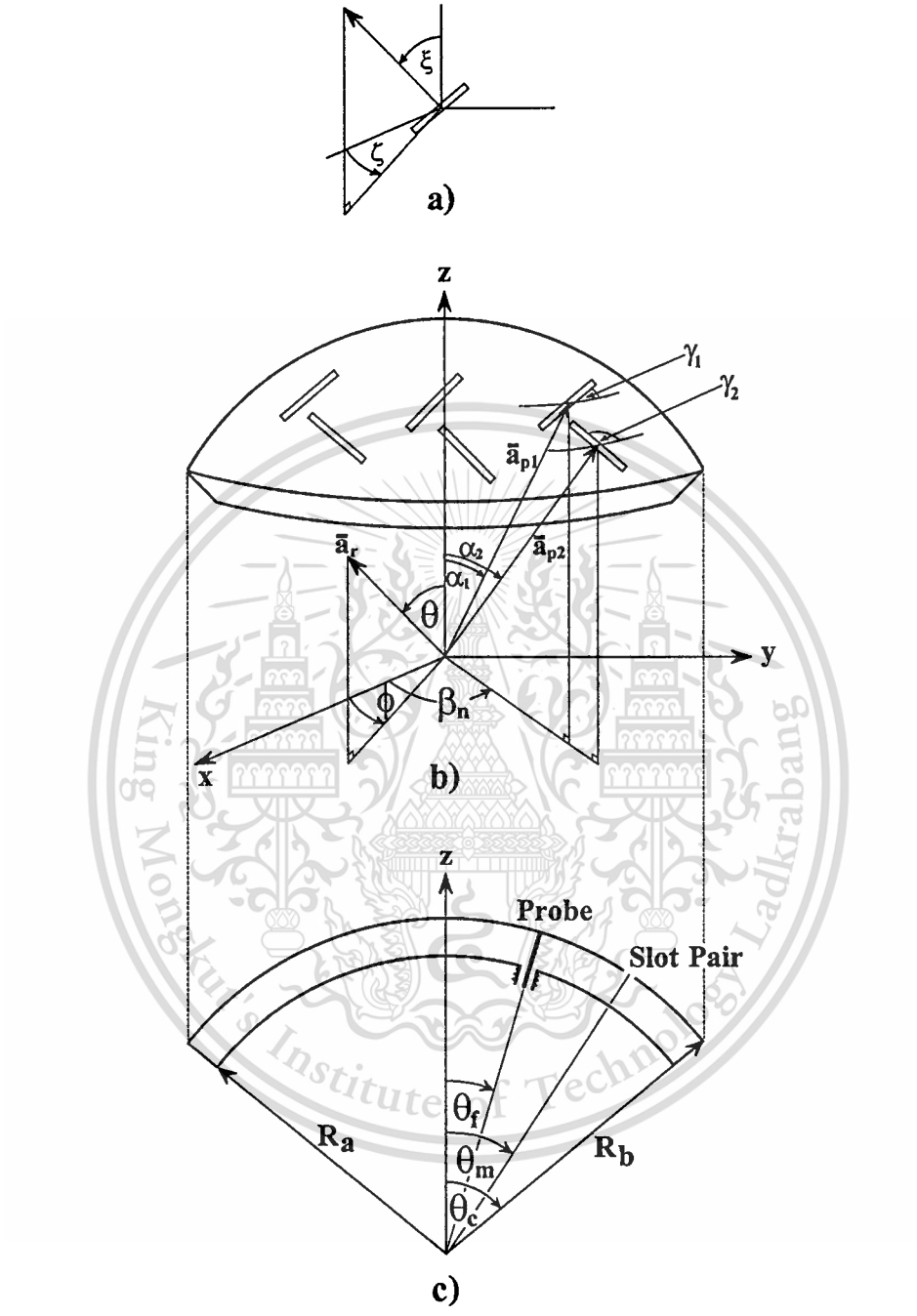

Fig.26 Geometry of a circularly polarized conical beam spherical slot array antenna

a) local coordinate of the slot element

b) perspective view

c) cross section view

Fig.26c shows the cross section view of the antenna. The inner and outer radii of the concentric conducting spherical cavity are R_a and R_b , respectively. These spherical conductors are closed by a conical conductor at an angle θ_c. The cavity is excited by a linear probe oriented along a radius at the position

$R_a \leq R \leq R_b$, $\theta = \theta_f$, $\phi = 0$. The center of each slot pair is located at the position where maximum surface current density occurs and it is denoted by an angle θ_m. Each slot in a pair is offset from this position in different direction so that phase quadrature between these slots is obtained. By this way, the weak coupling of the slots from the cavity is assumed.

From the antenna configuration in this case, the linear probe places along the radial direction. By considering the electric dyadic Green's function and the source function, it is obvious that the transverse magnetic mode was excited only [6-7]. It was found from [6-8] that the spherical radii can be determined from the characteristic equation

$$\frac{j_n'(kR_a)}{y_n'(kR_a)} = \frac{j_n'(kR_b)}{y_n'(kR_b)}, \tag{6.1}$$

where $j_n'(*)$ and $y_n'(*)$ denote the derivative with respect to the argument of the spherical Bessel functions of the first and second kinds of order n, respectively and k represents the propagation constant of the medium inside the cavity.

We can find the conical angle θ_c by using the relation that the electric field in radial direction at the boundary vanishes, thus

$$P_n^m(\cos\theta)\Big|_{\theta=\theta_c} = 0, \tag{6.2}$$

where $P_n^m(\cos\theta)$ denotes the associated Legendre function of the first kind of order *(n,m)*. Moreover, *m* represents the number of cycle of field variation in ϕ direction.

The position of the slot pair excitation θ_m is chosen where the surface current density is maximum. It can be found by maximizing that

$$\theta_m\Big|_{\theta}^{max} \frac{dP_n^m(\cos\theta)}{d\theta}. \tag{6.3}$$

The probe is located at an angle θ_f where

$$\theta_f\Big|_{\theta}^{max} P_n^m(\cos\theta) \tag{6.4}$$

is satisfied.

To obtain the right-hand circular polarization, we employ two perpendicular slots which are equally amplitude and quadrature phase excited. Since the surface current density that excites the slots is proportional to E_θ and H_ϕ which are proportional to the derivative of the associated Legendre function of cosine of angle θ [6-9] that is

$$E_\theta, H_\phi \propto \frac{dP_n^m(\cos\theta)}{d\theta}, \tag{6.5}$$

therefore, the orientation of these slots are $45°$ and $135°$ with respect to the horizontal line where the surface current density is maximum. The spacing between the center of these two slots along the elevation plane is adjusted so that phase difference of E_θ is $90°$. The slot array consists of a number of slot pairs arranged in the same manner as described above at the position so that the spacing between the center of each slot pair is equal to $2m\pi/N$ (N is the number of slot pairs).

6.3 Radiation Characteristics

According to fig.26b, the slot number *1* and *2* in a slot pair are oriented so that the inclination with the horizontal level are γ_1 and γ_2, respectively. Let us consider the half wavelength slot which is shown in fig.26a. The radiation pattern of each slot is manipulated by [6-10] and denoted by $f(R_b,\xi,\zeta)$, where (R_b,ξ,ζ) is the local coordinate of each slot. To provide the right-hand circular polarization from N slot pairs, the total electric field of the spherical slot array is formulated as [6-11]-[6-13]

$$\bar{E}(\theta,\phi) = \sum_{n=1}^{N}[\sum_{m=1}^{2}\{f(R_b,\xi,\zeta)(\bar{a}_\theta \sin\gamma_m - \bar{a}_\phi \cos\gamma_m) \times e^{jk[(\bar{a}_r,\bar{a}_{pm})+j\psi_{mn}]}\}] \quad (6.6)$$

where ψ_{mn} is the phase of the slot number m of the pair number n. It is noted that the phase difference of the two slot is $90°$. $\bar{a}_r$ and $\bar{a}_{pm}$ are the position vectors of the field point and the position of the slot number m, respectively, and are given by

$$\bar{a}_r = (\sin\theta\cos\phi, \sin\theta\sin\phi, \cos\theta) \tag{6.7}$$

$$\bar{a}_{pm} = R_b(\sin\alpha_m\cos\beta_n, \sin\alpha_m\sin\beta_n, \cos\alpha_m) \tag{6.8}$$

To analyze a six slot pairs circularly polarized conical beam spherical slot array antenna, directivity was calculated as a function of outer spherical radius (R_b) and the slot position (θ_m). Fig.27a illustrates patterns in an elevation plane of the antenna when R_b equals 1.43λ. It is apparent that the conical beam is obtained and the elevation angle is lowered when θ_m is small. The contour of directivity when R_b equals λ is shown in Fig.27b. We can observe that the antenna provides a $9\ dB_i$ directivity in the elevation angle direction $55°$ when the slot position is at $50°$. For the desired directivity $8\ dB_i$, on the $8\ dB_i$ contour, an appropriate slot position that lower the elevation angle to $70°$ at an angle θ_m is equal to or less than $18°$ can be chosen. Fig.27c shows the contour of directivity when θ_m is fixed at $40°$. If one chooses the spherical radius equals λ, a $8\ dB_i$ directivity can be obtained at the angle of $70°$. The contour of directivity illustrates that for the proper slot position and spherical radius, the directivity at particular direction can be designed.

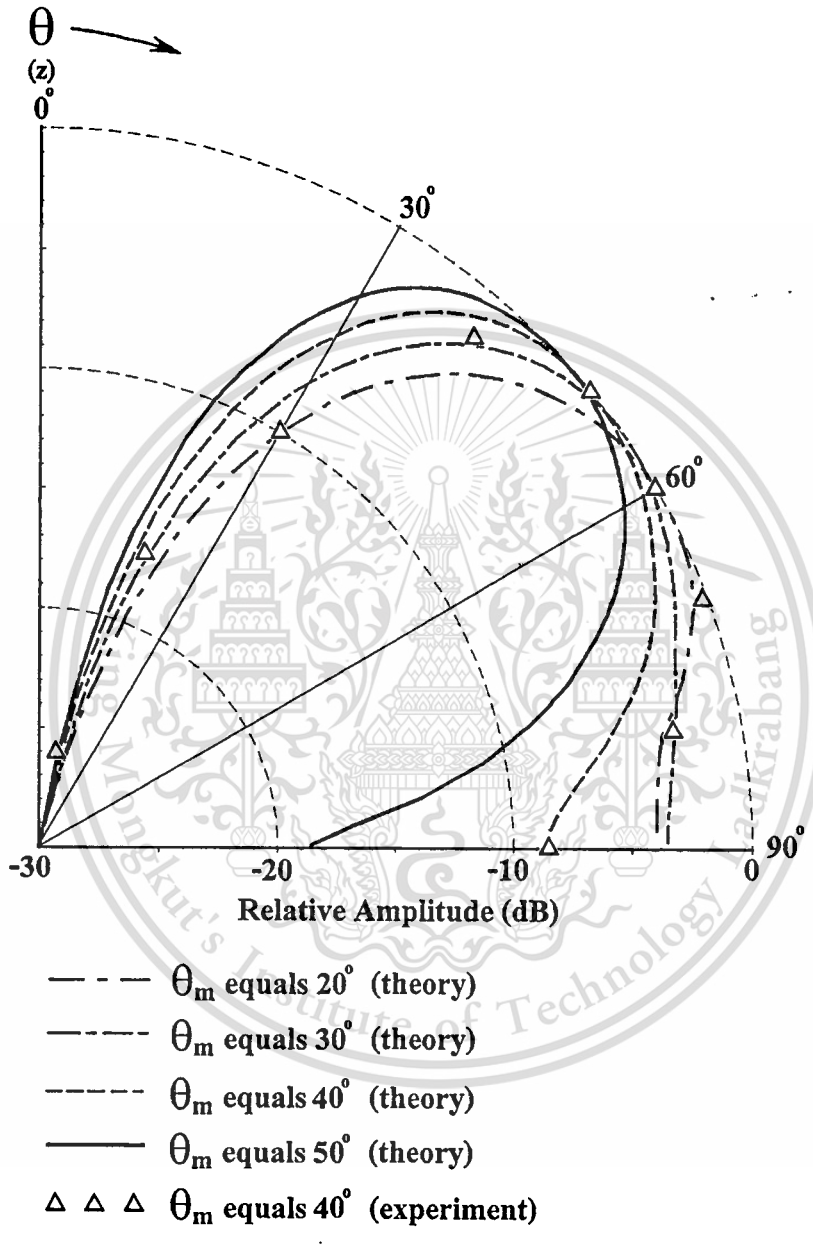

Fig.27 Radiation characteristics of a circularly polarized conical beam spherical slot array antenna

a) patterns in elevation plane

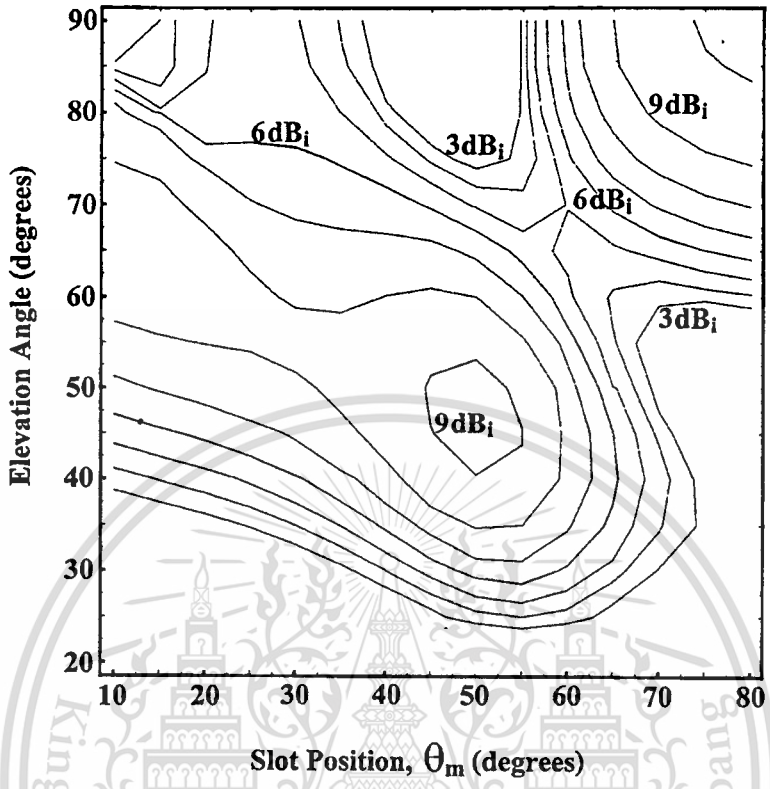

Fig.27(continued)

b) contour of directivity when R_b equals λ

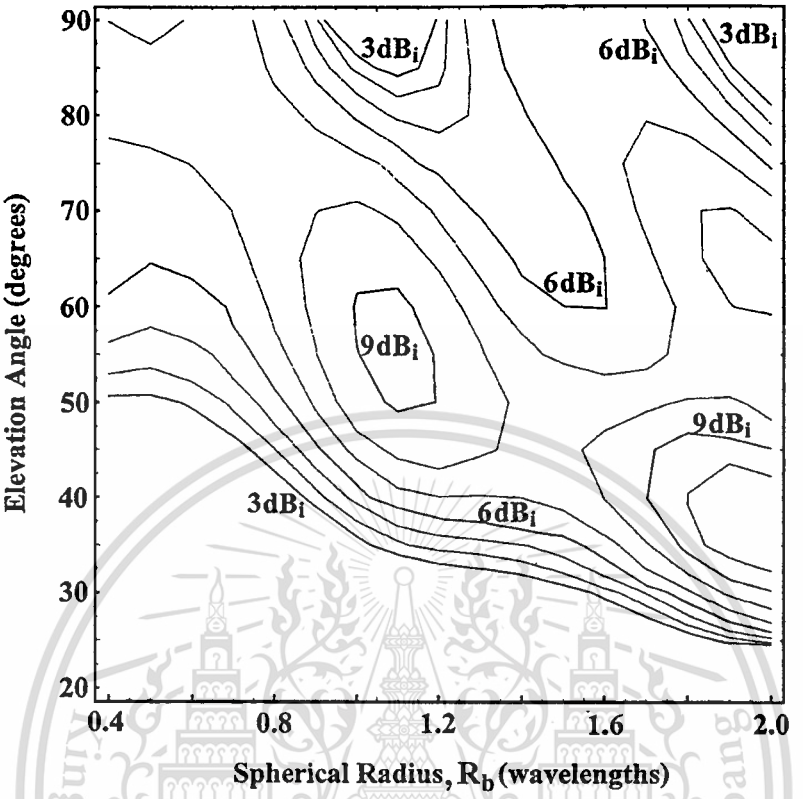

Fig.27(continued)

c) contour of directivity when θ_m is fixed at *40.00°*

Let us consider a pattern in the azimuthal plane of a conical beam spherical slot array antenna which has R_b equals 1.43λ in fig.28. The broken line shows the pattern of the antenna which has six slot pairs and are excited at θ_m equals *40°*. We can find that it is not uniform, the ripple of the pattern is in excess of *30* dB. When the number of slot pairs is increased to eight slot pairs as shown by the dashed line, the ripple is noticeably decreased to *4* dB. The uniform pattern can be achieved when the number of the slot pairs is twelve as illustrated by the solid line.

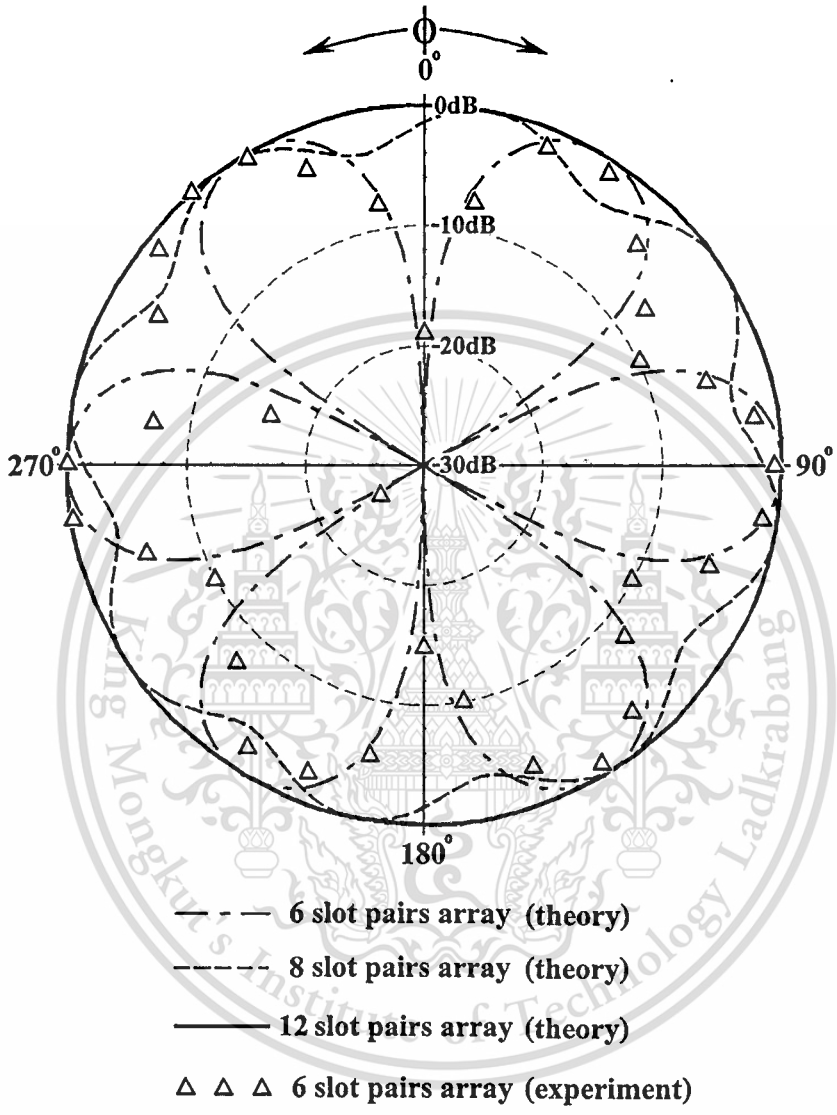

Fig.28 Patterns in the azimuthal plane

6.4 Antenna Design

For a specified directivity, the number of slot pairs, the outer spherical radius and the slot position will be determined. To design a

circularly polarized conical beam spherical slot array antenna, the concentric conducting spherical cavity is designed to excite the slot array first. When the number of slot pairs is fixed, the mode number m (the number of cycle along the tangential circumference of the cavity) can be determined to be one half of the number of slot pairs. We found from (6.1) that the spherical radii depend on the mode number n, therefore, n must be appropriately chosen for a particular directivity. Since the field distribution in the cavity depends on the mode of the cavity, hence the dimension, the slot position and the feed probe position are different. Fig.29 and fig.30 show the graphical characteristic in the radial and the elevation angle direction of the TM_{mn} mode for fixed $m = 3$ and varied $n = 6, 7, 8$ and varied $m = 3,6$, fixed $n = 8$. To estimate the orientation of the slot and the probe position, the electric and magnetic fields are revealed as depict in fig.31 and fig.32, respectively.

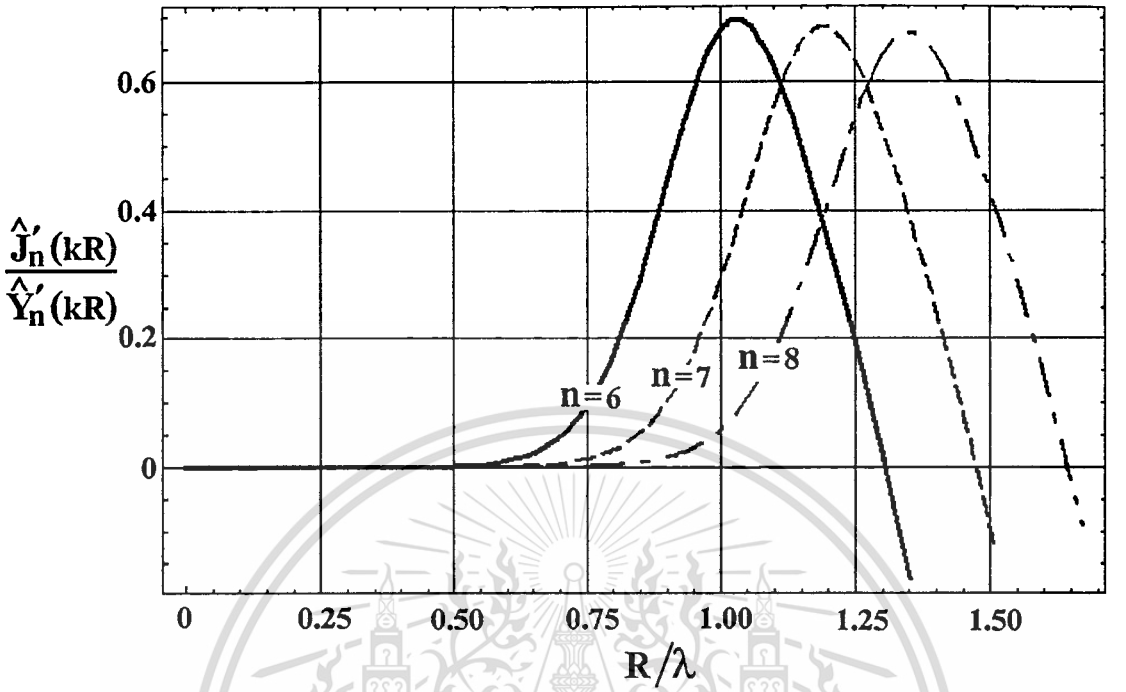

Fig.29 Graphical characteristic in the radial direction of the TM_{mn} mode (n=6,7,8)

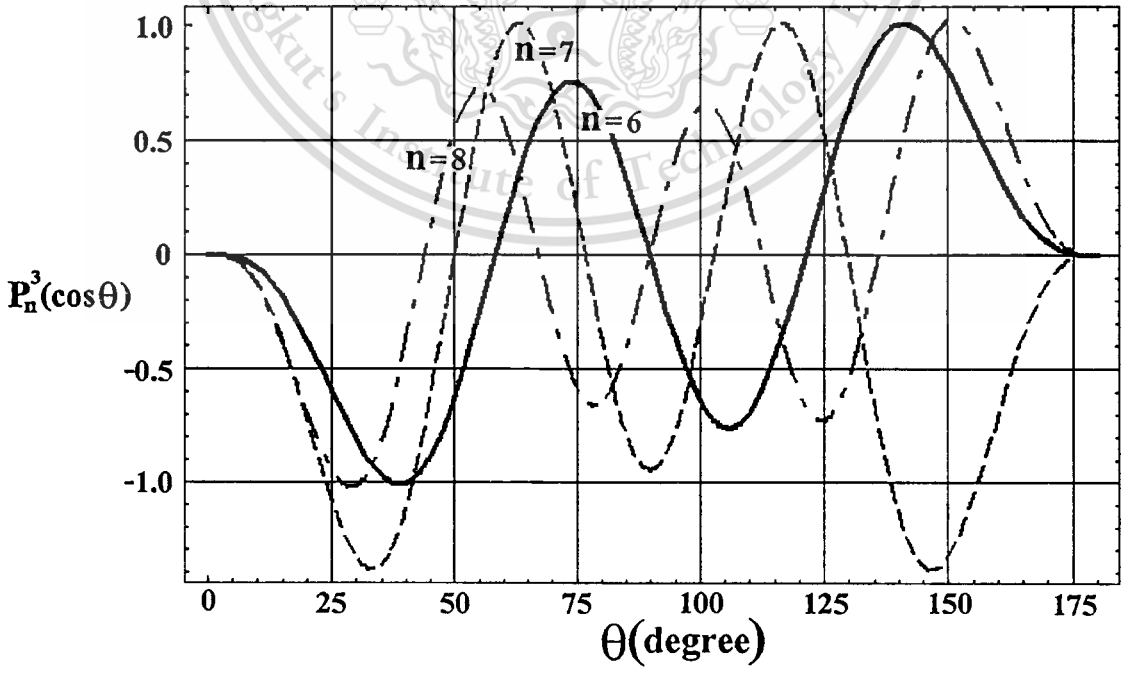

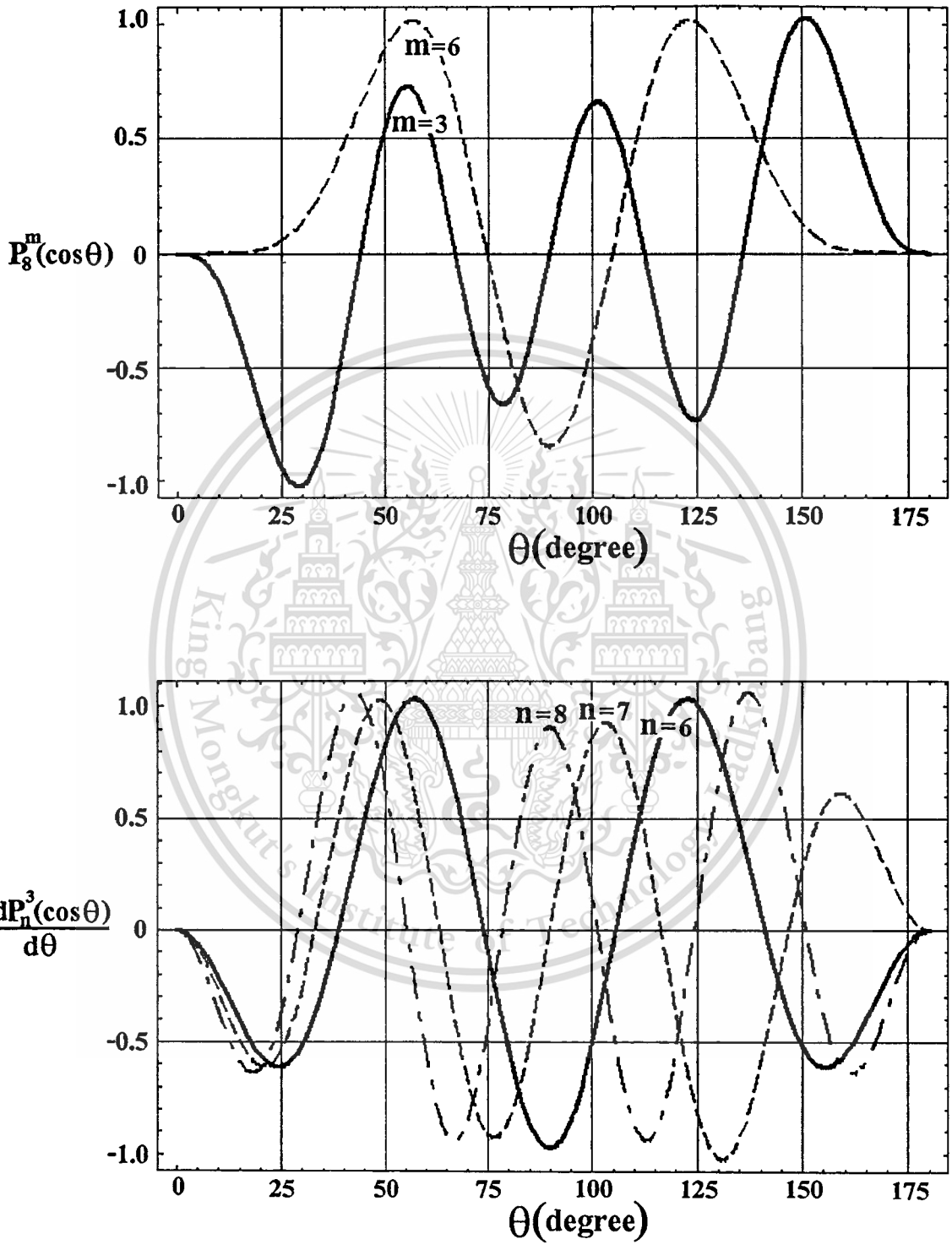

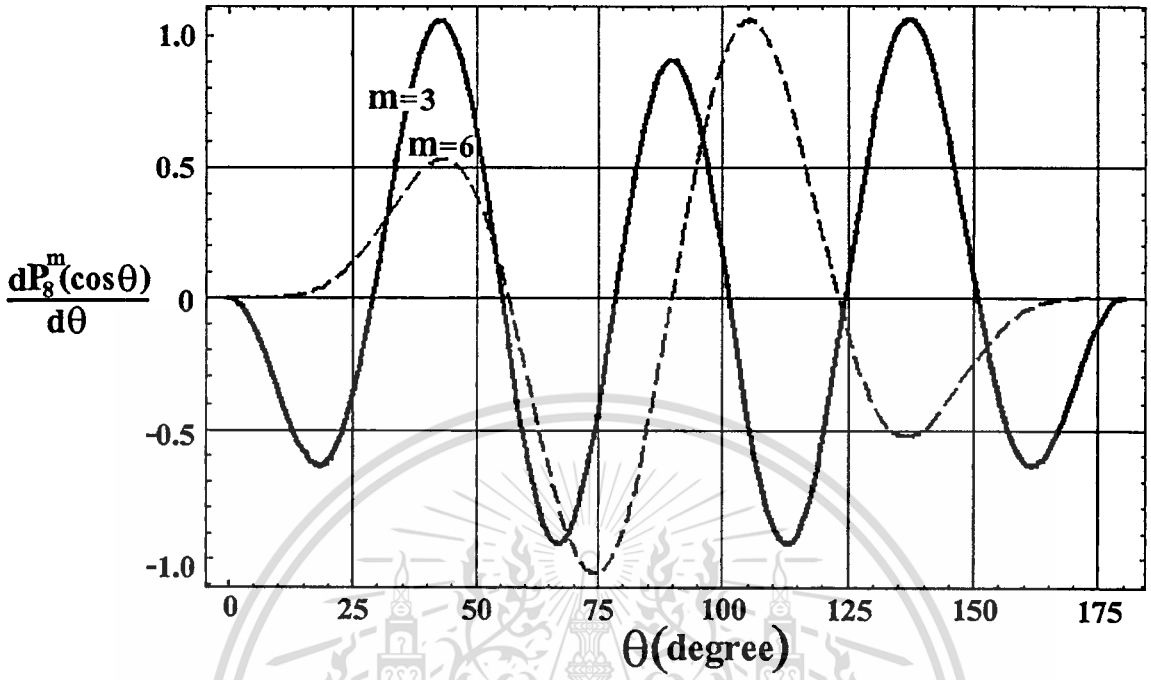

Fig.30 Graphical characteristics in the elevation angle direction of the TM_{mn} mode (m=3,n =6,7,8 and m=3,6,n=8)

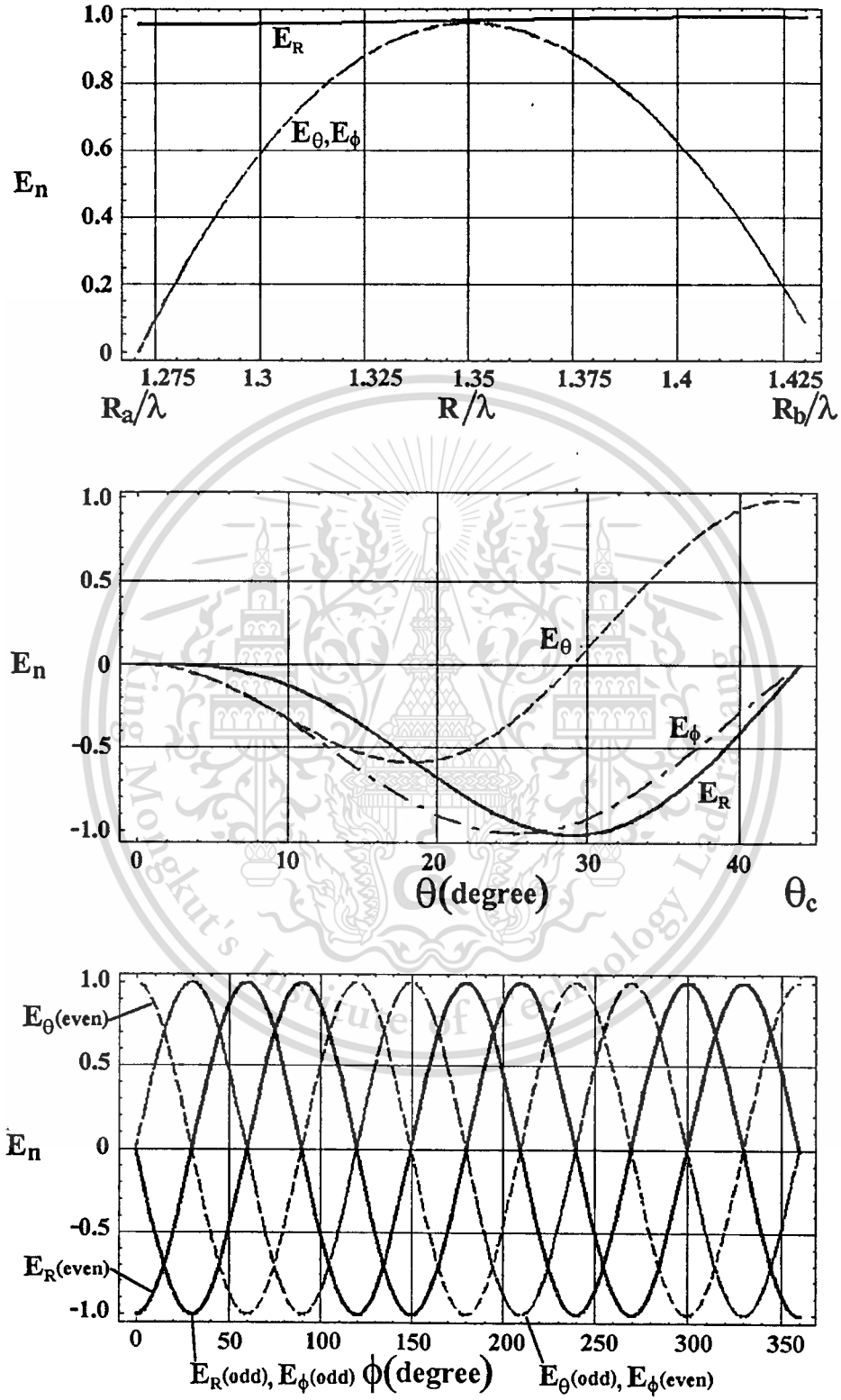

Fig.31 Electric field of TM_{38} mode

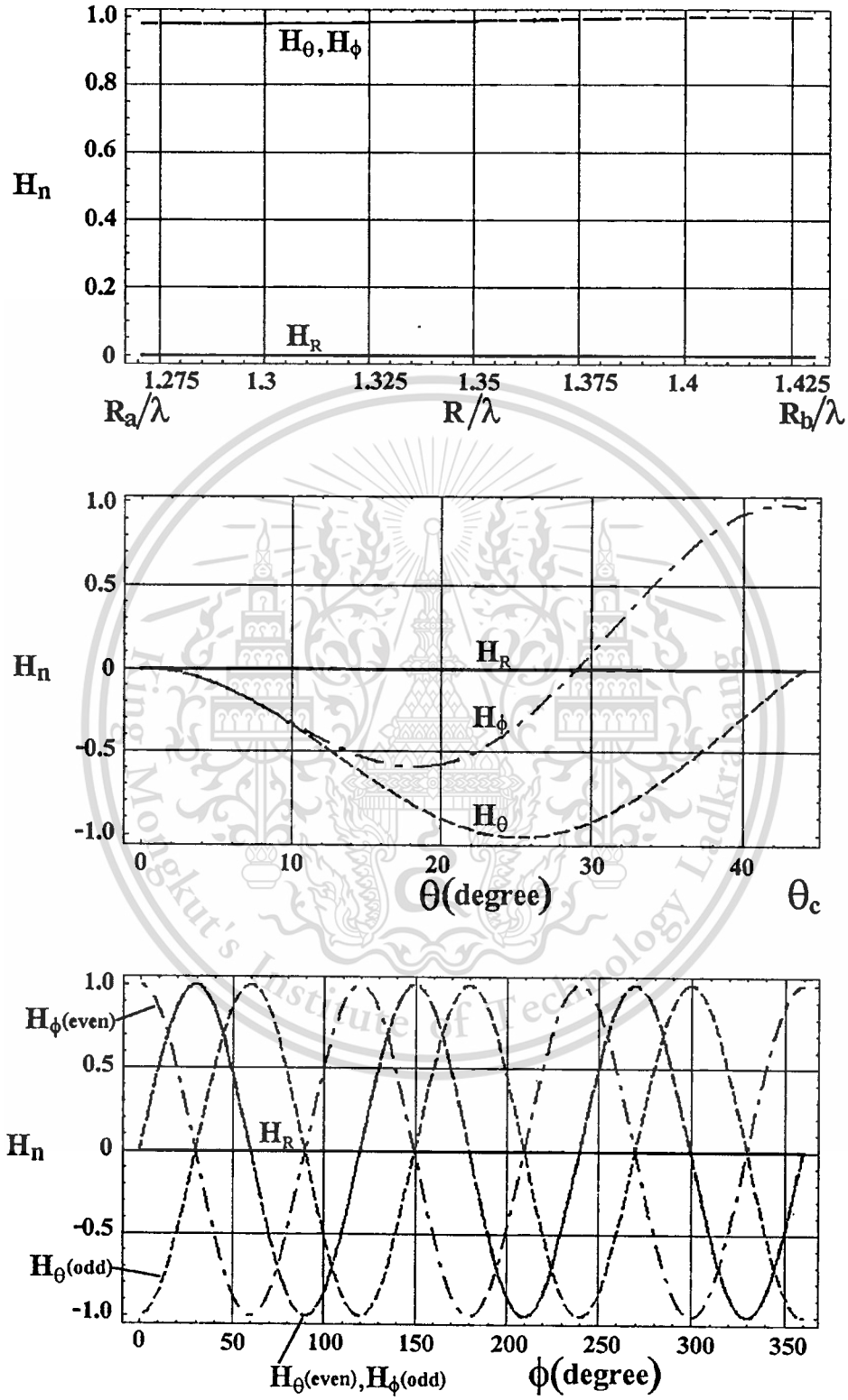

Fig.32 Magnetic field of TM_{38} mode

Table 6 summarizes the aforementioned quantity for four different mode cavities. In case of TM_{38}, for instance, the ratio of outer radius to inner radius is *9:8* and the outer spherical radius is 1.43λ. The conical angle can be at $43.96°$, $67.34°$ or $90.00°$ while the feed probe position is either at $29.08°$ or $55.42°$. The slot position is either at $16.19°$, $42.77°$ or $64.94°$. Let us compare the quantities of TM_{38} and TM_{68} modes surrounded by dashed lines, we can realize that eventhough they are somewhat different but the outer radius and the slot position (θ_m) are not significantly different. In this case, we can excite the different mode cavities with similar dimension of the outer radius and slot position. Therefore, the number of slot pairs can be increased to provide uniform azimuthal pattern by using the same size antenna.

Table 6 Dimensions of a concentric conducting spherical cavity, the feed probe position and the slot position

mode	R_b:R_a	R_b/λ	$\theta_c(°)$	$\theta_f(°)$	$\theta_m(°)$
TM_{36}	7:6	1.11	58.52	38.83	24.45
			90.00	74.12	57.26
			121.48		90.00
TM_{37}	8:7	1.27	50.16	33.22	20.91
			76.93	63.34	48.91
			103.07		76.64
TM_{38}	9:8	1.43	43.96	29.08	16.19
			67.34	55.42	42.77
			90.00		64.94
TM_{68}	9:8	1.43	75.04	56.79	41.13
			104.96	90.00	74.05

In the design, any values of those parameters can be chosen so that the antenna has the appropriated dimensions and slot position. After the cavity is designed and the probe position is set at $R_a \leq R \leq R_b$, $\theta = \theta_f$,$\phi = 0$ then the first slot pair is cut at a position ϕ equals $m\pi/N$ from the probe. The second slot pair which is at the position $2m\pi/N$ .The arrangement of the progressive slots are in the same as described above.

6.5 Experimental Results

From the design procedure as described in the previous section, for simplicity, the ring of six slot pairs circularly polarized conical beam spherical slot array antenna was designed to provide *7* dB_i directivity to verify the characteristics of the proposed antenna. The dimensions of this antenna is summarized in table 7. An antenna far-field test site was set up with the distance of *1* m (about twice of far field range). A *10*-turn helix was connected to HP 8720C network analyzer to transmit a right-hand circular polarized wave and the antenna under test was rotated to receive the transmitted wave at a *10°* per step. An output of antenna was connected to an HP8566B spectrum analyzer via a low noise block down converter. The pattern in the elevation plane is plotted and compared with the calculation as illustrated in fig.27. Fig.28 shows the azimuthal pattern in the beam peak direction. We can realize that the measured results in both planes are in good agreement with the predictions. The cross polarization patterns have been measured and found that it was rather high, the level is *-3* dB below the co-polar level. This might due to the radiated field is rather the linear polarization since quadrature phase between the slots in a pair is not realized. For impedance characteristic, the return loss is *-14* dB at the design frequency. It seems to be much better than one expected from weak coupling assumption.

Table 7 Dimensions of the antenna which is utilized in the experiment

operating frequency(f)	*3 GHz*
slot length(l)	0.5λ
operating mode	TM_{38}
outer:inner spherical radius(R_b:R_a)	*9:8*
outer spherical radius(R_b)	1.43λ
inner spherical radius(R_a)	1.27λ
conical angle(θ_c)	*67.34°*
center of slot array angle(θ_m)	*42.77°*
feed probe angle(θ_f)	*29.08°*

6.6 Conclusions

A circularly polarized conical beam spherical slot array antenna is proposed for applying to the land mobile satellite subscriber located far from the equator. The antenna consists of a ring of the perpendicular slot pairs cut on an outer surface of a concentric conducting spherical cavity which is very simple to fabricate. The design of the dimension of the concentric conducting spherical cavity, probe position and slot orientation on the spherical surface are obtained by using the electric

field inside the spherical cavity as derived in the previous chapter. However, since the purpose of this presentation is to demonstrate the practical application of the derivation and analysis of the electromagnetic field inside the concentric conducting spherical cavity, so the rigorous analysis of the complicate structure antenna is left for the further study.

It is found that the elevation pattern depends on the spherical radii and the position of the slot array on the spherical surface. The uniformity of the azimuth pattern depends on the number of the slot pairs. In this thesis, the slot coupling is assumed to be weak. This makes the phase quadrature to provide circularly polarized not realizable. The rigorous analysis of traveling wave in the exciting structure is under investigation.

References

[6-1] J.R.James and P.S.Hall, *Handbook of Microstrip Antennas*, Peter Peregrinus, London, 1989.

[6-2] Y.J. Guo, "A Circularly Patch Antenna for Radio LAN's," *IEEE Trans. Antennas Propagat*, vol. 45, pp. 177-178, 1997.

[6-3] J.Takada, A.Tanisho, K.Ito and M.Ando, "Circularly Polarised Conical Beam Radial Line Slot Antenna," *Electronic Letters*, vol. 30, pp. 1729-1730, 1994.

[6-4] J.Takada, A.Tanisho, K.Ito, M.Ando and N.Goto, "Radiation Characteristics of a Circularly Polarized Conical Beam Radial Line Slot Antenna," *Proceeding of the Asia-Pacific Microwave Conference*, pp. 101-104, 1994.

[6-5] J.Takada, T.Yamamoto, M.Ando and N.Goto, "Circularly Polarized

Multibeam Radial Line Slot Antennas for Mobile Satellite Communication," *Proceeding of the IEEE Antennas Propagation Society International Symposium*, pp. 1430-1433, 1995.

[6-6] J.Takada, T.Yamamoto, M.Ando and N.Goto, "An Azimuthal Multibeam Radial Line Slot Antennas for Mobile Satellite Communication," *Proceeding of the 4th IEEE International Conference on Universal Personal Communication*, pp. 571-574, 1995.

[6-7] C.Phongcharoenpanich, M.Krairiksh and J.Takada, "Dyadic Green 's Functions of the Concentric Conducting Spherical Cavity," *Proceeding of the 1997 Asia-Pacific Microwave Conference*, vol.2, pp.757-760, 1997.

[6-8] M.Krairiksh, T.Wakabayashi and W.Kiranon, "A Spherical Slot Array Applicator for Medical Applications," *IEEE Trans. Microwave Theory Tech.*, vol. 43, pp. 78-86, 1995.

[6-9] S.A. Schelkunoff, *Electromagnetic*, D.Van Nostrad, New York, 1943.

[6-10] Y. Mushiake and R.E. Webster, "Radiation Characteristics with Power Gain for Slots on Sphere," *IRE Trans. Antennas Propagat.*, vol.5, pp.47-55, 1957.

[6-11] M.Hoffman, "Conventions for the Analysis of Spherical Arrays," *IEEE Trans. Antennas Propagat.*, vol.11, pp.390-393, 1963.

[6-12] D.L.Sengupta, T.M.Smith and R.W.Larson, "Radiation Characteristics of a Spherical Array of Circularly Polarized Elements," *IEEE Trans. Antennas Propagat.*, vol.16, pp.2-7, 1968.

[6-13] T.Hori, N.Terada and K.Kagoshima, "Electronically Steerable

Spherical Array Antenna for Mobile Earth Station. *Proceeding of IEE.Conf. Antennas Propagat.,* pp.55-58, 1987.

Chapter 7

Conclusions and Discussions

Synopses of this thesis and discussions of the future studies are included in this chapter.

7.1 Summary of the Preceding Chapters

As mentioned in the preceding chapters that the aim of this thesis is to derive and analyze the electromagnetic field of the spherical geometry. The further application of this study is to use in the spherical cavity-backed slot array antenna as described in chapter 1. The coverage of this thesis is comprising of three configurations of the problem under consideration, they are the conducting spherical cavity, the concentric conducting spherical cavity enclosed by the conducting conical surface and the conducting spherical segment. The scope of the analysis includes the source and the source-free region. The derivation procedure is started with the Maxwell's equations and the continuity equation and then derived for the wave equations, subsequently. The details of the derivation are described in chapter 2. The general expression of the solution in the spherical coordinate system after the method of separation of variable is used for solving that partial differential equation consists of

1. linear combination of the spherical Bessel function of the first kind ($j_n(kR)$) and the spherical Bessel function of the second kind ($y_n(kR)$),

2. linear combination of the associated Legendre functions of the first and second kinds of order (n,m) of the cosine function($P_n^m(cos\theta)$ and $(Q_n^m(cos\theta))$,

3. linear combination of the cosine and sine functions $(^{cos}_{sin}m\phi)$.

After that, the vector potential is derived to obtain the electric and magnetic fields in both cases of the transverse electric and transverse magnetic fields. The solutions of the scalar eigenfunction, the difference is the solution in the radial direction, the spherical Bessel function. In chapter 3, electromagnetic field can be derived via the magnetic and electric vector potentials. The particular solutions in each cases as reported before can be obtained by applying the boundary conditions which are subjected to that geometry. The particular solution of the conducting spherical cavity is reduced by eleminating the second kind spherical Bessel function due to the restriction of the field at the origin and the second kind associate Legendre function from the singularities at θ equals 0 and π radians. The unknown coefficient was solved by using the boundary condition that the tangential electric field vanishes at that certain radius of the conducting spherical cavity. Based on the same fashion, the particular cavity solution of the concentric conducting spherical cavity enclosed by the conducting conical surface, the solution excludes the associated Legendre function of the second kind and the unknown coefficient was determined in the same way as desribed before. Similarly, for the event of the conducting spherical segment, the particular solution is similar to the case of the concentric conducting spherical cavity except the boundary condition at the azimuth plane is also included. Chapter 4 explains the theory of the dyadic Green's

function in electromagnetic problem, especially to consider the electromagnetic field in the source region, e.g., the radiation from the electric or magnetic current source inside the cavity. First, Maxwell's equation in dyadic form is derived and the order will be risen to keep away from the coupled property. Eventually, the dyadic Green's function is sub-divided into three categories by means of the boundary conditions which the field is satisfied. The first kind dyadic Green's function satisfies the Dirichlet boundary condition whereas the second kind satisfies the Neumann boundary condition. In the analysis of the multilayer media, the third kind dyadic Green's function is utilized to find the fields in each medium. The dyadic Green's function of the free space is determined to demonstrate the derivation. Electromagnetic field inside the concentric conducting spherical cavity in the source region is considered, subsequently. The dyadic Green's function in this case is derived by using the eigenfunction expansion which is obtained from the vector potential in the event of the source-free region. Accordingly, the electromagnetic field can be obtained by integrating the inner product of that dyadic Green's function and the source under consideration such as the electric current source, i.e., the linear electric probe or the magnetic current source, i.e., the linear slot on the conducting plane throughout the entire source configuration domain.

In chapter 5, the numerical results of the eigenmodes and the electromagnetic field inside the conducting spherical cavity are demonstrated to verify the calculation in various modes. Subsequently, the further practical application is revealed by proposing the concentric conducting spherical cavity-backed slot array antenna namely, the

circularly polarized conical beam spherical slot array antenna which is realized in chapter 6 by using the numerical results of the electromagnetic fields inside the cavity.

Finally, the summary of the material in this thesis and the discussion for the future studies are included in chapter 7, the last chapter. Appendices consist of, the first, includes the vector analysis in spherical coordinate system, the second, describes the spherical Bessel function and the last, the associated Legendre function is also presented. These two functions are very useful in the derivation of the problem involving the spherical configuration.

7.2 Remark for Future Studies

As mention before that the objective of the presentation of this thesis is to derive and analyze the electromagnetic field inside the concentric conducting spherical cavity, the concentric conducting spherical cavity and the conducting spherical segment. The expression of the electromagnetic fields are derived in both cases; source and source free. However, the numerical results are demonstrated only for the case of the source-free region due to an easy way in calculation. This simplification cannot be applied to the cavity in the source region such as the linear electric fed probe, accurately. To solve this problem, the dyadic Green's function can be applied. The expression of the electric and magnetic dyadic Green's function of the first and second kinds are presented in this thesis. Numerical results in this case are left for the further study.

The circularly polarized conical beam spherical slot array antenna is proposed by using the concentric conducting spherical cavity as the exciting structure. In this model, the weak slot coupling [6-1]-[6-2] is assumed. However, to achieve the strong coupling, the model of the excting structure must be modified to provide the traveling wave propagation [6-3].

References

[7-1] J.Takada, "A Study of the Slot Design for Radial Line Slot Antennas," Doctoral dissertation of Department of Electrical and Electronic Engineering, Tokyo Institute of Technology, 1991.

[7-2] J.Hirokawa, "A Study of Slotted Waveguide Array Antennas," Doctoral dissertation of Department of Electrical and Electronic Engineering, Tokyo Institute of Technology, 1993.

[7-3] J.S.Ajioka, "On the Conceptual Utility of Current Flow Lines in Waveguides," *IEEE Trans.Antennas Propagat.*,vol.34, no.2, 1996.

List of Publications

1. Works Concerning this Thesis

1.1 **C.Phongcharoenpanich** and M.Krairiksh, "Modal Expansion of Dyadic Green's Functions of the Conducting Spherical Segment," *Proceeding of the 20th Electrical Engineering Conference*, vol.1, pp. 243-248, 1997.

1.2 **C.Phongcharoenpanich,** M.Krairiksh and J.Takada, "Dyadic Green's Functions of the Concentric Conducting Spherical Cavity," *Proceeding of the 1997 Asia-Pacific Microwave Conference*, Hong Kong, vol.2, pp.757-760,1997.

1.3 M.Krairiksh, **C.Phongcharoenpanich**, K.Meksamoot and J.Takada, "A Circularly Polarized Conical Beam Spherical Slot Array-Antenna," submitted for publication in the *International Journal of Electronics*.

2. Related Works

2.1 K.Meksamoot, M.Krairiksh, **C.Phongcharoenpanich** and S. Kosulvit, "A Planar Slot Array Antenna for Thaicom Satellite Broadcasting Reception," *Proceedings of the 1997 Thailand-Japan Joint Symposium on Antennas and Propagation*, pp.55-59, 1997.

3. Other Interested Works

3.1 **C.Phongcharoenpanich**, M.Krairiksh, K.Meksamoot and T.

Wakabayashi, "Legendre Array," *Proceedings of the 1997 Thailand-Japan Joint Symposium on Antennas and Propagation*, pp.195-201, 1997.

3.2 **C.Phongcharoenpanich** and M.Krairiksh, "The Characteristics Comparison between Legendre and Two Kinds Tschebyscheff Arrays ," *Proceeding of the 20th Electrical Engineering Conference*, vol.1, pp. 207-212, 1997.

3.3 **C.Phongcharoenpanich** and M.Krairiksh, "A Modified One-Parameter Taylor Method for the Discrete Array Application," accepted for publication in the *Research and Development Journal of the Engineering Institute of Thailand.*

3.4 **C.Phongcharoenpanich** and M.Krairiksh, "The Discrete Array Pattern Synthesis which provides the Tapered Minor Lobes," accepted for publication in the *Thammasat International Journal of Science and Technology*.

Appendices

Appendix A

Vector Analysis in Spherical Coordinate System

A.1 The transformation of the vector in the spherical coordinate

A.1-1 Vector transformation from rectangular ↔spherical

The relation between rectangular and spherical coordinate system

$$x = R\sin\theta\cos\phi \tag{A.1}$$

$$y = R\sin\theta\sin\phi \tag{A.2}$$

$$z = R\cos\theta \tag{A.3}$$

and

$$R = \sqrt{x^2 + y^2 + z^2} \tag{A.4}$$

$$\theta = \tan^{-1}\frac{z}{\sqrt{x^2 + y^2}} \tag{A.5}$$

$$\phi = \tan^{-1}\frac{y}{x} \tag{A.6}$$

In matrix form, rectangular to spherical transformation matrix

$$\begin{bmatrix} A_R \\ A_\theta \\ A_\phi \end{bmatrix} = \begin{bmatrix} sin\theta cos\phi & sin\theta sin\phi & cos\theta \\ cos\theta cos\phi & cos\theta sin\phi & -sin\theta \\ -sin\phi & cos\phi & 0 \end{bmatrix} \begin{bmatrix} A_x \\ A_y \\ A_z \end{bmatrix} \quad (A.7)$$

In the vice versa, spherical to rectangular transformation matrix

$$\begin{bmatrix} A_x \\ A_y \\ A_z \end{bmatrix} = \begin{bmatrix} sin\theta cos\phi & cos\theta cos\phi & -sin\phi \\ sin\theta sin\phi & cos\theta sin\phi & cos\theta \\ cos\theta & cos\phi & 0 \end{bmatrix} \begin{bmatrix} A_R \\ A_\theta \\ A_\phi \end{bmatrix} \quad (A.8)$$

A.1-2 Vector transformation from cylindrical ↔spherical

The relation between cylindrical and spherical coordinate system

$$\rho = Rcos\theta \quad (A.9)$$

$$\phi = \phi \quad (A.10)$$

$$z = Rcos\theta \quad (A.11)$$

and

$$R = \sqrt{\rho^2 + z^2} \quad (A.12)$$

$$\theta = tan^{-1}\frac{z}{\rho} \quad (A.13)$$

$$\phi = \phi \quad (A.14)$$

In matrix form, cylindrical to spherical transformation matrix

$$\begin{bmatrix} A_R \\ A_\theta \\ A_\phi \end{bmatrix} = \begin{bmatrix} sin\theta & 0 & cos\theta \\ cos\theta & 0 & -sin\theta \\ 0 & 1 & 0 \end{bmatrix} \begin{bmatrix} A_\rho \\ A_\phi \\ A_z \end{bmatrix} \tag{A.15}$$

In the vice versa, spherical to cylindrical transformation matrix

$$\begin{bmatrix} A_\rho \\ A_\phi \\ A_z \end{bmatrix} = \begin{bmatrix} sin\theta & cos\theta & 0 \\ 0 & 0 & 1 \\ cos\theta & -sin\theta & 0 \end{bmatrix} \begin{bmatrix} A_R \\ A_\theta \\ A_\phi \end{bmatrix} \tag{A.16}$$

A.2 Vector differential operator in spherical coordinate

Gradient : ∇

$$\nabla\varphi = \frac{\partial\varphi}{\partial R}\hat{a}_R + \frac{1}{R}\frac{\partial\varphi}{\partial\theta}\hat{a}_\theta + \frac{1}{Rsin\theta}\frac{\partial\varphi}{\partial\phi}\hat{a}_\phi \tag{A.17}$$

Divergence : $\nabla\cdot$

$$\nabla\cdot\overline{F} = \frac{1}{R^2}\frac{\partial}{\partial R}(R^2F_R) + \frac{1}{Rsin\theta}\frac{\partial}{\partial\theta}(sin\theta F_\theta) + \frac{1}{Rsin\theta}\frac{\partial F_\phi}{\partial\phi} \tag{A.18}$$

Curl : $\nabla\times$

$$\nabla\times\overline{F} = \frac{1}{Rsin\theta}[\frac{\partial}{\partial\theta}(F_\phi sin\theta)-\frac{\partial F_\theta}{\partial\phi}]\hat{a}_R + \frac{1}{R}[\frac{1}{sin\theta}\frac{\partial F_R}{\partial\phi}-\frac{\partial}{\partial R}(RF_\phi)]\hat{a}_\theta + \frac{1}{R}[\frac{\partial}{\partial R}(RF_\theta)-\frac{\partial F_R}{\partial\theta}]\hat{a}_\phi \quad \text{(A.19)}$$

Laplacian : ∇^2

$$\nabla^2\varphi = \frac{1}{R^2}\frac{\partial}{\partial R}(R^2\frac{\partial\varphi}{\partial R})+\frac{1}{R^2sin\theta}\frac{\partial}{\partial\theta}(sin\theta\frac{\partial\varphi}{\partial\theta})+\frac{1}{R^2sin^2\theta}\frac{\partial^2\varphi}{\partial\phi^2} \quad \text{(A.20)}$$

Appendix B

Spherical Bessel Functions

One set of the Bessel and Hankel functions which are refered to as the ordinary spherical Bessel and Hankel functions are satisfied the ordinary spherical Bessel's differential equation

$$\frac{d^2}{dx^2}[xb_n(x)] + [1 - \frac{n(n+1)}{x^2}]xb_n(x) = 0, \tag{B.1}$$

where $b_n(x)$ are

$j_n(x)$: ordinary spherical Bessel function of the first kind of order n,

$y_n(x)$: ordinary spherical Bessel function of the second kind of order n,

$h_n^{(1)}(x)$: ordinary spherical Hankel function of the first kind of order n and $h_n^{(2)}(x)$ ordinary spherical Hankel function of the second kind of order n.

The ordinary spherical Bessel and Hankel functions are related to the regular (cylindrical) Bessel functions as

$$b_n(x) = \sqrt{\frac{\pi}{2x}} B_{n+\frac{1}{2}}(x), \tag{B.2}$$

where $B_n(x)$ is the regular Bessel function of order n.

Another set of the Bessel and Hankel functions which are usually used in determining the electromagnetic field in the spherical geometry are refered to as the Schelkunoff spherical Bessel and Hankel functions are satisfied the Schelkunoff spherical Bessel's differential equation

$$\frac{1}{\hat{B}_n(x)}\{x^2\frac{d^2\hat{B}_n(x)}{dx^2}\}+x^2-n(n+1)=0, \tag{B.3}$$

where $\hat{B}_n(x)$ are

$\hat{J}_n(x)$: Schelkunoff spherical Bessel function of the first kind of order n,

$\hat{Y}_n(x)$: Schelkunoff spherical Bessel function of the second kind of order n,

$\hat{H}_n^{(1)}(x)$: Schelkunoff spherical Hankel function of the first kind of order n

and $\hat{H}_n^{(2)}(x)$: Schelkunoff spherical Hankel function of the second kind of order n.

The Schelkunoff spherical Bessel and Hankel functions are related to the regular Bessel functions and the ordinary spherical Bessel functions as

$$\hat{B}_n(x)=\sqrt{\frac{\pi x}{2}}B_{n+\frac{1}{2}}(x)=xb_n(x). \tag{B.4}$$

Appendix C

Associated Legendre Functions

Associated Legendre functions are the functions which satisfied the associated Legendre's differential equation as

$$(1-x^2)\frac{d^2L_n^m(x)}{dx^2}-2x\frac{dL_n^m(x)}{dx}+[n(n+1)-\frac{m^2}{1-x^2}]L_n^m(x)=0, \quad \text{(C.1)}$$

where the solution $L_n^m(x)$ is

$$L_n^m(x) = A_1P_n^m(x)+B_1Q_n^m(x), \quad \text{(C.2)}$$

where $P_n^m(x)$: the associated Legendre function of the first kind of order (n,m) and $Q_n^m(x)$: the associated Legendre function of the second kind of order (n,m)

The relationship between the associated Legendre function and the ordinary Legendre function is

$$L_n^m(x) = (-1)^m(1-x^2)^{m/2}\frac{d^mL_n(x)}{dx^m}, \quad \text{(C.3)}$$

where $L_n(x)$ are $P_n(x)$: the ordinary Legendre function of the first kind of order n and $Q_n(x)$: the ordinary Legendre function of the second kind of order n.

Curriculum Vitae

Author : Chuwong Phongcharoenpanich

Date of Birth : September 11, 1974

Bachelor Degree : B.Eng.(Hons.) in Telecommunication Engineering

Institution : Faculty of Engineering
King Mongkut's Institute of Technology Ladkrabang

Year of Graduation : 1996

Undergraduate Research :

1. The Design of the Planar Slotted-Waveguide Array Antenna (1995)
2. The Design of Variable Phase Shifter (1994)
3. The Design of Phase Shifter From Partially-Filled Rectangular Waveguide (1994)

Scholarship : Local graduate Scholarship from the National Science and Technology Development Agency: NSTDA (1996-1997)

Experience : Graduate Research Assistant in Steerable Spherical Slot Array Antenna Project under the career development award of the National Science and Technology Development Agency: NSTDA (From 1997)